

https://dspace.org/

Synthesis and application of novel functionalized nanostructured membranes incorporating N-doped CNT supported metal nanoparticles in water treatment

Phao, Neo

2013-08-06
http://hdl.handle.net/10539/12999

Downloaded from a DSpace repository. https://dspace.org/

Synthesis and Application of Novel Functionalized Nanostructured Membranes Incorporating N-doped CNT Supported Metal Nanoparticles in Water Treatment

By

Neo Phao

Student Number: 0704197R

A dissertation submitted to the Faculty of Science, University of the Witwatersrand, Johannesburg, in fulfilment for the degree of Master of Science in Chemistry.

Supervisor: Dr. S.D. Mhlanga

Co-supervisors: Prof. B.B. Mamba

Dr. E.N. Nxumalo

University of the Witwatersrand May 2013

DECLARATION

I declare that the dissertation, which I hereby submit for the degree of Master of Science at the Faculty of Science, University of the Witwatersrand, Johannesburg, is my own work and has not previously been submitted by me to any institution.



_____

Neo Phao

On this _____ day of _____ 2013

DEDICATED TO

My parents Solly and Violet Phao;

my siblings Baatseba and Kelebogile Phao;

and to my late brother Matshobane Hathaway Phao.

"A man's dignity isn't measured by the people he has around him when he's at the peak of his success, but by his ability not to forget those who helped him when his need was greatest."

Paulo Coelho

ACKNOWLEDGEMENTS

I am grateful to my supervisors Dr S.D. Mhlanga, Prof B.B. Mamba and Dr E.N. Nxumalo for the great contributions to the success of this research study.

I am also grateful to Prof N.J. Coville for his input on certain aspects of this project, particularly the synthesis and analysis of N-CNTs.

All thanks to Ms Z.N. Tetana for babysitting me during my honours studies and for grooming me into a proper N-CNT synthesiser. Dr Lusilao you are not forgotten thanks for the initiation.

To the proper men and women of CATOMMAT for being such great colleagues and friends. Many thanks from myself exactly!!

DST/NIC Mintek Nanotechnology Innovation Centre, Bradlow and the University of the Witwatersrand local merit scholarship for financial support.

The University of Johannesburg for facilities and a working environment.

To Dr Kulsum Kondiah, for her assistance with the microbiological tests.

To Victoria, Banele, Derrick, Gcina and Bhekani for the constructive criticism. Thank you!

To my friends James, Lungile, Cynthia, Sello, Wilson and Funeka for their support and all the fun times. My mmata Angelo, you are the best buddy in the world!!

To Phumile and Asanda for making the UJ environment comfortable and conducive.

To my entire family, for the love and support. More importantly for attending all those graduations–employment will soon follow...LOL!!

Finally to the Almighty Father for the endless love, strength and courage through all those sleepless nights. Thank you!

PRESENTATIONS AND PUBLICATIONS

PRESENTATIONS AT CONFERENCES

- Neo Phao, Edward Nxumalo, Bhekie Mamba, Sabelo Mhlanga, Synthesis and application of N-doped CNT/Polyethersulfone ultrafiltration membranes in water treatment. **Oral presentation**. DST/MINTEK Nanotechnology Innovation Centre (NIC) annual symposium – Randburg, South Africa, November 2011.

- Neo Phao, Edward Nxumalo, Bhekie Mamba, Sabelo Mhlanga, Synthesis and application of N-doped CNT/Polyethersulfone ultrafiltration membranes in water treatment. **Oral presentation**. NanoAfrica 2012, the 4th International Conference on Nanoscience and Nanotechnology – University of the Free State, Bloemfontein, South Africa, 1 – 4 April 2012.

- Neo Phao, Edward Nxumalo, Bhekie Mamba, Sabelo Mhlanga, Synthesis and application of N-doped CNT/Polyethersulfone ultrafiltration membranes in water treatment. **Poster presentation**. Euromembrane Conference – United Kingdom, London, 23 –27 September 2012.

- Neo Phao, Edward Nxumalo, Bhekie Mamba, Sabelo Mhlanga, Synthesis and application of N-doped CNT/Polyethersulfone ultrafiltration membranes in water treatment. **Poster presentation**. University of the Witwatersrand 4th Cross Faculty Postgraduate Symposium, October 2012.

- Neo Phao, Edward Nxumalo, Bhekie Mamba, Sabelo Mhlanga, Synthesis and application of N-doped CNT/Polyethersulfone ultrafiltration membranes in water treatment. **Oral presentation.** 13th WaterNet Symposium – Birchwood Hotel, Boksburg, South Africa, November 2012.

PUBLICATIONS

1. Neo Phao, Edward Nxumalo, Bhekie Mamba, Sabelo Mhlanga, Synthesis and Study of Nanostructured Membranes Incorporating N-doped CNTs for water treatment, **submitted**, Physics and Chemistry of the Earth.

TABLE OF CONTENTS

DECLARATION i

DEDICATION ii

ACKNOWLEDGEMENTS iii

PRESENTATIONS AND PUBLICATIONS v

TABLE OF CONTENTS vii

ABSTRACT xii

LIST OF FIGURES xiii

LIST OF TABLES xvi

LIST OF ABBREVIATIONS xvii

Chapter 1 1

Introduction 1

1.1 Background 1

1.2 Motivation 2

1.3 Aims of project 4

1.4 Outline of the dissertation 5

1.5 References 6

Chapter 2 8

Literature review 8

2.1 Conventional water treatment methods 8
2.1.1 Activated carbon 8
2.1.2 Zeolites 8
2.1.3 Distillation 9
2.1.4 Classical Filtration 9
2.2 Membrane technology 10
2.2.1 Introduction 10
2.2.2 Membrane separation 12
2.2.3 Synthesis and preparation of membrane materials 14
2.2.3.1. Track etching 16
2.2.3.2 Film stretching 16
2.2.3.3 Phase inversion 16
2.2.4 Membrane structure 18
2.2.5 Membrane applications 20
2.2.5 Membrane fouling and its control 21
2.3 Carbon nanotubes 24
2.3.1 Synthesis methods for CNTs 25
2.3.2 Modification of the CNT structure 26
2.3.2.1 Purification of CNTs 27
2.3.2.2 Functionalisation of CNTs 27
2.3.2.3 Doping of CNTs 28

2.4 Antibacterial metals 29

2.5 Summary 29

2.6 References 31

Chapter 3 44

Experimental 44

3.1 Chemicals and materials 44

3.2 Preparation of Fe-Co/$CaCO_3$ catalyst 44

3.3 Synthesis of N-CNTs 44

3.4 Functionalization of N-CNTs 45

3.5 Membrane composition 46

3.6 Synthesis of Ag/N-CNTs 47

3.6.1 Anti-bacterial study of Ag/N-CNTs 47

3.7 Synthesis of Ag/N-CNT/PES membranes 48

3.7.1 Bacterial filtration test for Ag/N-CNT/PES 48

3.8 Characterisation 49

3.8.1 Transmission Electron Microscopy (TEM) 49

3.8.2 Scanning Electron Microscopy (SEM) 49

3.8.3 Zeta-Potential 49

3.8.4 Fourier Transform Infrared Spectroscopy 50

3.8.5 X-ray diffraction (XRD) 50

3.8.6 Brunauer-Emmett-Teller (BET) 50

3.8.7 Thermogravimetric analysis (TGA) 50

3.8.8 Atomic force microscopy (AFM) 50

3.8.9 Contact angle 51

3.8.10 Cross-flow system 52

3.9 References 53

Chapter 4 54

Results and discussion 54

4.1 Introduction 54

4.2 Catalyst characterisation 54

4.3 N-CNT characterisation 56

4.3.1 TEM analysis 56

4.3.2 CN Analysis of N-CNTs 58

4.3.3. Thermogravimetric analysis (TGA) and BET surface area analysis 60

4.3.4. FTIR spectroscopy and zeta potential measurements 61

4.4 Analysis of N-CNT/PES blend membranes 63

4.4.1 FTIR spectroscopy analysis 63

4.4.2 AFM and SEM analyses 64

4.4.3 Thermal stability of membranes 68

4.4.4 Mechanical properties of the *f*N-CNT/PES blend membranes 68

4.4.5 Membrane performance: flux, contact angle and rejection studies.....69

4.5 Fouling studies of N-CNT/PES membranes.....73

4.6 Synthesis of Ag/N-CNTs composites.....78

4.6.1 Leaching studies for Ag/N-CNTs.....80

4.6.2 Anti-microbial study of Ag/N-CNTs.....82

4.7 Synthesis of Ag/N-CNTs/PES membranes.....84

4.7.1 AFM and SEM analysis.....84

4.7.2 Anti-microbial study Ag/N-CNT/PES.....87

4.8 References.....89

Chapter 5.....92

Conclusions and recommendations.....92

5.1 Conclusions.....92

5.2 Recommendations for future work.....94

ABSTRACT

In relation to conventional water treatment methods, membrane separation has acquired a great audience due to its wide applicability, reliability, low cost, low energy demands, and ease of use. However, membrane fouling has been identified as the main downsizing factor in the application of this technology. To address this issue, several studies have suggested the use of inorganic additives for enhancement of the membrane antifouling properties.

In this study, silver (Ag) decorated nitrogen doped carbon nanotubes (N-CNTs) dispersed into polyethersulphone (PES) membranes for potential use in water treatment. Firstly, N-CNTs were synthesised using the chemical vapour deposition (CVD) method. The black soot was functionalised and characterised using transmission electron microscopy (TEM), scanning electron microscopy (SEM), thermogravimetric analysis (TGA) and Brunner-Emmett-Teller (BET). The N-CNTs were found to have an average diameter of 15 nm. The functionalised N-CNTs were then decorated with Ag nanoparticles (AgNPs) using the Polyol method. The resultant product was also characterised using TEM, the AgNPs were found to have an average diameter of 6 nm. The N-CNTs and Ag/N-CNTs were then uniformly dispersed into (PES) membranes to form N-CNT/PES and Ag/N-CNT/PES blend membranes, respectively. The membranes were then characterised using several series of techniques including scanning electron microscopy (SEM), atomic force microscopy (AFM), contact angle analyser and a cross-flow filtration system.

The blend membranes were investigated for any improved properties and tested for their efficiency in removing model pollutants (polyethylene glycol, humic acids, and bacteria) from water. The AFM results revealed a reduction in surface roughness from 23.9 nm for the pristine PES to 12.7 nm in the N-CNT/PES blend membranes. The mechanical stability increased from 3.7 MPa for the pristine PES to 4.4 MPa with a small addition of N-CNTs. Furthermore, the performance studies showed a 46% increase in pure water flux and a 13% increase in rejections for N-CNT blend PES membranes as compared to the pristine PES membrane. Antibacterial studies were also performed where Ag modified N-CNTs were found to inactivate *Enterohaemorrhagic E. coli* by almost twice the initial concentration in the bacterial suspensions. Finally, Ag/N-CNTs were immersed into PES membranes. The Ag/N-CNTs/PES membranes were then tested for their activity towards the bacteria.

LIST OF FIGURES

Chapter 2

Fig 2.1: Example of zeolite type structures 9

Fig 2.2: Solvent-nonsolvent exchange in a coagulation bath. 17

Fig 2.3: Example of a ternary phase diagram for the polymer-solvent-nonsolvent system during the immersion precipitation phase inversion process. 18

Fig 2.4: Schematic diagrams of isotropic membranes: (a) microporous (b) dense and (c) electrically charged membranes 19

Fig 2.5: Schematic diagrams of anisotropic membranes: (a) Loeb-Sourirajan (b) thin film composite membranes. 20

Fig 2.6: Arrangement of graphene to form various CNT morphologies. 25

Fig 2.7: Horizontal CCVD reactor for synthesis of CNTs. 26

Fig 2.8: Functionalisation of CNTs. 28

Chapter 3

Fig 3.1: Schematic diagram of CVD experimental setup. 45

Fig 3.2: Schematic diagram for preparation of N-CNT/PES membranes 46

Fig. 3.3: Schematic representation of contact angle measurements (a) large contact angle (b) small contact angle. 51

Fig. 3.4: Cross-flow filtration system used in this work. 52

Chapter 4

Fig. 4.1: TEM image of the as-synthesised Fe/Co/$CaCO_3$. 55

Fig. 4.2: XRD patterns of the $CaCO_3$ and the Fe/Co/$CaCO_3$ catalyst. 55

Fig. 4.3: EDS spectrum showing the presence of both the Fe and Co particles on the $CaCO_3$. 56

Fig. 4.4: TEM images of (a) as-grown N-CNTs and (b) *f*N-CNTs showing bamboo compartments (pointed by arrow insert); (c) diameter size distribution of N-CNTs before and after functionalisation. 57

Fig. 4.5: Types of nitrogen moieties that can be incorporated into graphitic carbon: (A) oxidized pyridinic; (B) pyridinic; (C) pyrrolic and (D) quaternary. 58

Fig. 4.6: XPS spectrum showing a deconvoluted N 1s spectrum of the functionalized N-CNT 59

Fig. 4.7: TGA profile of as-grown and *f*N-CNTs. 60

Fig. 4.8: FTIR spectra of as-grown and *f*N-CNTs. 62

Fig. 4.9: Zeta-potential profile for as-grown and *f*N-CNTs. 62

Fig. 4.10: FTIR spectra of the pristine PES and *f*N-CNT blend membranes having different *f*N-CNT loadings. 63

Fig. 4.11: AFM images of (a) pristine PES membrane and blend membranes with different *f*N-CNT loadings: (b) 0.02%, (c) 0.04%, (d) 0.08%, and (e) 0.5%.. 65

Fig 4.12: SEM images of membrane structure (a) surface structure (b) cross-sectional structure of the pristine PES (ai and bi), 0.04% N-CNT/PES (aii and bii) and 0.5% N-CNT/PES (aiii and biii) 67

Fig 4.13: TGA plots for the pristine and N-CNT blend PES membranes. 68

Fig. 4.14: Pure water flux as a function of pressure for the *f*N-CNT/PES membranes and the pristine membrane. 70

Fig. 4.15: Surface contact angle for the *f*N-CNT/PES blend membranes. 71

Fig. 4.16: Rejection of a 500 ppm PEG in aqueous solution using the *f*N-CNT/PES blend membranes. 72

Fig. 4.17: Flux decline behaviour of membranes during fouling studies with humic acid. 74

Fig. 4.18: Normalised flux for the filtration/backwashing experiments using humic acid as the foulant. 75

Fig. 4.19: AFM images of humic acid fouled membranes (a) Pristine PES (b) 0.02% N-CNT/PES (c) 0.04% N-CNT/PES (d) 0.08% N-CNT/PES (e) 0.5% N-CNT/PES. 76

Fig. 4.20: Surface roughness before and after fouling 77

Fig. 4.21: (a) TEM image Ag/N-CNTs (AgNPs can be seen as dark spots on surface of N-CNTs); (b) Diameter size distribution of AgNPs. 78

Fig. 4.22: An EDS spectrum and SEM image of 5% Ag/N-CNTs 79

Fig 4.23: XRD patterns of the pristine N-CNTs and the 5% Ag/N-CNTs. 80

Fig. 4.24: UV-vis spectra of DI water samples extracted from the sonicated samples containing Ag/N-CNTs. 81

Fig. 4.25: TEM image for Ag/N-CNTs after sonication 81

Fig. 4.26: Antibacterial activity of Ag/N-CNTs (a) N-CNTs (b) 5% Ag/N-CNT (c) 10% Ag/N-CNT (d) 20% Ag/N-CNT. 82

Fig. 4.27: Bacterial suspension incorporated with Ag/N-CNTs for antibacterial activity. From left to right is 0% Ag/N-CNT, 5% Ag/N-CNT, 10% Ag/N-CNT and 20% Ag/N-CNT. 84

Fig. 4.28: (a) AFM surface morphology and (b) SEM cross section images of Ag/N-CNT/PES membranes. 86

Fig. 4.29: Zone inhibition study of PES membrane with different concentration Ag incorporated onto N-CNTs. 88

LIST OF TABLES

Chapter 1

Table 1.1: Common pollutants in water systems 3

Chapter 2

Table 2.1: Contributions to membrane technology development 11

Table 2.2: Driving forces and their membrane processes. 13

Table 2.3: Summary of properties of pressure driven membranes. 14

Table 2.4: Polymers for membrane preparation 15

Table 2.5: Physiochemical properties that affect membrane fouling.....22

Chapter 3

Table 3.1: Composition of casting solutions.....47

Chapter 4

Table 4.1: BET surface area and pore volume of as-grown and *f*N-CNTs. 61

Table 4.2: AFM roughness parameters for different *f*N-CNT loadings in the PES membranes. 64

Table 4.3: Mechanical properties of *f*N-CNT/PES blend membranes. 69

Table 4.4: Zones of inhibition for Ag/N-CNTs. 83

Table 4.5: Cell concentrations of suspensions with Ag/N-CNTs. Initial concentration: $3x10^5$ 83

Table 4.6: Surface roughness before and after Ag incorporation. 85

LIST OF ABBREVIATIONS

Abbreviation	Description
AFM	Atomic force microscopy
AgNP(s)	Silver nanoparticle(s)
Ag/N-CNT/PES	Silver modified nitrogen doped carbon nanotubes blend in polyethersulphone membrane
BET	Brunner Emmett Teller
CA	Contact angle
CNT(s)	Carbon nanotube(s)
CVD	Chemical vapour deposition
DI	Deionised
DWCNT(s)	Doublewalled carbon nanotube(s)
E. coli	Escherichia coli
EHEC	Enterohaemorrhagic Escherichia coli
f	Functionalised
FTIR	Fourier transform infrared
h	Hour(s)
MWCNT(s)	Multiwalled carbon nanotube(s)
N	Nitrogen
N-CNT/PES	Nitrogen doped carbon nanotubes blend in polyethersulphone membrane
NMP	N-methylpyrrolidone
PEG	Polyethylene glycol
PES	Polyethersulphone
SWCNT(s)	Singlewalled carbon nanotube(s)
TEM	Transmission Electron Microscopy
TGA	Thermogravimetric analysis
UV-Vis	Ultra-violet visible
WHO	World Health Organisation
XRD	X-Ray Diffraction

CHAPTER 1

INTRODUCTION

1.1 Background

Environmental pollution alleviation and the increasing demand for clean safe water are amongst some of the most critical challenges faced by nations worldwide [1]. Besides water supply shortages, pollution caused by waterborne diseases and hazardous chemicals poses a great health threat to millions of people. In general, water quality in South Africa and around the world is deteriorating due to contamination by organic, inorganic and microbial substances [2]. Although conventional drinking water treatment methods employed can be effective, it is however, important to note the limitations of these methods. For example, activated carbon is unable to remove organic pollutants to acceptable levels. Classical filtration, which has large pores, is unable to filter very small contaminants e.g. bacteria, viruses etc. Also, distillation has high energy and cost requirements. Nevertheless, these methods will be discussed further in Section 2.1.

The ability to modify matter at the nanoscale has allowed the preparation of advanced nanocomposites and the fabrication of high performance membranes for water treatment possible [3]. Many water and gas purification techniques, such as filtration, distillation and reverse osmosis are reliant on membranes. Thus the development of novel membranes with a controlled architecture is important for obtaining more efficient and cost effective purification of water [4].

Membrane-based separations are potentially more economical and easier to implement than competing conventional separation technologies e.g. activated carbon. Also, their low energy and space requirement, as well as simplicity of operation renders them suitable for use in separation processes [3]. This technology has to date been widely used in pure and wastewater treatment for re-use. Also, membrane technologies have been employed in the treatment of municipal wastewater and oil spillages [5]. Membrane-based separation systems have many advantages over traditional drinking water and wastewater treatment processes. These include [5]:

- Fewer chemicals are used. This helps minimize the negative impact of these chemicals in the environment.
- Formation of barriers to colloids and microorganisms via size exclusion, which helps produce ultra-pure water.
- Formation of a compact and thin layer structure, which occupies less floor space.
- Recyclability of the permeate, resulting in water conservation, which typically reduces costs.

Membrane fouling is however still a serious factor limiting the use of membrane technologies [6]. According to Kuzmenko *et al* [7] membrane fouling is referred to as the decline of flux of a membrane filter caused by the accumulation of certain components in the feed water on the surface of the membrane or within the membrane matrix. In an attempt to solve the problems caused by fouling, many research groups have utilised carbon nanotubes (CNTs) as additives to improve the antifouling properties of the membranes. Previous studies by Shawky *et al* [8] have shown that multi walled carbon nanotubes (MWCNTs) blended polyamide membranes can improve mechanical and rejection properties. Celik *et al* [6] have shown that MWCNT blended polyethersulphone membranes show increased roughness, hydrophilicity, porosity and water flux, which subsequently enhances the resistance of the membranes to fouling.

1.2 Motivation

According to a study by the World Health Organisation (WHO) of 2004, 1 billion people in the world, mostly in developing countries, are without potable water and a further 2.6 billion people have no access to adequate sanitation [9]. In addition to the socio-economic and environmental impact of poor water shortages [10], the physical, mental and financial well being of people, particularly of susceptible groups such as children, the elderly and poor, are relatively linked to the availability of safe drinking water [11].

Indeed the world is facing formidable challenges in meeting the rising demands of clean water. The available supplies of pure water are decreasing due to mismanagement, population growth, pollution and more strict health regulations [12]. The presence of hazardous

pollutants in water remains a serious threat for water-supplying companies and municipalities. Organic, inorganic (especially heavy metals) and microbial pollutants are almost always present in water distribution networks (Table 1). The presence of these contaminants in drinking water poses a major risk to human health [13].

Table 1.1: Common pollutants in water systems.

Organic [14]	**Inorganic** [15]	**Microbial**
Polychlorinated biphenyls (PCBs)	Cadmium	Cryptosporidium [16-18]
Polyaromatic hydrocarbons (PAHs)	Lead	Escherichia coli [17, 18]
Dioxins	Mercury	SalmonellaVibrio [19]
Natural organic matter (NOM)	Hydrogen sulphide	Helicobacter [17]
Endocrine disrupting compounds (EDCs)	Chromium	Campylobacter [18]
	Arsenic	

Water treatment techniques for alleviation of these contaminants have been studied for decades. No one method has been found to manage all these pollutants [20]. Most of the conventional water purification methods employed have their limitations. Widely used disinfectants include chlorine, chloramines, ozone and UV light [21]. Each of these disinfection methods has drawbacks. For example, chlorine dissolves in water to form hypochlorous acid, which in turn reacts with NOM to form numerous disinfection by-products, including trihalomethanes, chlorinated byphenyls and other halogenated hydrocarbons [21].

Evidently, without quality drinking water, all scientific efforts become but only ideas without any substantial practical improvement in human development [22]. Challenges relating to drinking water quality cannot be alleviated with one solution. Methods involving advanced techniques at the nanoscale still have to be probed and smart solutions with high performance must be developed.

From this point of view, this study sought to synthesise an advanced membrane filtration technique incorporating silver (Ag) metal nanoparticles dispersed on nitrogen doped carbon nanotubes (N-CNTs). It was expected that the addition of the N-CNTs to the membranes will improve the physico-chemical properties of the materials. Moreover, it was envisaged that the addition of Ag/N-CNTs will improve the fouling/biofouling of the membrane structure.

1.3 Aims of project

The aim of the project was:

To synthesise and functionalise a membrane filtration system incorporating nitrogen doped CNT supported Ag nanoparticles (NPs).

The objectives of the research were as follows:

- To synthesise N-CNTs using the chemical vapour deposition method.
- To disperse AgNPs on the N-CNT using the Polyol method.
- To prepare N-CNT/polyethersulphone (PES) and Ag/CNTs/PES membranes using the phase inversion method.
- To characterise the nanostructured materials using a range of techniques including transmission electron microscopy (TEM), scanning electron microscopy (SEM), X-ray dispersive spectroscopy (EDS), thermogravimetric analysis (TGA), differential scanning calorimetry (DSC), fourier transform infrared spectroscopy (FTIR), Brunauer-Emmett-Teller (BET), cross-flow filtration system and the contact angle analyser. In order to see any structural and performance changes upon modification of the membranes
- To test the nanotechnology-enabled membrane filtration system for the removal of pollutants from water e.g. humic acids.

- To study the capability of the new system in fouling resistance.

- To test the antibacterial activity of the Ag modified N-CNT/PES membranes.

1.4 Outline of the dissertation

Chapter 1: In this chapter a brief background of problems relating to water quality, membrane technology and the motivation of the study are discussed. Furthermore, the chapter addresses the aim of the study and the steps undertaken to achieve it.

Chapter 2: This chapter provides a general insight in the use of membrane technology, carbon nanotubes and carbon nanotube membrane composites for water treatment. A review of their structural properties, methods of preparation, ways of modification and unique properties relative to conventional water treatment technologies is presented.

Chapter 3: This chapter gives a detailed description of the procedures employed for preparation of the calcium carbonate ($CaCO_3$) supported iron (Fe) - cobalt (Co) catalyst, N doped CNTs, Ag modified N-CNTs, N-CNT/Polyethersulphone (PES) and Ag/N-CNT/PES blend membranes. The characterisation techniques used in this research study are also discussed in this chapter.

Chapter 4: This chapter follows from the hypothesis made in Chapter 1. The chapter displays the results obtained in synthesis of N-CNTs and Ag/N-CNTs using the CVD and the Polyol method respectively. The incorporation of these nanotubes into membrane systems, and the subsequent implications they have on the membrane properties (e.g. physiochemical, permeation, fouling and antibacterial properties)

Chapter 5: This chapter provides a summary and conclusion of the study. In addition, it provides recommendations for future work.

1.5 References

1. Likodimos, V., Dionysiou, D.D., and Falaras, P. 2010. Clean water: Water detoxification using innovative photocatalysts. Reviews in Environmental Science and Bio/Technology, 9, 87-94.
2. Mhlanga, S.D., Mamba, B.B., Krause, R.W., and Malefetse, T.J. 2007. Removal of organic contaminants from water using nanosponge cyclodextrin polyurethanes. Journal of Chemical Technology & Biotechnology, 82, 382-388.
3. Tarabara, V.V. 2009. Chapter 5 - multifunctional nanomaterial-enabled membranes for water treatment. William Andrew Publishing: Boston, 59-75.
4. Sears, K., Dumée, L., Schütz, J., She, M., Huynh, C., Hawkins, S., Duke, M., and Gray, S. 2010. Recent developments in carbon nanotube membranes for water purification and gas separation. Materials, 3, 127-149.
5. Chen, J.P., Mou, H., Wang, L.K., Matsuura, T., and Wei, Y. 2008. Membrane separation: Basics and applications membrane and desalination technologies. Humana Press, 271-332.
6. Celik, E., Park, H., Choi, H., and Choi, H. 2011. Carbon nanotube blended polyethersulfone membranes for fouling control in water treatment. Water Research, 45, 274-282.
7. Kuzmenko, D., Arkhangelsky, E., Belfer, S., Freger, V., and Gitis, V. 2005. Chemical cleaning of uf membranes fouled by BSA. Desalination, 179, 323-333.
8. Shawky, H.A., Chae, S.-R., Lin, S., and Wiesner, M.R. 2011. Synthesis and characterization of a carbon nanotube/polymer nanocomposite membrane for water treatment. Desalination, 272, 46-50.
9. (WHO), W.H.O. 2004. Meeting the mdg drinking water and sanitation target: A mid-term assessment of progress. Geneva.
10. Mara, D.D. 2003. Water, sanitation and hygiene for the health of developing nations. Public health, 117, 452-456.
11. Eshelby, K. 2007. Dying for a drink. British Medical Journal, 334, 610-612.
12. Savage, N. and Diallo, M.S. 2005. Nanomaterials and water purification: Opportunities and challenges. Journal of Nanoparticle Research, 7, 331-342.

13. Malefetse, T., Mamba, B., Krause, R., and Mahlambi, M. 2009. Cyclodextrin-ionic liquid polyurethanes for application in drinking water treatment. Water SA, 35, 729-734.
14. Salipira, K.L. 2006. Polymerisation of cyclodextrin and multiwalled carbon nanotubes for use in water purification. Master of Technology in Chemistry. Unviversity of Johannesburg.
15. http://www.clihouston.com/knowledge-base/common-inorganic-pollutants-of-water-pollution.html, Accessed 11 September 2012.
16. Payment, P., Waite, M., and Dufour, A. 2003. Introducing parameters for the assessment of drinking water quality. In assessing microbial safety of drinking water improving methods and approaches. Organisation for economic cooperation and development, 47-78.
17. Hunter, P.R., Colfod, J.M., Le Chevallier, M.W., Binder, S., and Berger, P.S. 2001. Waterborne diseases. Emerging Infectious Diseases, 7, 544-545.
18. Szewzyk, U., Szewzyk, R., Manz, W., and Schleifer, K.H. 2000. Microbiological safety of drinking water. Annual Review of Microbiology, 54, 81-127.
19. Lee, D.G. and Kim, S.J. 2003. Bacterial species in biofilm cultivated from the end of the seoul water distribution system. Journal of Applied Microbiology, 95, 317-324.
20. Bambo, M.F. 2007. Synthesis, characterisation and application of nanoporous cyclodextrin polymers. Master of Technology in Chemistry. Unviversity of Johannesburg.
21. Freese, S.D., and Nozaic, D.J. 2004. Chlorine: Is it really so bad and what are the alternatives? Water SA, 30, 18-24.
22. Pradeep, T. and Anshup. 2009. Noble metal nanoparticles for water purification: A critical review. Thin Solid Films, 517, 6441-6478.

CHAPTER 2

LITERATURE REVIEW

2.1 Conventional water treatment methods

Various physico-chemical water purification processes are being utilised for removal of contaminants in polluted water systems. Most of these processes while effective, are costly, energy and time consuming and very often have disadvantages associated with them [1].

2.1.1 Activated carbon

Activated carbons are carbon based materials that have been chemically and physically treated to increase their surface area and thus their capacity to adsorb organic contaminants from polluted water. They have been utilised for various unique applications (e.g. purification of antibiotics in pharmaceuticals, decolourisation of liquid sugars in food industries [2]), both as structural and functional materials [3]. Their use in purifying water dates as far back as the Roman era [4]. Two types of activated carbon exist, namely: powdered and granular activated carbon (PAC and GAC). These have been used in water purification [5] and gas separation [6]. Their flexible coordination chemistry and ability to react with foreign atoms e.g. nitrogen, hydrogen has made them ideal candidates for use in separation processes [3].

Activated carbon has its own limitations. These include [2, 5, 7]:

- Matrix effect in water which can reduce the adsorption capacity of the material.
- Inability of the material to remove organic contaminants to the acceptable levels (µg/L)
- Complex recycling process
- Regeneration

2.1.2 Zeolites

Zeolites are porous crystalline minerals composed of silicon, aluminium, and oxygen atoms which are connected via a bronsted acid type interaction [8, 9]. Their structure consists of a

pore system of molecular dimension with pore sizes ranging between 3-30 Å, consequently providing size and shape selectivity for foreign atoms (Fig 2.1) [10, 11]. Zeolites have been adopted for use in removal of transition metals, large micro-organisms and organic impurities in polluted water systems [12, 13].

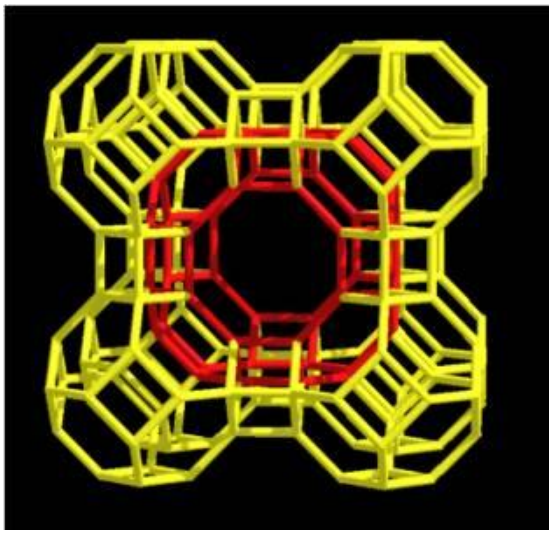

Fig. 2.1: Example of zeolite type structures. The yellow portion represents the framework whereas the red region indicates the region where the primary units combine [14]

Zeolites exhibit exceptional properties with respect to both activity and selectivity because of their ability to adsorb and transform molecules in their inner pores [15]. Although they have great attributes, they have a low affinity for organic compounds. Furthermore, they interact with moisture, which decreases their adsorptive properties [11].

2.1.3 Distillation

Distillation is a process that involves evaporation of water in order to purify it [16]. This technique is one of the oldest in treating water [16, 17]. It has generally been used for removing organic, inorganic and microbial pollutants from water [17]. Despite the above mentioned capabilities, distillation still cannot manage certain pollutants, such as organics with boiling points lower than 100 °C.

2.1.4 Classical Filtration

The original filtration process involves separating phases from each other based on their physical differences [18]. Filtration basically operates by sieving particles according to their

sizes and shapes, such that particles above a certain size will not pass through the filter barrier. The filters used in this process have various morphologies and pore sizes, and are often made of sand, gravel or charcoal [19].

Filtration methods can be cost effective, easy to use and reliable. Moreover they can be cleaned and reused. However, that does not guarantee the removal of all viruses, bacteria, and organic impurities etc. which require filtering with very small pores to separate them. As such, improved and new technological developments need to be put in place to avoid the limitations of current methods and assist in mitigating the prevalence of toxic contaminants in water.

Having considered the advantages and disadvantages of conventional water treatment methods, it is important to discuss membrane based technologies for their use in water separation and purification since these materials were investigated in this study.

2.2 Membrane technology

2.2.1 Introduction

The term membrane has been defined in a number of ways. The most appealing definitions to us are the following:

“ A selective separation barrier for one or several components in solution or suspension” [20].

“ A thin layer of material that is capable of separating materials as a function of their physical and chemical properties when a driving force is applied across the membrane” [21].

Membranes are important materials which form part of our daily lives. Their long history and use in biological systems has been extensively studied throughout the scientific field. The preparation of synthetic membranes is however a more recent invention which has received a great audience due to its applications [22]. Membrane technology like most other methods has undergone a developmental stage, which has validated the technique as a cost-effective treatment option for water [23]. The level of implementation of membrane technologies is

still extending and it is stimulated by the use of additives to improve the mechanical and thermal properties, as well as the permeability, selectivity, rejection and fouling of the membranes [24].

Membranes can be fabricated to possess different morphologies. However, most membranes that have found practical use are mainly of asymmetric structure [25, 26]. Separation in membrane processes takes place as a result of differences in the transport rates of different species through the membrane structure, which is usually polymeric or ceramic [25].

The versatility of membrane filtration has allowed their use in many processes where their properties are suitable in the feed stream. Although membrane separation does not provide the ultimate solution to water treatment, it can be economically connected to conventional treatment technologies by modifying and improving certain properties (e.g. reducing disinfection by products normally encountered when using chlorine) [25-27].

The preparation, operation and application of membrane materials have a long history. There are many books, presentations and papers which have reviewed and discussed these membranes [20, 22, 28]. Table 2.1 presents a brief history of the developments in membrane technologies.

Table 2.1: Contributions to membrane technology development [28].

Contributors	Year	Contributions
Abbe Nollet	1748	Discovering of osmosis phenomenon in natural membranes
Matteucci	1845	Research on anisotropy of natural membranes
Fick	1865	First synthetic membrane from nitrocellulose
Graham	1866	Research on dialysis, research on gas separation on rubber membranes
Traube	1867	Research on osmosis on synthetic membranes
Pfeffer	1877	Research on osmosis on ceramic membranes

Gibbs I van Hoff	1877	Theory of osmosis phenomenon
Donnan	1911	Distribution Law
Abel	1926	Research on dialysis
Michaels, Manegold, McBain	1926-31	Research on reverse osmosis
Elder i in.	1934	Research on electrodialysis
Kammermeyer	1957	Gas separation on silicone rubber and pervaporation of azeotropic mixtures
Londsdale	1960	Research on composite membranes
Loeb-Surirayan	1962	Preparation of asymmetric membranes and pore size controlling in membranes
Mahon	1963	Capillary membranes
Merten	1963	Concentration polarisation
Porter	1975	Classification of pressure-driven processes
Goddard	1977	Models of facilitated transport
Leblanc	1980	Membranes with immobilized carriers
Yoshikawa	1986	Membranes with active centres
Cussler, Aris, Brown	1989	The chain model of facilitated transport
Rautenbach	1990	Membrane hybrid processes

2.2.2 Membrane separation

Synthetic membranes show a large variety in their structural forms. The material used in their production determines their function and their driving forces. Typically the driving force is pressure across the membrane barrier (see Table 2.2) [29-31]. Formation of a pressure gradient across the membrane allows separation in a sieve-like manner. Some other forms of separation that exist include charge effects and solution diffusion. In this “sieve-like” separation, the smaller particles are allowed to pass through as permeates whereas the larger molecules (macromolecules) are retained. The retention and/or permeation of these species is dictated by the pore architecture as well as pore sizes of the membrane employed. Therefore

based on the pore sizes, these pressure driven membranes can be divided into microfiltration, ultrafiltration, nanofiltration and reverse osmosis membranes [32-36].

Table 2.2: Driving forces and their membrane processes [37].

Driving force	**Membrane process**
Pressure difference	Microfiltration, Ultrafiltration, Nanofiltration, Reverse osmosis
Chemical potential difference	Pervaporation, Pertraction, Dialysis, Gas separation, Vapour permeation, Liquid membranes
Electrical potential difference	Electrodialysis, Membrane electrophoresis, Membrane electrolysis
Temperature difference	Membrane distillation

(i) Microfiltration (MF) membranes

MF membranes have the largest pore sizes and thus use less pressure. They involve removing chemical and biological species with diameters ranging between 100 to 10000 nm. Components smaller than this, pass through as permeates [31].

(ii) Ultrafiltration (UF) membranes

UF membranes operate within the parameters of the micro- and nanofiltration membranes. Therefore UF membranes have smaller pores as compared to MF membranes. They involve retaining macromolecules and colloids from solution which range between 2 – 100 nm e.g. large organic molecules and proteins [31].

(iii) Nanofiltration (NF) membranes

NF membranes are distinguished by their pore sizes of between 0.5 – 2 nm. They are mainly used for the removal of small organic molecules and di- and multivalent ions. Additionally, according to van Bruggen *et al,* NF membranes have surface charges that make them suitable for retaining ionic pollutants from solution [31].

(iv) Reverse osmosis (RO) membranes

RO membranes are dense semi-permeable membranes mainly used for desalination of sea water [38]. Contrary to MF and UF membranes, RO membranes have no distinct pores. As a result, high pressures are applied to increase the permeability of the membranes [31]. The properties of the various types of membranes are summarised in Table 2.3.

Table 2.3: Summary of properties of pressure driven membranes [31].

	MF	**UF**	**NF**	**RO**
Permeability ($L/h.m^2.bar$)	1000	10 – 1000	1.5 – 30	0.05 – 1.5
Pressure (bar)	0.1 – 2	0.1 – 5	3 – 20	5 – 120
Pore size (nm)	100 – 10000	2 – 100	0.5 – 2	< 0.5
Separation mechanism	Sieving	Sieving	Sieving, charge effects	Solution diffusion
Applications	Removal of Bacteria	Removal of bacteria, fungi, viruses	Removal of multivalent ions	Desalination

2.2.3 Synthesis and preparation of membrane materials

The synthesis of reliable, high performance synthetic membranes is an important aspect in the field of membrane technology. The membrane preparation procedure stands as the most significant element in membrane research. Considering the different types of membranes available for various applications, it is important to discuss a few preparation routes. Furthermore, given the wide use of the phase inversion synthesis method, this technique will be discussed in greater detail.

It is important to note, even though both ceramic and polymeric membranes are used, polymer membranes are preferred. Therefore the synthesis methods discussed in this work are related to polymeric membranes. The polymer materials generally used during membrane preparation are presented in Table 2.4.

Table 2.4: Polymers for membrane preparation [39].

Material	Membrane formation	Application
CA: cellulose acetate	Casting/ Melt extr	RO, UF, MF, D, GS
CTA: cellulose triacetate	Casting	RO
CN: cellulose nitrate	Casting	UF
PE: polyethylene	Melt extr	PV,GS
PVC: poly(vinyl chloride)	Casting	MF
PVDF: poly(vinylidene fluoride)	Casting	UF,MF, ED
PTFE: polytetrafluorethylene	Melt extr	MF, ED
PAN: polyacrylonitrile	Casting	D, UF
PMMA: polymethyl methacrilate	Casting	D
PVA: poly(vinyl alcohol)	Casting	D, PV
PP: polypropylene	Melt extr	MF, MD
PMP: poly(methyl pentenal)	Melt extr	GS
PET: poly(ethylene terephtalate)	Melt extr	MF
PBTP: poly(butylenes terephtalate)	Melt extr	GS
PC: polycarbonate	Casting	D, MF
PDMS: polydimethylsiloxane	Casting	GS, PV
PTMSP: polytrimethylsilyl propyne	Casting	GS
Psu: polysulphone	Casting	UF
PESu: poly(ether sulfone)	Casting	UF
PPO: poly(phenylene oxide)		UF, GS
PA: polyamide	Melt extr	UF
PEBA: poly(etyher block amide)	Casting	PV
PEI: poly(ether imide)	Casting	GS
PAI: poly(amide imide)	Casting	GS, UF
PPN: polyphosphazene	Casting	GS, PV
PEEK: poly(ether ether ketone)	Melt/Casting	GS

D = Dialysis; G = Gas separation; PV = Pervaporation; MD = Membrane distillation; ED = Electrodialysis

2.2.3.1. Track etching

The formation of polymer membranes with distinct and well-structured nano- and micro pores is highly desirable. Track etching allows fabrication of such structures, by controlled chemical etching of tracks formed by irradiating a polymeric film with heavy ions (e.g. Ni^{7+}, Li^{3+} etc) [40, 41]. Typically, this method involves exposing a polymer film to high energy particles which produce tracks along the entire film. Subsequently these tracks may be strategically etched by a chemical solution in order to form pores [40, 42-44].

2.2.3.2 Film stretching

Membrane stretching is achieved by either uniaxially or biaxially stretching a semi crystalline polymer membrane in order to form pores [45, 46]. Two commonly used routes for making these membranes includes particle stretching and dry stretching [47]. In particle stretching a polymer material is mixed with particles and this mixture is then extruded, whereby pores are formed at the interface of the two components used [47]. However, this method includes costly cleanup processes of solvents and particle contamination. According to Sadeghi *et al,* the preparation of membranes by dry stretching is achieved by three steps: (i) fabrication of the nascent film with lamellar architecture, (ii) annealing the film to thicken the lamellar and (iii) extruding the membrane at low and high temperatures to form small and large pores exponentially [46, 48].

2.2.3.3 Phase inversion

The phase inversion synthesis technique is of highly complex nature, since thermodynamics, kinetics and structural changes play a major role during the synthesis process. Although over the years several methods have been proposed (some of which are mentioned above) for synthesis of polymer membranes, the phase inversion method still remains the most relevant and highly used technique. Experimentally, the phase inversion process can be applied in different ways and by varying certain conditions [49].

(i) Thermal based phase inversion

This method involves mixing a polymer in a diluent (e.g. dimethyl sulphone [50]) at high temperatures (e.g. ± 500 K [51]). The solution is then cooled to induce phase separation. The diluent is then removed to allow the formation of pores on the membrane [50-53].

(ii) Reaction based phase inversion

The reaction based phase inversion processes occurs by liquid-liquid separation to provide a well ordered phase separated structure during a reaction [54]. This is due to the increase in the molecular weight of the polymer and subjection of this polymer to a reaction [55, 56].

(iii) *Immersion precipitation method*

The immersion precipitation process is the most widely used phase inversion method in research and industrially. Generally, the technique involves a polymer dissolved in a organic solvent such as N-methylpyrrolidone (NMP), dimethyl formamide (DMF) or dimethyl actamide (DMAc). The solution is uniformly spread on a solid support. The coated surface is then immersed into a non-solvent (water) bath. Phase inversion then occurs *via* evaporation of the solvent as well as the solvent-nonsolvent exchange (usually water) [36, 57-59]. As a result of evaporation of the solvent and solvent-nonsolvent exchange in the coagulation bath (Fig. 2.2), precipitation of the cast film occurs [60]. This film serves as the actual membrane and can be used as a barrier layer for separation of different components.

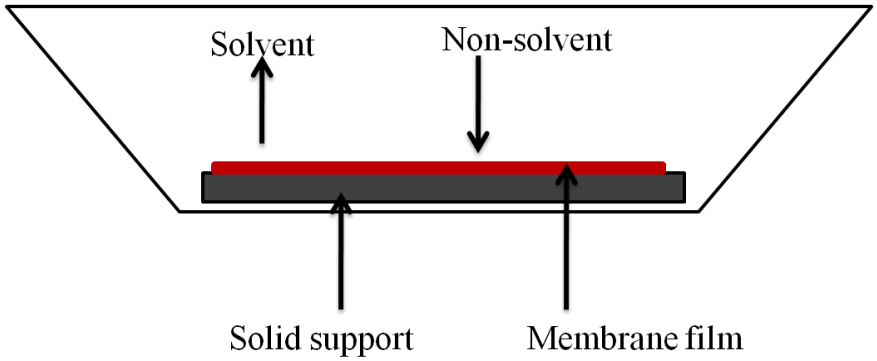

Fig. 2.2: Solvent-nonsolvent exchange in a coagulation bath [60].

Several models have been established to describe the formation of membranes using the phase inversion process. Ternary phase diagrams are used to depict the behaviour of the polymer, solvent and non-solvent phases under various conditions. In Fig. 2.3 the three vertices of a triangle depict the pure components used in the process, whereas any point within the diagram represents a combination of the three materials [20, 58]. The phase

changes that occur during membrane fabrication can be described by paths a – d, where **a** represents the initial polymer solution and **d** the resultant porous membranes. The intermediary points describe the regions of liquid-liquid demixing and solidification respectively. The phase inversion process thus undertakes a sequential route for membrane formation [20, 49, 58].

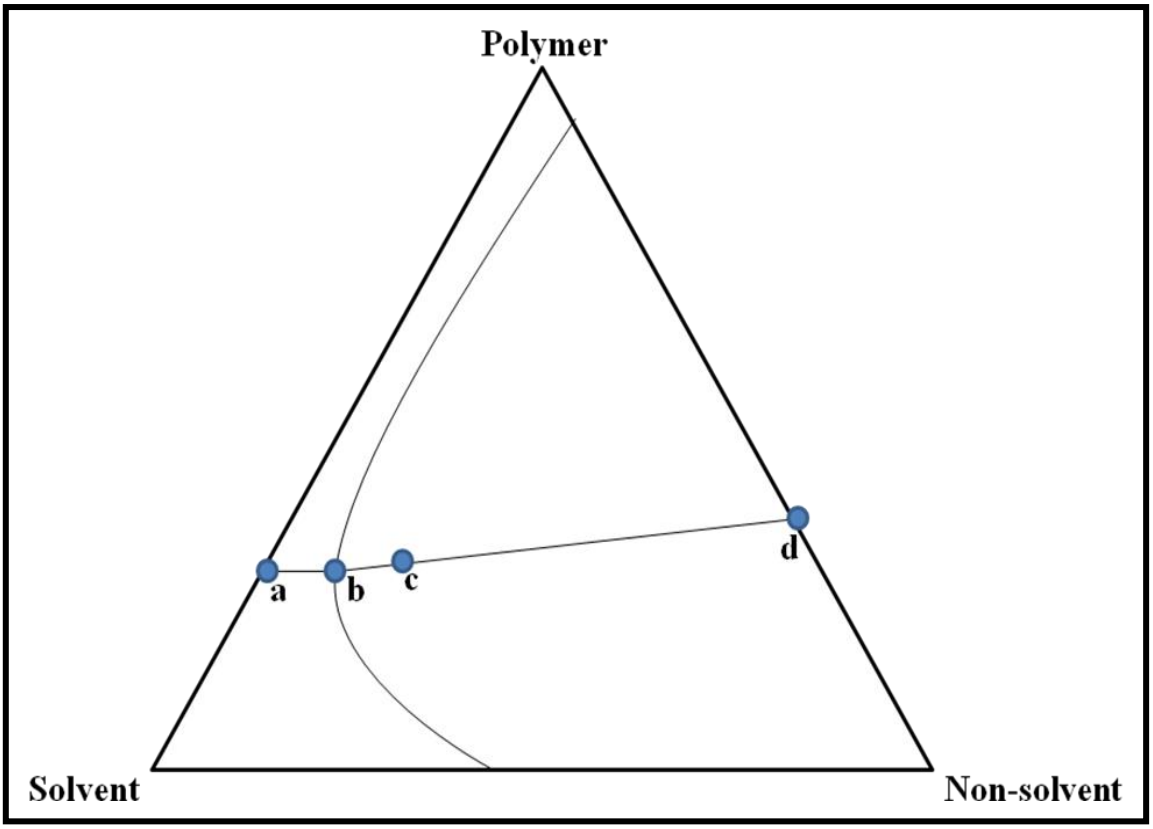

Fig. 2.3: Example of a ternary phase diagram for the polymer-solvent-nonsolvent system during the immersion precipitation phase inversion process [58]. Points **a – d** represent the following; **a** - initial polymer solution **b** - liquid-liquid demixing **c** - solidification **d** - resultant porous membrane.

2.2.4 Membrane structure

The performance of any polymeric membrane in a given process is highly dependent on both the chemical structure of the matrix and the physical arrangement of the membrane [61]. Moreover, the structural integrity of a membrane is very important since it determines its permeation and selectivity efficiency. As such, polymer membranes should be seen as much

more than just sieving filters, but as intrinsic complex structures which can either be homogenous (isotropic) or heterogeneous (anisotropic), porous or dense, liquid or solid, organic or inorganic [61, 62].

(i) Isotropic membranes

Isotropic membranes are typically homogeneous/uniform in composition and structure [63]. They are divided into three subgroups, namely: microporous, dense and electrically charged membranes [63, 64]. Isotropic microporous membranes have evenly distributed pores (Fig 2.4a) [65]. Their pore diameters range between 0.01 – 10 µm and operate by the sieving mechanism. The microporous membranes are mainly prepared by the phase inversion method albeit other methods can be used [64]. Conversely, isotropic dense membranes do not have pores and as a result they tend to be thicker than the microporous membranes (Fig 2.4b). Solutes are carried through the membrane by diffusion under a pressure, concentration or electrical potential gradient [63]. Electrically charged membranes can either be porous or non-porous. However in most cases they are finely microporous with pore walls containing charged ions (Fig 2.4c) [66].

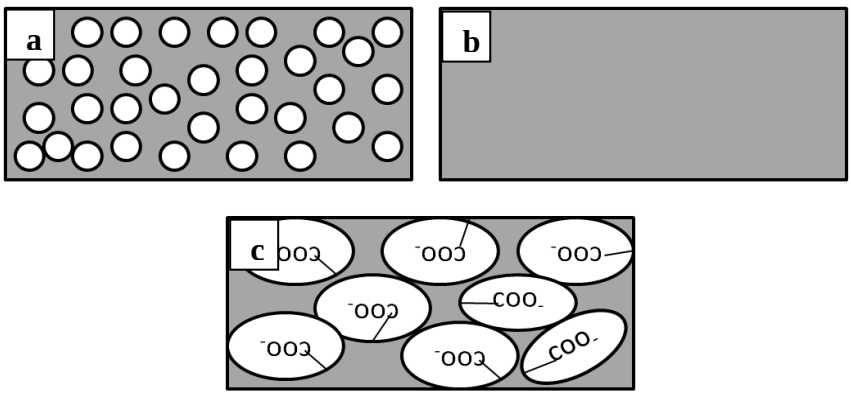

Fig 2.4: Schematic diagrams of isotropic membranes: (a) microporous; (b) dense; and (c) electrically charged membranes

(ii) Anisotropic membranes

Anisotropic membranes are often referred to as Loeb-Sourirajan, based on the scientists who first synthesised them [36, 57, 58]. They are the most widely used membranes in industries. They are represented by non-uniform structures which consist of a thin active skin layer and a highly porous support layer. The active layer dictates the efficiency of the membrane, whereas the porous support layer influences the mechanical stability of the membrane. Anisotropic membranes can be divided into two groups, namely: (i) integrally skinned membranes where the active layer is formed from the same material as the supporting layer, (ii) composite membranes where the polymer of the active layer differs from that of the supporting sub-layer [67].

The detail provided above about isotropic and anisotropic membranes mainly refers to flat film membranes. However, these physical properties are also found in hollow fibre membranes [63].

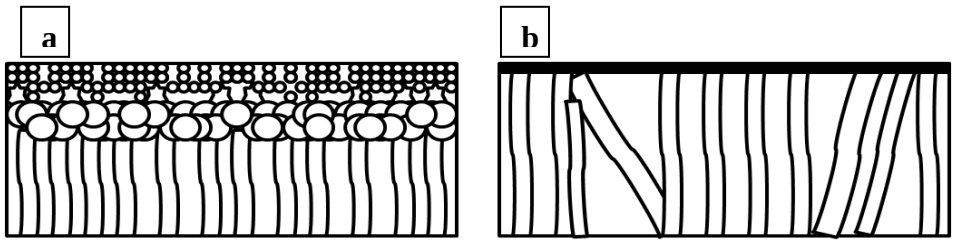

Fig 2.5: Schematic diagrams of anisotropic membranes: (a) Loeb-Sourirajan and (b) thin film composite membranes.

2.2.5 Membrane applications

Advances in membrane research has resulted to an increased use of synthetic membranes (mainly polymer synthetic membranes) in polymer science, medicine, biology, chemistry and engineering. Faiz and Li reported on the use of polymeric membranes for light olefin/paraffin separation in the petrochemical industry. The membranes cost less than cryogenic distillation [68].

Choi *et.al,* showed that the modification of Nafion membranes with graphene oxide could effectively improve the physical and transport properties of the membrane, which is essential for the application of fuel cells [69]. Budd and McKeown published a detailed review on the

application of polymeric membranes for gas separation. They discussed their use in hydrogen recovery, nitrogen generation and the removal of carbon dioxide (CO_2) [70]. In addition to the above mentioned applications, membranes are increasingly applied in water purification. Until recently, most applications of membranes have been on desalination, however, with the different membrane structures that exist, several other opportunities have been explored [71]. These include removal of organic, inorganic and microbial contaminants from water.

Other applications of polymeric membranes can be found in the food industry [72, 73], pharmaceutical industry [74], electrodes [75], biomedicine [76], and beverages [77-79]. Although the applications of membranes in water treatment are vast, the deposition, accumulation and sometimes the adsorption of rejected materials on/in the membrane structure is inevitable. This occurs *via* a process known as membrane fouling.

2.2.5 Membrane fouling and its control

Membrane fouling can be referred to as the deposition and aggregation of solid matter on the surface and within the pores of a membrane [80]. The solid matter can take several forms ranging from microorganisms, colloids to even particulates. Fouling mechanisms are thus extremely complex and interconnected. The most common categories of membrane fouling mechanisms are:

(i) Adsorption of solid matter on the surface and within the pores of the membrane.

(ii) Cake layer formation on the membrane surface.

(iii) Pore blocking by rejected solutes.

(iv) Occurrence of biofouling due to microorganisms.

In addition, based on the matter that deposits on the surface of the membrane (foulant) membrane fouling can be classified as: inorganic, organic, colloidal and biofouling [64, 81]:

(a) *Inorganic fouling:* precipitation of inorganic salts in/on the membrane structure.

(b) *Biofouling:* adherence and growth of bacteria, viruses, fungi etc. on the membrane surface.

(c) *Organic fouling:* adsorption of organic species on/in the membrane.

(d) *Colloidal fouling:* accumulation of colloidal particles on the surface of the membrane, such that a thick cake layer is formed.

Membrane fouling can cause an overall reduction in the permeate flux and selectivity and thus an increase in the energy consumption and eventually an increase in cost [80, 81]. The level of fouling is also directly linked to the physiochemical properties of the membrane used (Table 2.5).

Table 2.5: Physiochemical properties that affect membrane fouling [82]

Physical properties	Chemical properties
Surface roughness	Hydrophobicity/hydrophilicity
Pore sizes/architecture	Membrane charge

(a) Surface hydrophilicity

Most of the pressure driven membranes are hydrophobic because of the nature of the polymers used in their preparation. The hydrophobicity of these membranes tends to promote fouling [83]. Consequently, research is being carried out to produce membranes that are less hydrophobic. Indeed several research groups have embarked on projects to enhance the performance of membranes by fine tuning their surface properties. For example, polyvinylpyrrolidone (PVP) has been widely used as a polymer additive to provide hydrophilicity and to increase membrane permeability [84-86]. Likewise polyethylene glycol has been used to improve the membrane hydrophilicity. A more recent trend is on the study of surface grafted membranes in order to introduce hydrophilic functional groups on the membrane surface [87, 88].

(b) Surface charge

Surface charge interactions between the membrane and the solutes from the water being treated play an important role in the fouling process [89, 90]. Workers have used membranes

with similar charge to the foulant charge. The repulsive forces between the two components would prevent the deposition or adsorption of the foulant on the membrane thereby reducing fouling [83, 89].

(c) Surface roughness

The surface roughness of a membrane is directly linked to membrane fouling [91, 92]. A highly rough surface has peaks and depressions through which the solutes are transported. As such, the depressions preferentially accumulate these solutes which subsequently block the membrane pores and surface leading to flux decline [93]. Elimelech *et al* [94] studied the fouling behaviour of cellulose acetate and aromatic polyamide thin film composite reverse osmosis membranes at identical permeation rates. They observed that thin film composite membranes fouled more as compared to the cellulose acetate membrane. This was due to the higher surface roughness observed for the composite membrane as compared to the acetate membranes [94]. Similarly, Bartels *et al* [95] described the low fouling ESNA1 – CF series membrane as having a smooth surface and a neutral charge, which minimizes organic fouling.

Recently, carbon nanomaterials have been used as additives to improve the membrane properties such as the mechanical strength. For example, carbon nanotubes (CNTs) have high thermal stability, high mechanical strength, chemical inertness, and transport properties which could enhance the overall physicochemical properties of membranes [96, 97]. However, as-grown CNTs tend to bundle up due to the strong van der Waals forces that exist between them, thus making them insoluble in polar organic solvents and/or water [98-105]. As such, this affects the interfacial adhesion between the CNTs and a polymer, affecting the uniform dispersion of the CNTs in the membrane polymer matrix [106, 107].

According to Sung *et al* [108] and Ismail *et al* [109], aligning of CNTs in a polymer matrix can potentially improve the physical properties (e.g. mechanical strength), flux, and selectivity of membranes. However, due to the flexibility and high aspect ratio of the CNTs, such a modification has proven to be difficult to achieve. Therefore, to resolve these issues chemical modification and functionalisation of the CNTs have been proposed by several researchers [84, 110, 111]. For example, Wu *et al* [112] prepared ultrafiltration membranes by incorporating carboxyl multiwalled carbon nanotubes (MWCNTs) into a matrix of brominated polyphenylene oxide using triethanolamine as a linking agent. They observed an

increase in membrane hydrophilicity, permeability, separation performance and chemical stability. In another study, Choi *et al* [84] synthesised MWCNT/polysulphone (PSf) blend membranes using the phase inversion method. Before preparing the membranes, they first functionalised the MWCNTs to introduce acid groups on the surface and make them easily dispersible in organic solvents [84]. The results showed that MWCNTs were good membrane modifiers by controlling the hydrophilicity and adjusting the membrane pore sizes and porosity. Also, the flux and solute rejection of the membrane was increased. These results correlate well with work carried by several other researchers [112-117].

2.3 Carbon nanotubes

The need for new technological processes, scientific innovations and development of a sustainable society are the main driving forces for new material development [118]. Therefore, much attention has been directed towards nanostructured materials [119], in particular CNTs. CNTs are of great interest both from a principal frame of reference for nanomaterials and for future applications [120]. Recent work has shown that certain properties of CNTs depend on their structure [121]. Much attention has been placed on controlling the structure and morphology of CNTs [121].

CNTs can be described as seamless cylinders derived from the honeycomb lattice of graphite sheet [122]. They can exist in three major categories namely, single, double and multi-walled CNTs (SWCNTs, DWCNTs and MWCNTs). SWCNTs are made from a one atom thick sheet of graphene rolled up into a cylinder. When an additional layer of graphene exists around a central SWCNT, a double-walled CNT is formed. On the other hand, MWCNTs can be seen as a series of concentric SWCNTs (Fig 2.6) [123]. Such cylindrically arranged carbon materials have phenomenal properties that make them potentially relevant in various applications.

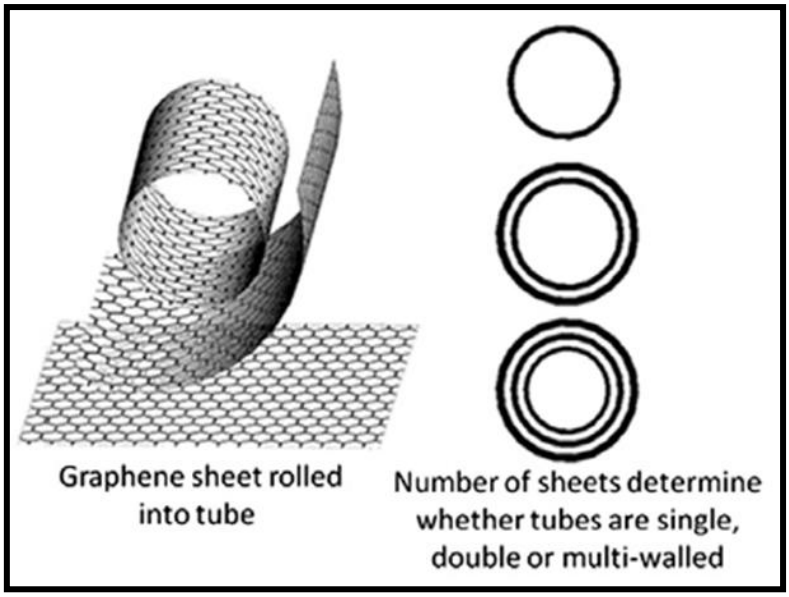

Fig 2.6: Arrangement of graphene to form various CNT morphologies [124].

These unique and novel properties of CNTs include: high tensile strength, high elasticity, high thermal conductivity and high aspect ratio [125]. The outstanding qualities of CNTs find potential applications in numerous fields including biosensors [119], catalysis [126], polymer composites [127], and water purification [1]. Due to their high surface area CNTs have also been used as additives/fillers for modification of various membrane properties [128, 129].

2.3.1 Synthesis methods for CNTs

The synthesis of CNTs can be achieved by employing one of three conventional methods, namely; arc discharge, laser ablation or catalytic chemical vapour deposition (CCVD). The CCVD method is, however, more superior to the other two techniques due to its low cost, versatility and controlled growth of the CNTs under given conditions. The system typically involves a tubular furnace equipped with a quartz-tube, temperature controller and gas sources. The setup can be vertically or horizontally arranged (Fig. 2.7).

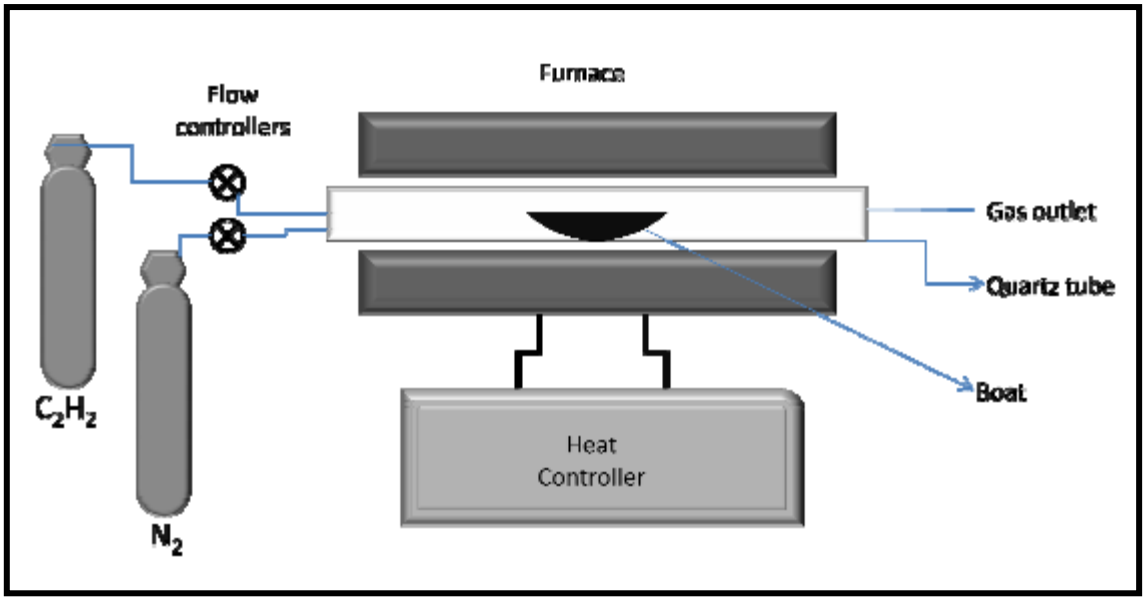

Fig 2.7: Horizontal CCVD reactor for synthesis of CNTs.

The growth process involves heating a metal catalyst (e.g. Fe, Co, Ni) to high temperatures (typically 600 – 1100 °C) in the reactor furnace, followed by passing a hydrocarbon gas (e.g. methane, acetylene, for a period of time). The catalyst serves as a active site on which the CNTs grow. This process can either use a supported catalyst or a floating catalyst. In the former procedure, the metal catalyst is supported by another material and in the latter both the carbon source and the catalyst can be introduced in a gaseous form. Both procedures rely on optimization of certain experimental parameters, such as temperature, synthesis time, carbon precursor and catalyst in order to fabricate the desired CNTs.

The problems associated with the use of the CCVD method include (i) the formation of structural defects, (ii) an excess fabrication of carbonaceous materials, and (iii) the presence of a residual catalyst in the final product. Thus, while the method can be cost effective and readily upscalable, it is important to note that the quality of CNTs can be compromised.

2.3.2 Modification of the CNT structure

Although CNTs have extraordinary properties, exploiting them in membrane composites and other fields seems to be presenting a serious problem for many researchers. CNTs tend to have several impurities despite the method of synthesis. To solve these problems, different channels of modification have been presented. According to Shaikjee [130], modification can enhance the chemical and physical properties. Indeed, many strategies have been employed to modify the structure of CNTs. These methods include functionalisation, doping and even the

incorporation of metals. Consequently, before these modifications can be performed, the CNTs have to be purified.

2.3.2.1 Purification of CNTs

As-grown CNTs synthesised by conventional techniques unavoidably contain metal catalyst or particles (Ni, Co, Fe) and carbonaceous impurities such amorphous carbon, graphitic carbon [131, 132]. Since these impurities can influence the properties of the CNTs, purification becomes an essential tool to employ for addressing this issue. Common purification methods are either based on oxidation liquids (acids and bases) or gaseous oxidants (oxygen etc.) [133]. The choice of purification method is greatly dictated by the intended use of the CNTs [126]. Our discussion will focus mainly on liquid based oxidation methods which are suitable for the purification of our materials. Several mild oxidising acid solutions, such as nitric acid (HNO_3) [126, 134-136], sulphuric acid (H_2SO_4) and potassium permanganate ($KMnO_4$) [133] are preferred for the removal of metal particles and amorphous carbon. Additionally, the use of these oxidants can introduce functional groups on the walls of the CNTs. The CNTs synthesised in our labs could easily be purified by stirring in mild HNO_3.

2.3.2.2 Functionalisation of CNTs

CNTs are composed of pure chemically inert carbon atoms without any functional moieties. As a consequence, this makes them difficult to disperse in most solvents. In addition, this renders them incompatible with polymer matrices. To overcome these issues, surface functionalisation is employed. Through treatment with an oxidant, CNTs are purified and made chemically reactive by introducing oxygen containing groups such as –C=O and –COOH groups, on the surface of the structure (Fig. 2.8). The presence of these groups helps separate to the CNT bundles, and increase their solubility and dispersibilty in different solvents [136, 137]. The presence of oxygen containing groups is especially important when using CNTs as reinforcements in composite materials such as membranes. This is because they increase the interfacial adhesion between themselves and the surrounding environment. This process further also in transferring these unique properties to the CNT-based composites [137].

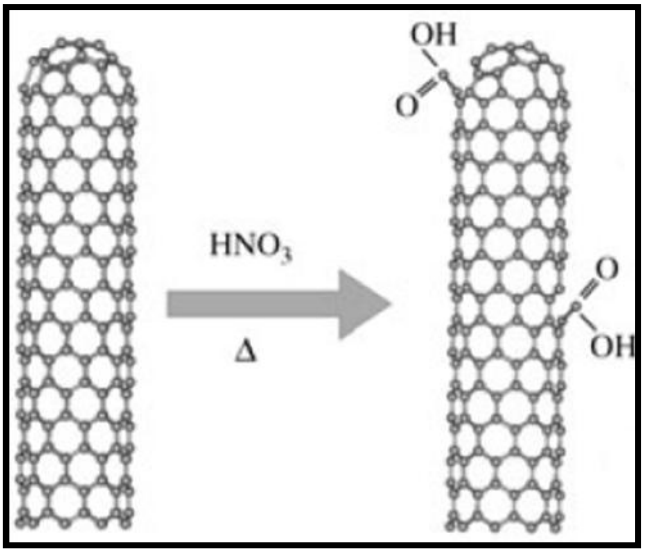

Fig. 2.8: Functionalisation of CNTs [138].

2.3.2.3 Doping of CNTs

Improving physico-chemical properties of CNTs by chemical modification is essential for their application. As mentioned above, elemental doping is one other effective method for achieving this. Typically, substitution of carbon with nitrogen (N) provides an alternative to surface oxidation as it renders the surface of CNTs chemically active, leads to higher surface areas, narrows the tube diameters and bamboo structures within the inner compartments of the CNTs. Nitrogen can be introduced into the CNT lattice by treatment with nitrogen containing materials e.g. ammonia, acetonitrile, urea etc. In this process N can be seen as a *n*-type heteroatom providing an extra electron for donation and substituting carbon in the graphite system [139].

Nitrogen doped CNTs can be produced in two ways:

(1) In–situ doping: direct doping during the CNT synthesis. This method is generally employed for preparation of N-doped CNTs and carbon nanofibers (CNFs) [140].

(2) Post doping: post incorporation of N in pre-synthesised carbon nanomaterials at high temperatures (600 – 900 °C) under a nitrogen atmosphere [141-143].

The use of N doped CNTs as additives in polymer membranes has not yet been explored. One of the objectives of this work was to synthesise N-CNTs and use them as functional particles

in the formation of PES membranes. Moreover, modify the N-CNTs with Ag and use for antibacterial activity of PES membranes.

2.4 Antibacterial metals

A large number of heavy metals are used for antibacterial work. This is because they can form interactions with protein molecules and thus deactivate their functionalities [144]. Metals such as Zn, Cu, Mn, Au and Ag have some toxic properties towards micro-organisms. However, Ag is the most studied metal for anti-bacterial growth.

The domestic use of Ag in the form of silver nitrate ($AgNO_3$), metallic Ag etc for the treatment of burns, wounds and other bacterial infections dates a few centuries back [145]. With the existence of microorganisms immune to antibiotics, the impetus on Ag based materials is being regenerated [146]. The emphasis being on Ag nanoparticles as a result of their enhanced activity at the nanoscale [146].

The proposed mechanism through which Ag destroys bacteria follows a few steps [147-149]:

- Attachment of the Ag nanoparticles onto the bacterial cell membrane,
- Interaction of the nanoparticles with thiol groups containing proteins,
- The release of potassium ions (K^+) from the cell,
- The nanoparticles attack the DNA,
- Interaction of the nanoparticles with thiol groups of enzymes, inhibiting cell growth,
- Finally-cell destruction.

2.5 Summary

It is evident from the literature survey presented in this dissertation that water contamination is an adverse condition that requires serious attention. Current and potential water purification methods still exhibit shortcomings, which make them inefficient in addressing most water related problems. Polymer membranes are presented as an alternative method to overcome these disadvantages, in particular polymer membranes incorporated with Ag loaded nitrogen doped CNTs. It is anticipated that the blend membrane system will have

enhanced characteristics, such as improved hydrophilicity, reduced surface roughness, better mechanical stability, good permeation, and enhanced anti-fouling/biofouling properties.

2.6 References

1. Savage, N. and Diallo, M.S. 2005. Nanomaterials and Water Purification: Opportunities and Challenges. Journal of Nanoparticle Research, 7, 331-342.
2. Przepiórski, J. 2006. Chapter 9 Activated carbon filters and their industrial applications. Interface Science and Technology, Elsevier, 421-474.
3. Bandosz, T.J. and Ania, C.O. 2006. Chapter 4 Surface chemistry of activated carbons and its characterization. Interface Science and Technology, Elsevier, 159-229.
4. http://www.calgoncarbon.com/documents/ACPrinciples.pdf, Accessed 08 September 2012.
5. Karanfil, T. 2006. Chapter 7 Activated carbon adsorption in drinking water treatment. Interface Science and Technology, Elsevier, 345-373.
6. Sircar, S., Golden, T.C., and Rao, M.B. 1996. Activated carbon for gas separation and storage. Carbon, 34, 1-12.
7. http://www.chemeng.lth.se/ket050/Finalreport2009/Stamicarbon.pdf, Accessed 27 November 2012.
8. Ibrahim, S.A.B. 2007. Synthesis and characterisation of zeolites from sodium aluminosilicate solution. Master of Science. University of Malaysia.
9. van Santen, R.A. and Kramer, G.J. 1995. Reactivity theory of zeolitic broensted acidic sites. Chemical Reviews, 95, 637-660.
10. Tao, Y., Kanoh, H., Abrams, L., and Kaneko, K. 2006. Mesopore modified zeolites: preparation, characterization, and applications. Chemical Reviews, 106, 896-910.
11. Bambo, M.F. 2007. Synthesis, characterisation and application of nanoporous cyclodextrin polymers. Master of Technology in Chemistry. Unviversity of Johannesburg.
12. Kalló, D. 2001. Applications of natural zeolites in water and wastewater treatment. Reviews in Mineralogy and Geochemistry, 45, 519-550.
13. Widiastuti, N., Wu, H., Ang, M., and Zhang, D.-K. 2008. The potential application of natural zeolite for greywater treatment. Desalination, 218, 271-280.
14. Roy, A.H., Broudy, R.R., Auerbach, S.M., and Vining, W.J. 1999. Teaching materials that matter: an interactive, multi-media module on zeolites in general chemistry. The Chemical Educator, 4, 114-118.
15. van Donk, S. 2002. Adsorption, diffusion and reaction studies of hydrocarbons on zeolite catalysts. Doctor of Philosophy. University of Utrecht.

16. Kamrin, M. 1990. Distillation for home water treatment. Water Quality Series. Michigan State University.
17. Dvorak, B.I., and Skipton, S.O. 2008. Drinking water treatment: Distillation. Neb Guide. University of Nebraska-Lincoln Extension,.
18. Sutherland, K. 2008. Section 1 - Basic principles in filters and filtration handbook. Elsevier, Oxford, 1-40.
19. http://www.safewater.org/PDFS/knowthefacts/conventionalwaterfiltration.pdf, Accessed 08 September 2012.
20. Doménech-Carbó, M.T. and Aura-Castro, E. 1999. Evaluation of the phase inversion process as an application method for synthetic polymers in conservation work. Studies in Conservation, 44, 19-28.
21. http://www.ultra-flo.com.sg/images/wenton.pdf, Accessed 07/10/12.
22. Strathmann, H., Giorno, L., Drioli, E. 2006. An introduction to membrane science and technology. Rende: Institute on Membrane Technology.
23. Asia, W.A.W. 2005. Membrane filtration-its history and future direction.
24. Chen, J.P., Mou, H., Wang, L.K., Matsuura, T., and Wei, Y. 2008. Membrane separation: Basics and applications membrane and desalination technologies. Humana Press, 271-332.
25. Mortazavi, S. 2008. Application of membrane separation technology to mitigation of mine effluent and acidic drainage. MEND Report 3.15.1.
26. Porter, M.C. 1990. Handbook of industrial membrane technology. William Andrew Publishing/Noyes, 136-259.
27. Weber, W.F., and Bowman, W. 1986. Membranes replacing other separation technologies. 82. New York, NY, ETATS-UNIS: American Institute of Chemical Engineers.
28. Koltuniewicz, A.B. 2005. The history and state of the art in membrane technologies. Tarragona, Erasmus.
29. Macedonio, F. and Drioli, E. 2008. Pressure-driven membrane operations and membrane distillation technology integration for water purification. Desalination, 223, 396-409.
30. Merdaw, A.A., Sharif, A.O., and Derwish, G.A.W. 2011. Mass transfer in pressure-driven membrane separation processes, Part I. Chemical Engineering Journal, 168, 215-228.

31. Van Der Bruggen, B., Vandecasteele, C., Van Gestel, T., Doyen, W., and Leysen, R. 2003. A review of pressure-driven membrane processes in wastewater treatment and drinking water production. Environmental Progress, 22, 46-56.
32. Shirazi, S., Lin, C.-J., and Chen, D. 2010. Inorganic fouling of pressure-driven membrane processes —A critical review. Desalination, 250, 236-248.
33. Pendergast, M.M. and Hoek, E.M.V. 2011. A review of water treatment membrane nanotechnologies. Energy & Environmental Science, 4, 1946-1971.
34. Ulbricht, M. 2006. Advanced functional polymer membranes. Polymer, 47, 2217-2262.
35. Mulder, M. 1996. Basic principles of membrane technology. Dordrecht: Kluwer.
36. Kesting, R.E. 1990. The four tiers of structure in integrally skinned phase inversion membranes and their relevance to the various separation regimes. Journal of Applied Polymer Science, 41, 2739-2752.
37. Timmer J.M.K. 2001. Properties of nanofiltration membranes: model development and industrial application. Doctor of Philosophy. Eindhoven University of Technology.
38. Kasher, R. 2009. Membrane-based water treatment technologies: Recent achievements, and new challenges for a chemist. Bulletin of the Israel Chemical Society, (24), 10-18.
39. Ozdemir, S.S., Buonomenna, M.G., and Drioli, E. 2006. Catalytic polymeric membranes: Preparation and application. Applied Catalysis A: General, 307, 167-183.
40. Kaur, J., Singh, S., Kumar, R., Kanjilal, D., and Chakarvarti, S.K. 2011. Nano/micro structure synthesis on semiconducting substrate and their characterization. Superlattices and Microstructures, 50, 713-721.
41. Awasthi, K., Kulshreshtha, V., Tripathi, B., Acharya, N.K., Singh, M., and Vijay, Y.K. 2006. Transport through track etched polymeric blend membrane. Bulletin of materials science, 29, 261-264.
42. Quinn, J.A., Anderson, J.L., Ho, W.S., and Petzny, W.J. 1972. Model pores of molecular dimension: The preparation and characterization of track-etched membranes. Biophysical Journal, 12, 990-1007.
43. Yamazaki, I.M., Paterson, R., and Geraldo, L.P. 1996. A new generation of track etched membranes for microfiltration and ultrafiltration. Part I. Preparation and characterisation. Journal of Membrane Science, 118, 239-245.

44. Apel, P. 2001. Track etching technique in membrane technology. Radiation Measurements, 34, 559-566.
45. Flaris, V. 2011. Improving the porosity of polypropylene/polysulfone membranes. Antec, 1-3.
46. Sadeghi, F., Ajji, A., and Carreau, P.J. 2007. Analysis of microporous membranes obtained from polypropylene films by stretching. Journal of Membrane Science, 292, 62-71.
47. Tabatabaei, S.H., Carreau, P.J., and Ajji, A. 2009. Microporous membranes obtained from PP/HDPE multilayer films by stretching. Journal of Membrane Science, 345, 148-159.
48. Sadeghi, F., Tabatabaei, S.H., Ajji, A. and Carreau, P.J. 2009. Effect of PVDF characteristics on extruded film morphology and porous membranes feasibility by stretching. Journal of Polymer Science Part B: Polymer Physics, 47, 1219-1229.
49. van de Witte, P., Dijkstra, P.J., van den Berg, J.W.A., and Feijen, J. 1996. Phase separation processes in polymer solutions in relation to membrane formation. Journal of Membrane Science, 117, 1-31.
50. Wu, Q.-Y., Wan, L.-S., and Xu, Z.-K. 2012. Structure and performance of polyacrylonitrile membranes prepared via thermally induced phase separation. Journal of Membrane Science, 409–410, 355-364.
51. Lloyd, D.R., Kim, S.S., and Kinzer, K.E., Microporous membrane formation via thermally-induced phase separation. II. Liquid-liquid phase separation. Journal of Membrane Science, 1991. 64(1-2): p. 1-11.
52. Lloyd, D.R., Kinzer, K.E., and Tseng, H.S., Microporous membrane formation via thermally induced phase separation. I. Solid-liquid phase separation. Journal of Membrane Science, 1990. 52(3): p. 239-261.
53. Funk, C.V., Hanks, P.L., Kaczorowski, K.J., and Lloyd, D.R., Diluent crystal alignment in the formation of membranes via liquid-solid thermally induced phase separation. Journal of Porous Materials, 2009. 16(4): p. 453-458.
54. Li, W., Ryan, A.J., and Meier, I.K., Morphology Development via Reaction-Induced Phase Separation in Flexible Polyurethane Foam. Macromolecules, 2002. 35(13): p. 5034-5042.

55. Borrajo, J., Riccardi, C.C., Williams, R.J.J., Cao, Z.Q., and Pascault, J.P., Rubber-modified cyanate esters: thermodynamic analysis of phase separation. Polymer, 1995. 36(18): p. 3541-3547.
56. Girard-Reydet, E., Sautereau, H., Pascault, J.P., Keates, P., Navard, P., Thollet, G., and Vigier, G., Reaction-induced phase separation mechanisms in modified thermosets. Polymer, 1998. 39(11): p. 2269-2279.
57. Kim, I.-C., Yoon, H.-G., and Lee, K.-H., Formation of integrally skinned asymmetric polyetherimide nanofiltration membranes by phase inversion process. Journal of Applied Polymer Science, 2002. 84(6): p. 1300-1307.
58. Strathmann, H. and Kock, K., The formation mechanism of phase inversion membranes. Desalination, 1977. 21(3): p. 241-255.
59. Kesting R, E., Phase Inversion Membranes, in Materials Science of Synthetic Membranes1985, American Chemical Society. p. 131-164.
60. Beier, S.P., Pressure driven membrane processes. ebooks at bookboon.com, 2007: p. 1-22.
61. Naylor, T.d. and Rapra Technology, L., Polymer membranes : materials, structures and separation performance, Shawbury, Shrewsbury, Shropshire, UK: Rapra Technology Limited, 1996.
62. Strathmann, H., Introduction to membrane science and technology, Weinheim, Germany: Wiley-VCH Verlag & Co, 2011.
63. Baker, R.W. Membrane technology and applications. 2004; Available from: http://public.eblib.com/EBLPublic/PublicView.do?ptiID=219708.
64. Wang, L.K. Membrane and desalination technologies. 2008; Available from: http://rave.ohiolink.edu/ebooks/ebc/9781597452786.
65. Ng, S.-F., Rouse, J.J., Sanderson, F.D., and Eccleston, G.M., The relevance of polymeric synthetic membranes in topical formulation assessment and drug diffusion study. Archives of Pharmacal Research, 2012. 35(4): p. 579-593.
66. Nath, K., Membrane separation processes, New Delhi: Prentice-Hall of India, 2008.
67. Khulbe, K.C., Feng, C.Y., and Matsuura, T. Synthetic polymeric membranes characterization by atomic force microscopy. 2008; Available from: http://public.eblib.com/EBLPublic/PublicView.do?ptiID=337999.
68. Faiz, R. and Li, K., Polymeric membranes for light olefin/paraffin separation. Desalination, 2012. 287(0): p. 82-97.

69. Choi, B.G., Huh, Y.S., Park, Y.C., Jung, D.H., Hong, W.H., and Park, H., Enhanced transport properties in polymer electrolyte composite membranes with graphene oxide sheets. Carbon, 2012. 50(15): p. 5395-5402.
70. Budd, P.M. and McKeown, N.B., Highly permeable polymers for gas separation membranes. Polymer Chemistry, 2010. 1(1): p. 63-68.
71. Geise, G.M., Lee, H.-S., Miller, D.J., Freeman, B.D., McGrath, J.E., and Paul, D.R., Water purification by membranes: The role of polymer science. Journal of Polymer Science Part B: Polymer Physics, 2010. 48(15): p. 1685-1718.
72. Akin, O., Temelli, F., and Köseoğlu, S., Membrane Applications in Functional Foods and Nutraceuticals. Critical Reviews in Food Science and Nutrition, 2012. 52(4): p. 347-371.
73. Gyura, J., Šereš, Z., and Eszterle, M., Influence of operating parameters on separation of green syrup colored matter from sugar beet by ultra-and nanofiltration. Journal of Food Engineering, 2005. 66(1): p. 89-96.
74. López-Fernández, R., Martínez, L., and Villaverde, S., Membrane bioreactor for the treatment of pharmaceutical wastewater containing corticosteroids. Desalination, 2012. 300: p. 19-23.
75. Huang, M., Ding, Y., and Li, X., Improvement of lower detection limit of ion-selective electrodes based on PVC membrane. Progress in Chemistry, 2012. 24(8): p. 1560-1571.
76. Ramakrishna, S., Ma, Z., and Matsuura, T., Polymer membranes in biotechnology : preparation, functionalization and application, London: Imperial College Press, 2011.
77. Garcia-Castello, E.M. and McCutcheon, J.R., Dewatering press liquor derived from orange production by forward osmosis. Journal of Membrane Science, 2011. 372(1-2): p. 97-101.
78. Grassino, A.N., Milardović, S., Grabarić, Z., and Grabarić, B.S., Simple and reliable biosensor for determination of glucose in alcoholic beverages. Food Research International, 2012. 47(2): p. 368-373.
79. Yazdanshenas, M., Nejad, S.A.R.T., Soltanieh, M., Tavakkoli, A., Babaluo, A.A., and Fillaudeau, L., Dead-end microfiltration of rough nonalcoholic beer by different polymeric membranes. Journal of the American Society of Brewing Chemists, 2010. 68(2): p. 83-88.

80. Mohanty, K. and Purkait, M.K., Membrane technologies and applications2012, Boca Raton , FL: CRC Press.
81. Zhang, T.C., Environmental, Water Resources Institute . Membrane Technology Task, C., and American Society of Civil, E., Membrane technology and environmental applications, Reston, VA: American Society of Civil Engineers, 2012.
82. Roest, H.F.V.D., Bentem, A.G.N.D., and Lawrence, D.P., Membrane bioreactors for municipal wastewater treatment, London: IWA Publ. 2002.
83. Hilal, N., Khayet, M., and Wright, C.J., Membrane modification : technology and applications, Boca Raton: Taylor & Francis, 2012.
84. Choi, J.-H., Jegal, J., and Kim, W.-N., Fabrication and characterization of multi-walled carbon nanotubes/polymer blend membranes. Journal of Membrane Science, 2006. 284(1–2): p. 406-415.
85. Han, M.J. and Nam, S.T., Thermodynamic and rheological variation in polysulfone solution by PVP and its effect in the preparation of phase inversion membrane. Journal of Membrane Science, 2002. 202(1-2): p. 55-61.
86. Lee, K.-W., Seo, B.-K., Nam, S.-T., and Han, M.-J., Trade-off between thermodynamic enhancement and kinetic hindrance during phase inversion in the preparation of polysulfone membranes. Desalination, 2003. 159(3): p. 289-296.
87. Tu, C.-Y., Liu, Y.-L., Lee, K.-R., and Lai, J.-Y., Hydrophilic surface-grafted poly(tetrafluoroethylene) membranes using in pervaporation dehydration processes. Journal of Membrane Science, 2006. 274(1–2): p. 47-55.
88. Wang, C., Zhao, S., and Wei, Y., Hydrophilic Modification of Microporous Polysulfone Membrane via Surface-Initiated Atom Transfer Radical Polymerization and Hydrolysis of Poly(glycidylmethacrylate). Chinese Journal of Chemistry, 2012: p. 2473-2482.
89. Van der Bruggen, B., Mänttäri, M., and Nyström, M., Drawbacks of applying nanofiltration and how to avoid them: A review. Separation and Purification Technology, 2008. 63(2): p. 251-263.
90. Elimelech, M., Chen, W.H., and Waypa, J.J., Measuring the zeta (electrokinetic) potential of reverse osmosis membranes by a streaming potential analyzer. Desalination., 1994. 95(3): p. 269.

91. Zhu, X. and Elimelech, M., Colloidal Fouling of Reverse Osmosis Membranes: Measurements and Fouling Mechanisms. Environmental Science & Technology., 1997. 31(12): p. 3654.
92. Vrijenhoek, E.M., Hong, S., and Elimelech, M., Influence of membrane surface properties on initial rate of colloidal fouling of reverse osmosis and nanofiltration membranes. Journal of Membrane Science, 2001. 188(1): p. 115-128.
93. Chennamsetty, R.K., Evolution of two polymeric nanofiltration membranes following ion beam irradiation, 2007.
94. Elimelech, M., Xiaohua, Z., Childress, A.E., and Seungkwan, H., Role of membrane surface morphology in colloidal fouling of cellulose acetate and composite aromatic polyamide reverse osmosis membranes. Journal of Membrane Science, 1997. 127(1): p. 101-109.
95. Bartels, C., Wilf, M., Casey, W., and Campbell, J., New generation of low fouling nanofiltration membranes. Desalination Desalination, 2008. 221(1-3): p. 158-167.
96. Dai, H., Carbon Nanotubes: Synthesis, Integration, and Properties. Accounts of Chemical Research, 2002. 35(12): p. 1035-1044.
97. Dresselhaus, M.S., Dresselhaus, G., Charlier, J.C., and Hernández, E., Electronic, thermal and mechanical properties of carbon nanotubes. Philosophical Transactions of the Royal Society of London. Series A: Mathematical, Physical and Engineering Sciences, 2004. 362(1823): p. 2065-2098.
98. Lin, Y., Meziani, M.J., and Sun, Y.-P., Functionalized carbon nanotubes for polymeric nanocomposites. Journal of Materials Chemistry, 2007. 17(12): p. 1143-1148.
99. Thostenson, E.T., Ren, Z., and Chou, T.W., Advances in the science and technology of carbon nanotubes and their composites: a review. Composites science and technology., 2001. 61(13): p. 1899-1912.
100. Harris, P.J.F., Carbon nanotube composites. International materials reviews., 2004. 49: p. 31-43.
101. Andrews, R. and Weisenberger, M.C., Carbon nanotube polymer composites. Current Opinion in Solid State and Materials Science, 2004. 8(1): p. 31-37.
102. Coleman, J.N., Khan, U., and Gunko, Y.K., Mechanical Reinforcement of Polymers Using Carbon Nanotubes. Advanced Materials -Deerfield Beach then Weinheim-, 2006. 18(6): p. 689-706.

103. Moniruzzaman, M. and Winey, K.I., Polymer Nanocomposites Containing Carbon Nanotubes. Macromolecules, 2006. 39(16): p. 5194-5205.
104. Van der Bruggen, B., The Separation Power of Nanotubes in Membranes: A Review. ISRN Nanotechnology ISRN Nanotechnology, 2012. 2012(3): p. 1-17.
105. Sun, Y.-P., Fu, K., Lin, Y., and Huang, W., Functionalized Carbon Nanotubes: Properties and Applications. Accounts of Chemical Research, 2002. 35(12): p. 1096-1104.
106. Shawky, H.A., Chae, S.-R., Lin, S., and Wiesner, M.R., Synthesis and characterization of a carbon nanotube/polymer nanocomposite membrane for water treatment. Desalination, 2011. 272(1–3): p. 46-50.
107. Li, W.-H., Chen, X.-H., Chen, C.-S., Xu, L.-S., Yang, Z., and Wang, Y.-G., Preparation and shear properties of carbon nanotubes/poly(butyl methacrylate) hybrid material. Polymer Composites, 2008. 29(9): p. 972-977.
108. Sung, J.H., Kim, H.S., Jin, H.-J., Choi, H.J., and Chin, I.-J., Nanofibrous Membranes Prepared by Multiwalled Carbon Nanotube/Poly(methyl methacrylate) Composites. Macromolecules, 2004. 37(26): p. 9899-9902.
109. Ismail, A.F., Goh, P.S., Sanip, S.M., and Aziz, M., Transport and separation properties of carbon nanotube-mixed matrix membrane. Separation and Purification Technology, 2009. 70(1): p. 12-26.
110. Celik, E., Park, H., Choi, H., and Choi, H., Carbon nanotube blended polyethersulfone membranes for fouling control in water treatment. Water Research, 2011. 45(1): p. 274-282.
111. Kim, J. and Van der Bruggen, B., The use of nanoparticles in polymeric and ceramic membrane structures: Review of manufacturing procedures and performance improvement for water treatment. Environmental Pollution, 2010. 158(7): p. 2335-2349.
112. Wu, H., Tang, B., and Wu, P., Novel ultrafiltration membranes prepared from a multi-walled carbon nanotubes/polymer composite. Journal of Membrane Science, 2010. 362(1–2): p. 374-383.
113. Vatanpour, V., Madaeni, S.S., Moradian, R., Zinadini, S., and Astinchap, B., Fabrication and characterization of novel antifouling nanofiltration membrane prepared from oxidized multiwalled carbon nanotube/polyethersulfone nanocomposite. Journal of Membrane Science, 2011. 375(1–2): p. 284-294.

114. Ahn, C.H., Baek, Y., Lee, C., Kim, S.O., Kim, S., Lee, S., Kim, S.-H., Bae, S.S., Park, J., and Yoon, J., Carbon nanotube-based membranes: Fabrication and application to desalination. Journal of Industrial and Engineering Chemistry, 2012. 18(5): p. 1551-1559.
115. Hu, S.Y., Zhang, Y., Lawless, D., and Feng, X., Composite membranes comprising of polyvinylamine-poly(vinyl alcohol) incorporated with carbon nanotubes for dehydration of ethylene glycol by pervaporation. Journal of Membrane Science, 2012. 417-418: p. 34-44.
116. Vatanpour, V., Madaeni, S.S., Moradian, R., Zinadini, S., and Astinchap, B., Novel antibifouling nanofiltration polyethersulfone membrane fabricated from embedding TiO2 coated multiwalled carbon nanotubes. Separation and Purification Technology, 2012. 90(0): p. 69-82.
117. Rahimpour, A., Jahanshahi, M., Khalili, S., Mollahosseini, A., Zirepour, A., and Rajaeian, B., Novel functionalized carbon nanotubes for improving the surface properties and performance of polyethersulfone (PES) membrane. Desalination, 2012. 286(0): p. 99-107.
118. Oosthuizen, R.S. and Nyamori, V.O., Carbon nanotubes as supports for palladium and bimetallic catalysts for use in hydrogenation reactions. Platinum Metals Review, 2011. 55(3): p. 154-169.
119. Trojanowicz, M., Analytical applications of carbon nanotubes: a review. TrAC Trends in Analytical Chemistry, 2006. 25(5): p. 480-489.
120. http://students.chem.tue.nl/ifp03/WondrousWorldofCarbonNanotubes_Final.pdf, Wondrous World of Carbon Nanotubes, in Eindehoven University of Technology, Accessed 13 August 2012.
121. Wu, X., Tao, Y., Mao, C., Wen, L., and Zhu, J., Synthesis of nitrogen-doped horn-shaped carbon nanotubes by reduction of pentachloropyridine with metallic sodium. Carbon, 2007. 45(11): p. 2253-2259.
122. http://arxiv.org/ftp/cond-mat/papers/0611/0611484.pdf, Bond Lengths of Single-Walled Carbon Nanotubes, in Accessed 13 August 2012.
123. Mhlanga, S.D., Synthesis and study of carbon nanotubes and carbon spheres, in School of Chemistry2009, University of the Witwatersrand: Johannesburg, South Africa.

124. Shaikjee, A. and Coville, N.J., The synthesis, properties and uses of carbon materials with helical morphology. Journal of Advanced Research, 2012. 3(3): p. 195-223.
125. Ebbesen, T.W., Carbon nanotubes: Preparation and properties, 1997, CRC Press.
126. Motchelaho, M.A.M., Xiong, H., Moyo, M., Jewell, L.L., and Coville, N.J., Effect of acid treatment on the surface of multiwalled carbon nanotubes prepared from Fe–Co supported on CaCO3: Correlation with Fischer–Tropsch catalyst activity. Journal of Molecular Catalysis A: Chemical, 2011. 335(1–2): p. 189-198.
127. Ajayan, P.M., Schadler, L.S., Giannaris, C., and Rubio, A., Single-Walled Carbon Nanotube–Polymer Composites: Strength and Weakness. Advanced Materials, 2000. 12(10): p. 750-753.
128. Celik, E., Liu, L., and Choi, H., Protein fouling behavior of carbon nanotube/polyethersulfone composite membranes during water filtration. Water Research, 2011. 45(16): p. 5287-5294.
129. Jirage, K.B. and Martin, C.R., New developments in membrane-based separations. Trends in Biotechnology, 1999. 17(5): p. 197-200.
130. Shaikjee, A., Synthesis of carbon nano-structured materials. Doctor of Philosophy. University of the Witwatersrand, 2011.
131. Hou, P.-X., Liu, C., and Cheng, H.-M., Purification of carbon nanotubes. Carbon, 2008. 46(15): p. 2003-2025.
132. Dementev, N., Osswald, S., Gogotsi, Y., and Borguet, E., Purification of carbon nanotubes by dynamic oxidation in air. Journal of Materials Chemistry, 2009. 19(42): p. 7904-7908.
133. Pełech, I., Narkiewicz, U., Moszyński, D., and Pełech, R., Simultaneous purification and functionalization of carbon nanotubes using chlorination. Journal of Materials Research, 2012. FirstView: p. 1-7.
134. Dujardin, E., Ebbesen, T.W., Krishnan, A., and Treacy, M.M.J., Purification of Single-Shell Nanotubes. Advanced Materials, 1998. 10(8): p. 611-613.
135. Hu, H., Zhao, B., Itkis, M.E., and Haddon, R.C., Nitric Acid Purification of Single-Walled Carbon Nanotubes. The Journal of Physical Chemistry B, 2003. 107(50): p. 13838-13842.
136. Rinzler, A.G., Liu, J., Dai, H., Nikolaev, P., Huffman, C.B., Rodríguez-Macías, F.J., Boul, P.J., Lu, A.H., Heymann, D., Colbert, D.T., Lee, R.S., Fischer, J.E., Rao, A.M., Eklund, P.C., and Smalley, R.E., Large-scale purification of single-wall carbon

nanotubes: process, product, and characterization. Applied Physics A: Materials Science & Processing, 1998. 67(1): p. 29-37.

137. Datsyuk, V., Kalyva, M., Papagelis, K., Parthenios, J., Tasis, D., Siokou, A., Kallitsis, I., and Galiotis, C., Chemical oxidation of multiwalled carbon nanotubes. Carbon, 2008. 46(6): p. 833-840.

138. Balasubramanian, K. and Burghard, M., Chemically Functionalized Carbon Nanotubes. Small, 2005. 1(2): p. 180-192.

139. Nieto-Marquez, A., Toledano, D., Sanchez, P., Romero, A., and Valverde, J.L., Impact of nitrogen doping of carbon nanospheres on the nickel-catalyzed hydrogenation of butyronitrile. Journal of Catalysis -New York-, 2010. 269(1): p. 242-251.

140. Shao, Y., Yin, G., Gao, Y., and Sui, J., Nitrogen-doped carbon nanostructures and their composites as catalytic materials for proton exchange membrane fuel cell. Applied Catalysis B: Environmental, 2008. 79(1): p. 89-99.

141. Sidik, R.A., Anderson, A.B., Subramanian, N.P., Kumaraguru, S.P., and Popov, B.N., O~2 Reduction on Graphite and Nitrogen-Doped Graphite: Experiment and Theory. The Journal of Physical Chemistry. B, Condensed matter, materials, surfaces, interfaces & biophysical., 2006. 110(4): p. 1787-1793.

142. Jiang, L. and Gao, L., Modified carbon nanotubes: an effective way to selective attachment of gold nanoparticles. Carbon, 2003. 41(15): p. 2923-2929.

143. Roy, S.C., Harding, A.W., Russell, A.E., and Thomas, K.M., Spectroelectrochemical Study of the Role Played by Carbon Functionality in Fuel Cell Electrodes. Journal of The Electrochemical Society, 1997. 144(7): p. 2323-2328.

144. Kim, S.J., Effect of heavy metals on natural populations of bacteria from surface micro-layers and subsurface water. Marine Ecology Progress Series, 1985. 26: p. 203-206.

145. Rai, M., Yadav, A., and Gade, A., Silver nanoparticles as a new generation of antimicrobials. Biotechnology Advances, 2009. 27(1): p. 76-83.

146. Kim, J.S., Kuk, E., Yu, K.N., Kim, J.H., Park, S.J., Lee, H.J., Kim, S.H., Park, Y.K., Park, Y.H., Hwang, C.Y., Kim, Y.K., Lee, Y.S., Jeong, D.H., and Cho, M.H., Antimicrobial effects of silver nanoparticles. Nanomedicine: Nanotechnology, Biology, and Medicine, 2007. 3(1): p. 95-101.

147. Liau, S.Y., Read, D.C., Pugh, W.J., Furr, J.R., and Russell, A.D., Interaction of silver nitrate with readily identifiable groups: relationship to the antibacterial action of silver ions. Letters in Applied Microbiology, 1997. 25(4): p. 279-283.
148. Klasen, H.J., A historical review of the use of silver in the treatment of burns. II. Renewed interest for silver. Burns : journal of the International Society for Burn Injuries, 2000. 26(2): p. 131-138.
149. Du Plessis, D.M. Fabrication and characterization of anti-microbial and biofouling resistant nanofibers with silver nanoparticles and immobilized enzymes for application in water filtration. 2011; Available from: http://hdl.handle.net/10019.1/40237.

CHAPTER 3

EXPERIMENTAL

3.1 Chemicals and materials

The reagents used in this research were purchased from Sigma-Aldrich (Johannesburg, South Africa) except for the polyethersulphone (PES), which was acquired from Solvay Advanced Polymers (South Africa). All chemicals were used without further purification except sterilisation for the microbiological tests.

3.2 Preparation of Fe-Co/$CaCO_3$ catalyst

A 10 wt% Fe-Co/$CaCO_3$ catalyst with 5 wt% Fe and 5 wt% Co was prepared using the wet impregnation method [1, 2]. Iron nitrate Fe $(NO_3)_3$•9H2O and Cobalt nitrate Co $(NO_3)_2$•$6H_2O$ were used as the sources of Fe and Co for preparation of the catalyst. $CaCO_3$ was used as a support. Calculated amounts of Fe and Co nitrate were added into distilled water and stirred until they were completely dissolved. The solution was then added dropwise to 30 g $CaCO_3$ while stirring, until a homogeneous slurry was obtained. The slurry was left to stir for a further 30 min at room temperature and left to dry in air for 30 min before it was inserted into an oven at 120 °C for 12 h. The product was then removed from the oven and allowed to cool at room temperature it was then ground and screened through a 150 µm sieve and calcined at 400 °C for 16 h in a static oven to remove any excess nitrates. The resulting powder shall herein in after be referred to as the catalyst.

3.3 Synthesis of N-CNTs

The multiwalled N-CNTs were synthesised in a single stage furnace in which a quartz tube about 150 cm in length was inserted horizontally into the furnace with the inlet of the tube connected to a bubbler (see Fig 3.1). The heating rate of the chamber was controlled by a temperature controller, which was connected to a thermocouple placed at the centre of the furnace. The tube reactor inlet-bubbler setup was connected to the gas sources (nitrogen and acetylene) via a mass flow controller and the outlet was attached to an exhaust pipe.

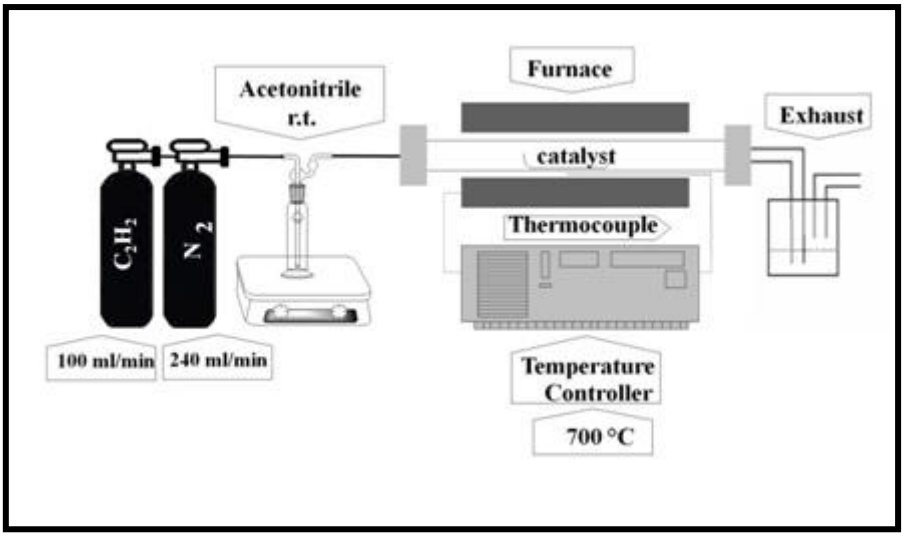

Fig 3.1: Schematic diagram of CVD experimental setup.

N-CNTs were synthesised by a modified chemical vapour deposition (CVD) method [3, 4]. Typically, a 10 wt% Fe-Co/$CaCO_3$ catalyst was uniformly spread in a quartz boat and placed in the central position in a quartz tube, which was inserted in a furnace. First, a nitrogen gas (N_2) flow was introduced through the quartz tube at a flow rate of 50 ml/min while the furnace was heated up to the desired synthesis temperature (700 °C) wherein acetylene gas was passed over the catalyst (by bubbling through acetonitrile) together with N_2 (flow rate 240 ml/min) for 1 h. The furnace was then cooled to room temperature by passing N_2 gas through the reactor. The boat was removed from the reactor and weighed to establish the amount of N-CNTs formed. This method was chosen because it is environmentally friendly and the catalyst used to synthesise the N-CNTs could easily be removed from the final product dissolving in dilute acids e.g. 35% HNO_3 [2, 4, 5].

3.4 Functionalization of N-CNTs

The N-CNTs were functionalized by adding them to a solution of 35% HNO_3, and stirred under reflux for 4 h at 110 °C. The solution was then filtered and the filtered N-CNTs were further washed with distilled water until the pH of the washings was neutral. They were then dried in an oven at 120 °C for 12 h. The degree of functionalisation was studied through zeta potential measurements. This was important in this study since the degree of functionalisation relates to the hydrophilicity of the N-CNTs which could subsequently have an impact on the hydrophilicity of the nanostructured membranes.

3.5 Membrane composition

N-CNT/PES blend membranes were prepared by the immersion precipitation phase inversion method. The schematic diagram for the preparation of membranes is shown in Fig. 3.2. N-CNT/N-methylpyrrolidone (NMP) having various fractions of N-CNT to NMP was mixed with PES to form the membrane casting solutions. In all solutions, the content of PES remained constant at 15 wt% whereas the proportions of N-CNTs were 0, 0.02, 0.04, 0.08 and 0.5 wt%. (See Table 3.1).

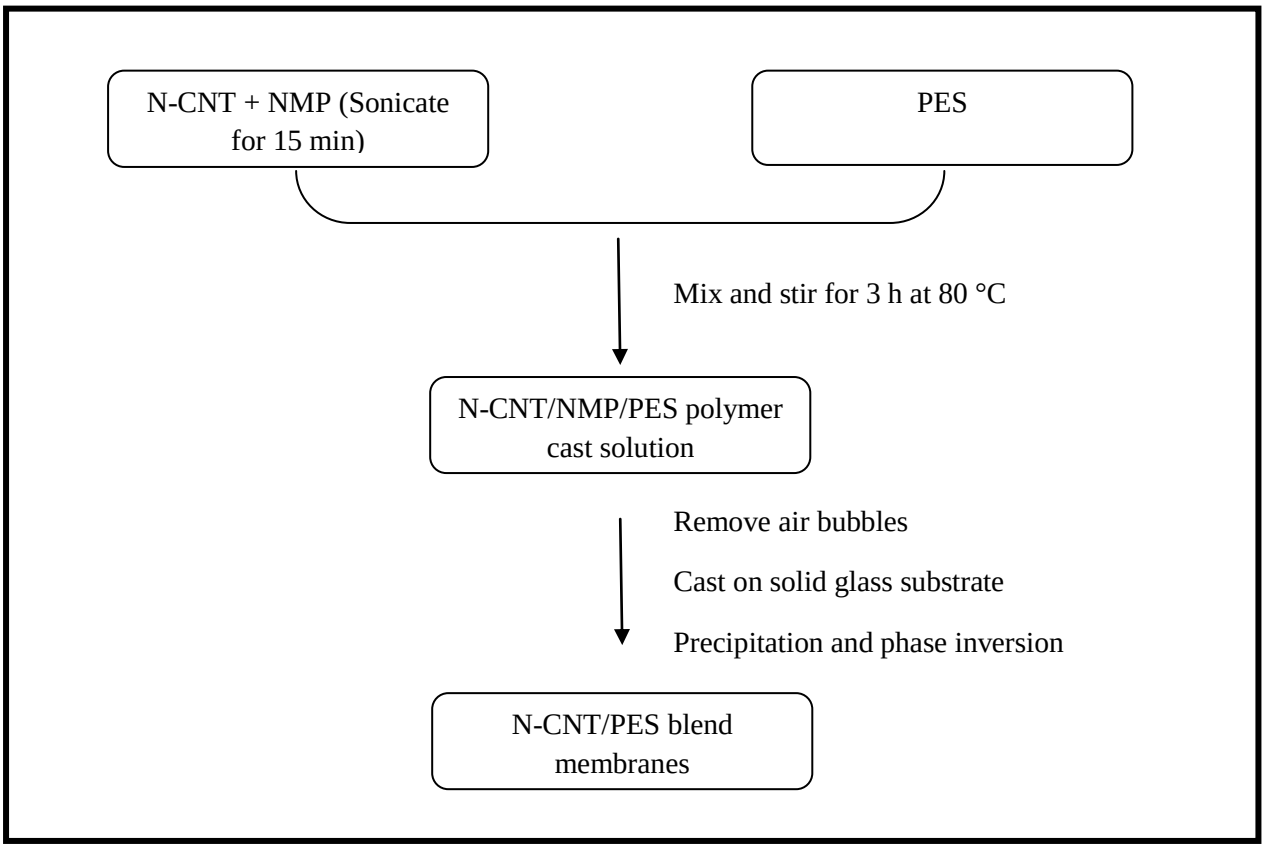

Fig 3.2: Schematic diagram for preparation of N-CNT/PES membranes

Table 3.1: Composition of casting solutions

Prepared identification	Composition of PES (wt. %)	Composition of NMP (wt. %)	Proportions of N-CNTs (wt. %)
1	15	85	0
2	15	85	0.02
3	15	85	0.04
4	15	85	0.08
5	15	85	0.5

PES was supplied by Solvay Advanced Polymer (South Africa). 1-Methyl-2-pyrrolidone (NMP) was used as a solvent of choice due to its good interaction with polymers and miscibility in water [6]. Water was used as the non-solvent. The N-CNT/PES blend membranes were prepared by first dispersing the N-CNTs in NMP to form a homogenous mixture. After dispersing the functionalised N-CNTs in solvent, PES was dissolved in the N-CNT/NMP solution by continuous stirring and heating at 80 °C for 3 h. The resultant solution was then left overnight to allow the product to settle and remove air-bubbles.

3.6 Synthesis of Ag/N-CNTs

A measured amount of functionalised N-CNTs was added to 150 ml of ethylene glycol. The mixture was sonicated for 15 min followed by stirring for 30 min at room temperature. The silver metal solution ($AgNO_3$) was then added dropwise to the mixture, which was stirred for a further 3 h at room temperature. The solution was then refluxed for 3 h at 180°C and filtered thereafter. The filtrates were washed with 20 ml of acetone and distilled water. The acquired product was then oven dried at 80°C for 12 h.

3.6.1 Anti-bacterial study of Ag/N-CNTs

The bactericidal activity of the Ag/N-CNTs was tested against a pathogenic strain of *Escherichia coli*. A single colony of *Enterohaemorrhagic E. coli* (EHEC) inoculums was cultured in 5 ml of nutrient broth and grown overnight at 37 °C while shaking at 200 rpm. Appropriate culture suspensions were diluted to get a standard concentration of approximately 1 x 10^5 cells/ml. The Ag/N-CNTs were then tested by placing 0.003 g in 10 ml

of culture (for 1, 3 and 24 h) and by spotting for any changes on HiChrome plates with a standard concentration of cells. All samples and apparatus were sterilised before conducting any tests.

3.7 Synthesis of Ag/N-CNT/PES membranes

The N-CNT/PES blend membranes were synthesised using the phase inversion method. 1-Methyl-2-pyrrolidone (NMP) was used as a solvent of choice and water was as the non-solvent (coagulant). The Ag/N-CNT/PES blend membranes were prepared by first dispersing the Ag/N-CNTs in NMP to form a homogenous mixture. After dispersing the functionalised Ag/N-CNTs in solvent, PES was dissolved in the Ag/N-CNT/NMP solution by continuous stirring and heating at 80 °C for 3 h. The resultant solution was then left overnight to allow the product to settle and remove air-bubbles.

The polymer solution was cast on a glass plate using a 200 µm thick casting knife. The glass plate, coated with a wet polymer solution was left to air-dry for 40 s. This was followed by dipping the glass plate into a water bath (deionised water). The formed membranes were subsequently stored in deionised water until use.

3.7.1 Bacterial filtration test for Ag/N-CNT/PES

(i) Plate counts

The antibacterial experiments for PES blend membranes were also carried out using the gram negative EHEC. The bacterial cultures were grown overnight in 5 ml nutrient broth. 25 ml of nutrient broth was then inoculated and grown to an optical density of 600 (OD_{600}). The bacteria were harvested by centrifugation at 6468 rpm for 20 min and the pellet was washed once with 0.01M phosphate buffer saline (PBS, pH 7.2) and once with water. The pellet was resuspended to give a final concentration of 1 x 10^7 cells/ml in a total volume of 55 ml of water. 1 ml of spiked water was used to make 10^0 – 10^{-6} dilutions. From the 1 ml, 100 µl of each dilution was then plated on HiChrome selective agar in triplicate. Subsequently, 10^0 – 10^{-6} dilutions of filtered samples were made, from each, 100 µl was placed on HiChrome selective agar in triplicate. All plates were then incubated at 37 °C for 24 h.

(ii) Filtration test

The same procedure as above (section 3.7.1(i)) was performed for preparation of the bacterial samples. However, in this case 50 ml of the spiked water was immediately transferred to a sterile bottle. The contents of the bottle were then filtered through the Ag/N-CNT/PES membranes. After the filtration, the membrane was aseptically removed from the vacuum filtration setup and placed on a HiChrome selective agar. The plate was incubated at 37 °C for 24 h. All samples and apparatus were sterilised before conducting any tests.

3.8 Characterisation

3.8.1 Transmission Electron Microscopy (TEM)

The two dimensional morphology and microstructure of the catalyst, as grown and functionalised N-CNTs were studied using the FEI Tecnai Spirit G2 transmission electron microscope operating at 120 kV. Samples were prepared by ultrasonic suspension of the materials in methanol. The suspensions were then dropped onto a carbon coated copper grid and were allowed to dry at room temperature before analysis.

3.8.2 Scanning Electron Microscopy (SEM)

The topographical information of N-CNTs and surface morphology of the PES and N-CNT/PES membranes were characterised using the Nova nanoSEM 200. Samples were prepared by mounting them on aluminium studs with carbon tape. Prior to analysis, samples were coated with gold to make them conductive.

3.8.3 Zeta-Potential

The degree of functionalisation was studied through zeta potential measurements. A Malvern Zetasizer nano-series instrument was used to quantify the zeta potentials of the as-grown and functionalized N-CNTs. The N-CNTs were dispersed in 100 ml of deionised water and the pH of the suspension was adjusted from 2.0 to 12.0 by adding 0.1 M HCl or 0.1 M NaOH. By measuring the zeta potential as a function of pH, the isoelectric point was determined.

3.8.4 Fourier Transform Infrared Spectroscopy

The presence of acid functional groups on the N-CNT surfaces and the chemical bonding of N-CNTs with the PES matrix were established by the Bruker TENSOR 27 FTIR spectrometer.

3.8.5 X-ray diffraction (XRD)

The phase composition of $CaCO_3$ (catalyst support) and the catalyst were obtained by means of XRD. The diffraction patterns were obtained from the Bruker D2 phaser.

3.8.6 Brunauer-Emmett-Teller (BET)

The BET technique is typically used to determine the total surface area, pore volume and pore size of solid samples. Prior to analysis, approximately 250 mg of each sample was degassed in N_2 at 150 °C for 4 h using a Micrometrics Flow Prep 060 degas system. The surface areas and the pore properties were then acquired by the BET method [2, 8] using the Micrometrics TRISTAR 3000 analyser.

3.8.7 Thermogravimetric analysis (TGA)

TGA is an important tool for determining the thermal stability and purity of materials by monitoring the mass change of a sample as a function of temperature. In a standard run, 10 mg of sample was placed in a ceramic pan and placed in the furnace of the Perkin Elmer STA 4000 analyzer. The samples were heated at 10 °C/min under an air or N_2 atmosphere (20 ml/min) from 30-900 °C. Data was retrieved from a PC connected to the instrument.

3.8.8 Atomic force microscopy (AFM)

An AFM is a very effective microscope for imaging materials at the nanoscale. Moreover, it enables visualisation of species in three dimensions. The membrane surface morphologies were measured by AFM with tapping mode in air using a Dimension 3100 Veeco AFM.

3.8.9 Contact angle

The wettability and surface hydrophilicity of the nascent PES, N-CNT/PES and Ag/N-CNT/PES membranes were evaluated by the DATA Physics optical contact angle using the sessile drop measurement method. A 2 µl drop of deionised (DI) water was placed on a flat membrane surface using a Gilmont syringe. Using the SCA20 version 4.1.12 build 1019 software, the advancing angle (θ) was measured as the water droplet was placed on the surface. In general, the larger the angle, the lower the hydrophilicity and the smaller the angle the higher the hydrophilicity (Fig 3.3). According to Violleau *et al* [9] contact angle measurements do not give absolute values, but rather allow the comparison between each sample.

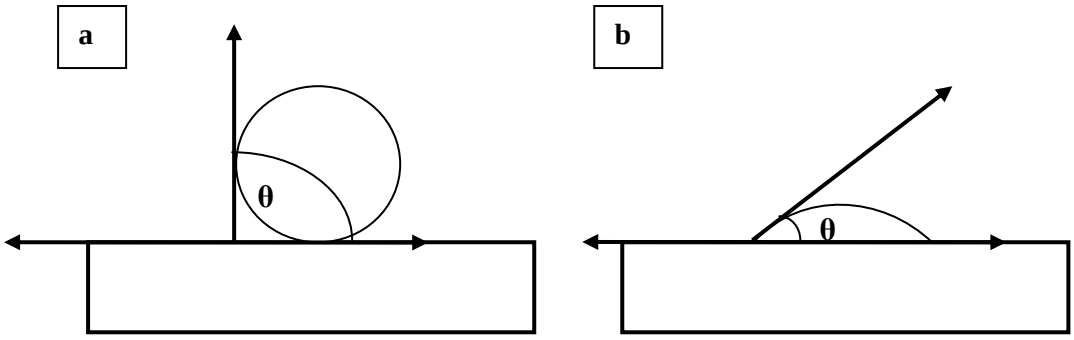

Fig. 3.3: Schematic representation of contact angle measurements (a) large contact angle (b) small contact angle [10].

3.8.10 Cross-flow system

The performances of the N-CNT/PES blend membranes were studied by measuring the pure water flux and rejections of 500 ppm polyethylene glycol (PEG) (10 000). Experiments were done using the cross-flow filtration system (Fig. 3.3) (Sterlitech, USA) with a membrane area of 14.6 cm^2 at room temperature. The membranes were preconditioned by compacting with deionised water at an applied pressure until steady fluxes were obtained. Water flux (J_w) was measured according to Eq. 1.

$$Jw = \frac{V}{A \times \Delta T} \tag{1}$$

where V is the volume of the permeation water. A is the area of the membrane, and ΔT is the time taken to acquire each measurement. The rejection was calculated using Eq. 2

$$R\% = 1 - \frac{Cp}{Cf} \tag{2}$$

where C_p is the permeate concentration, and C_f the feed concentration.



Fig. 3.4: Cross-flow filtration system used in this work.

3.9 References

1. Mhlanga, S.D. and Coville, N.J. 2008. Iron–cobalt catalysts synthesized by a reverse micelle impregnation method for controlled growth of carbon nanotubes. Diamond and Related Materials, 17, 1489-1493.
2. Motchelaho, M.A.M., Xiong, H., Moyo, M., Jewell, L.L., and Coville, N.J. 2011. Effect of acid treatment on the surface of multiwalled carbon nanotubes prepared from Fe–Co supported on $CaCO_3$: Correlation with fischer–tropsch catalyst activity. Journal of Molecular Catalysis A: Chemical, 335, 189-198.
3. Nxumalo, E.N. and Coville, N.J. 2010. Nitrogen doped carbon nanotubes from organometallic compounds: A review. Materials Materials, 3, 2141-2171.
4. Mhlanga, S.D., Mondal, K.C., Carter, R., Witcomb, M.J., and Coville, N.J. 2009. The effect of synthesis parameters on the catalytic synthesis of multiwalled carbon nanotubes using Fe-Co/$CaCO_3$ catalysts. South African Journal of Chemistry, 62, 67-76.
5. Tetana, Z.N., Mhlanga, S.D., Bepete, G., Coville, N.J., and Krause, R.W.M. 2012. The synthesis of nitrogen-doped multiwalled carbon nanotubes using an Fe-Co/$CaCO_3$ catalyst. South African Journal of Chemistry, 65, 39-49.
6. Ahmad, A.L., Sarif, M., and Ismail, S. 2005. Development of an integrally skinned ultrafiltration membrane for wastewater treatment: Effect of different formulations of psf/nmp/pvp on flux and rejection. Desalination., 179, 257.
7. Malgas, G.F., Arendse, C.J., Cele, N.P., and Cummings, F.R. 2008. Effect of mixture ratios and nitrogen carrier gas flow rates on the morphology of carbon nanotube structures grown by CVD. Journal of Materials Science, 43, 1020-1025.
8. Idakiev, V., Yuan, Z.Y., Tabakova, T., and Su, B.L. 2005. Titanium oxide nanotubes as supports of nano-sized gold catalysts for low temperature water-gas shift reaction. Applied Catalysis A, 281, 149-155.
9. Violleau, D., Essis-Tome, H., Habarou, H., Crou, J.P., and Ponti, M. 2005. Fouling studies of a polyamide nanofiltration membrane by selected natural organic matter: An analytical approach. Desalination, 173, 223-238.
10. Nascimento, R.M.D., Martinelli, A.E., and Buschinelli, A.J.A. 2003. Review article: Recent advances in metal-ceramic brazing. Cerâmica, 49, 178-198.

CHAPTER 4

RESULTS AND DISCUSSION

4.1 Introduction

This chapter presents the results obtained in this research work. It includes the characterisation of N-CNTs and N-CNT/PES blend membranes using the methods and techniques discussed in chapter 3. The performance tests of these membranes using ultrapure water for permeation studies, PEG as a model pollutant for rejection studies and humic acids as foulants for fouling studies are discussed in detail. In addition, results relating to the antibacterial activity of the Ag/N-CNT/PES blend membranes are presented.

4.2 Catalyst characterisation

Figure 4.1 presents a low magnification TEM image of freshly prepared 10 wt.% Fe/Co/$CaCO_3$ catalyst. The image demonstrates catalyst fragments that are mainly composed of $CaCO_3$ (support) in which the Fe-Co particles are embedded. The BET surface areas of the commercial $CaCO_3$ and the Fe/Co/$CaCO_3$ catalyst were 9.3 and 8.9 m^2/g, respectively. This suggests that the metal particles had no influence on the $CaCO_3$ structure.

Analysis of the XRD patterns for the commercial $CaCO_3$ and the Fe/Co/$CaCO_3$ further confirmed the presence of the $CaCO_3$. However, no metal particles were observed on the XRD pattern (Fig. 4.2). This is due to the low detection limit of the instrument with regards to the small amount of metals dispersed in the $CaCO_3$ matrix. Therefore, the energy dispersive X-ray spectroscopy (EDS) was used to verify the presence of the metal particles. The EDS spectrum showed that both Fe and Co were present on the $CaCO_3$ support (Fig. 4.3).

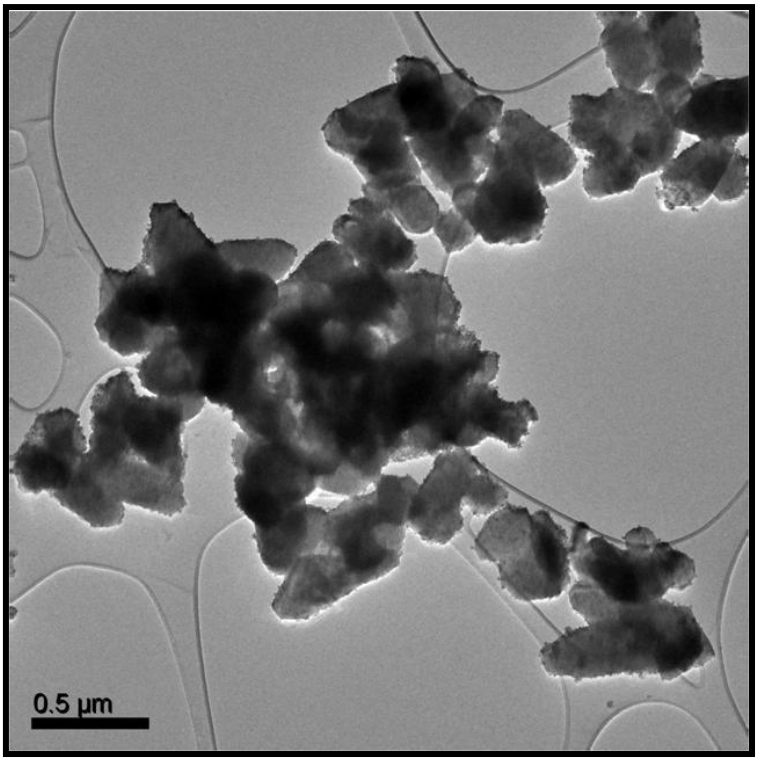

Fig. 4.1: A TEM image of as-synthesised Fe/Co/$CaCO_3$.

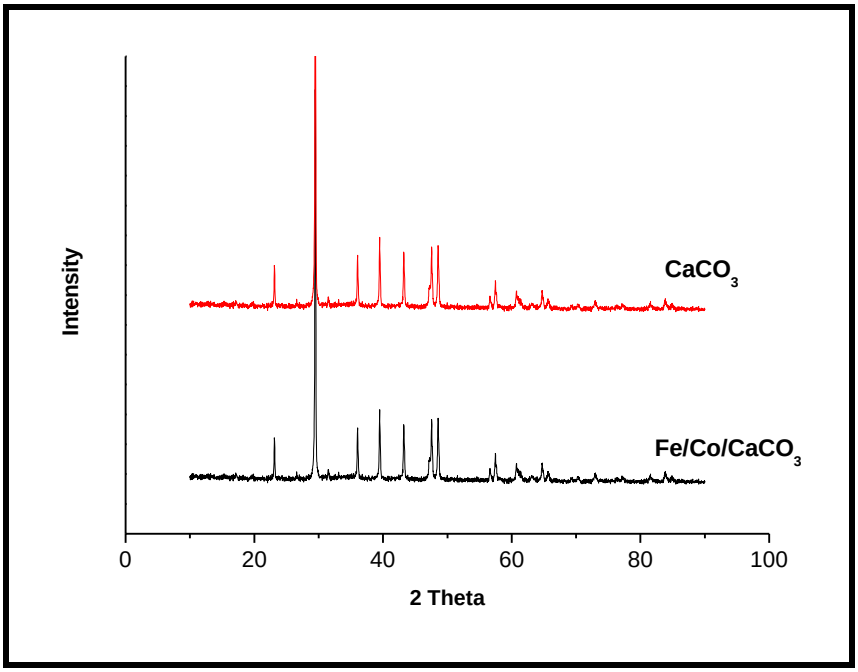

Fig. 4.2: XRD patterns of $CaCO_3$ and Fe/Co/$CaCO_3$ catalyst.

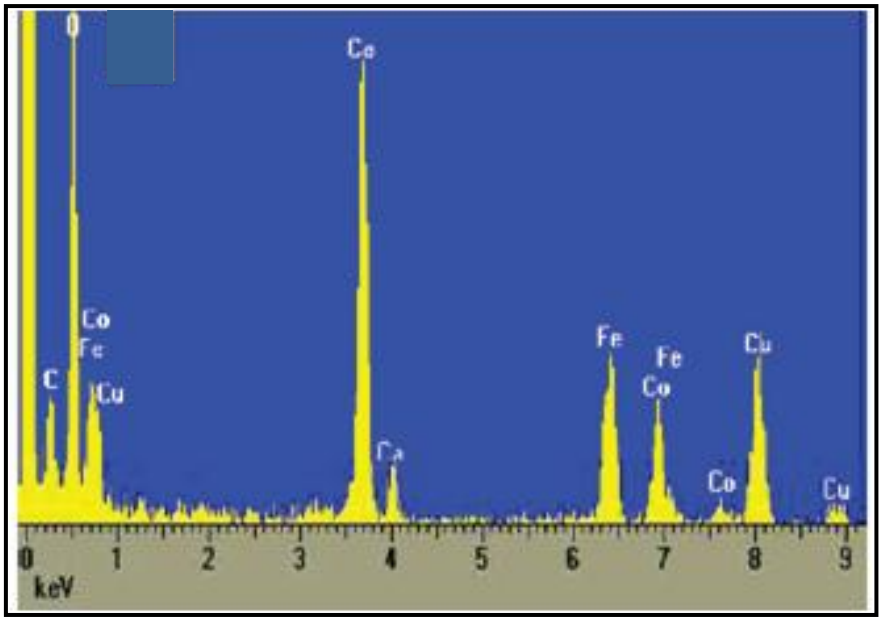

Fig. 4.3: EDS spectrum showing the presence of Fe and Co nanoparticles on the $CaCO_3$ support.

4.3 N-CNT characterisation

4.3.1 TEM analysis

Figure 4.4a shows a TEM image of the purified and functionalised N-CNTs (*f*N-CNTs). The TEM image reveals the formation of tubular structures with bamboo-like compartments. This structure is observed when N is doped into the CNT structure [1]. The N-CNTs were found to have outer diameters ranging between 30 – 45 nm (Fig. 4.4c). After acid treatment of the N-CNTs the average diameters decreased slightly as shown by the distribution graph in Fig. 4.4c. According to Motchelaho *et al* [2] the reduction in diameter is due to the interaction of the acid with the outer most graphene layers of the N-CNTs.

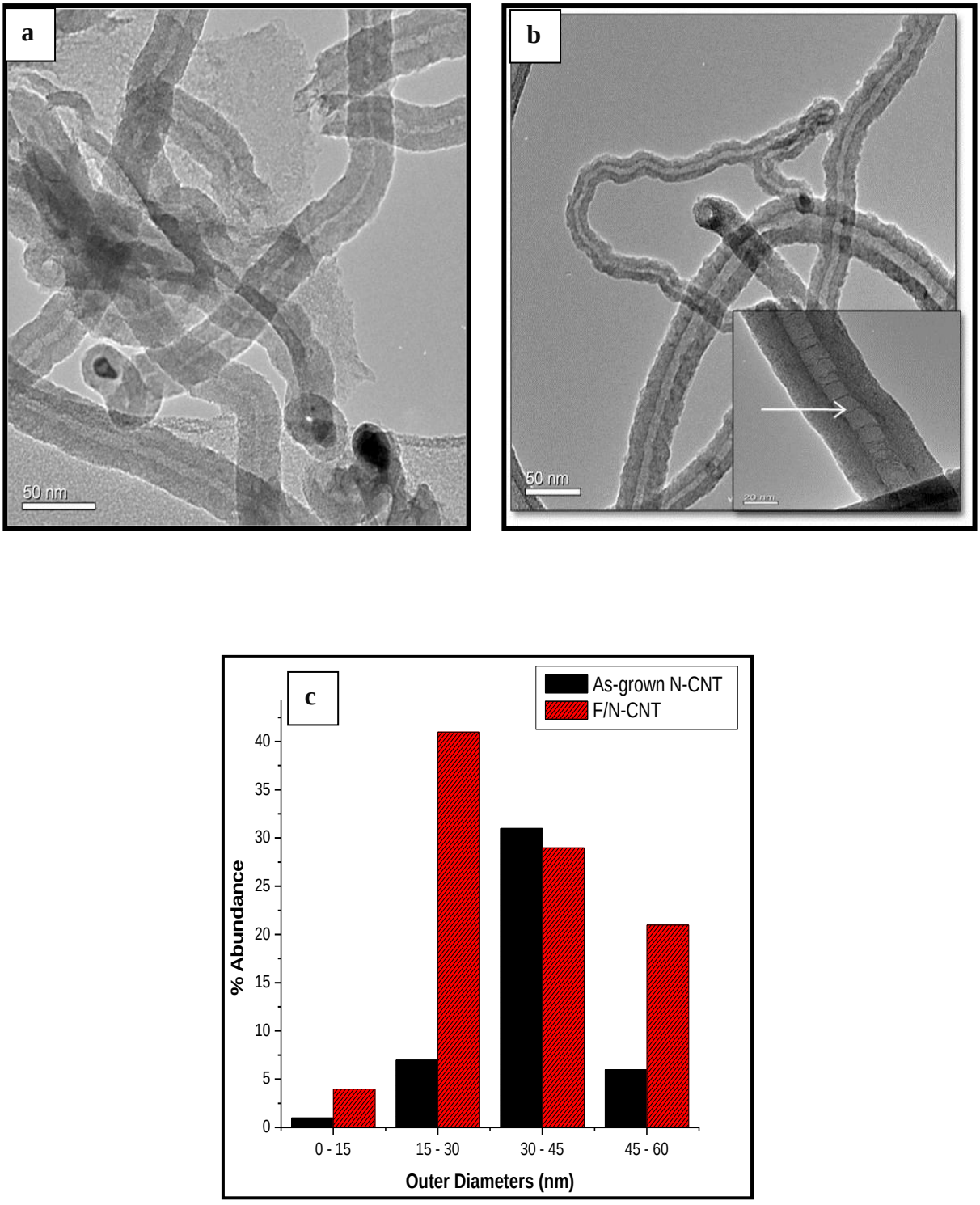

Fig. 4.4: TEM images of (a) as-grown N-CNTs; (b) *f*N-CNTs showing bamboo compartments (pointed by arrow insert); and (c) size distribution of N-CNTs before and after functionalisation.

4.3.2 CN analysis of N-CNTs

To quantify the nitrogen content in the N-CNTs, carbon and nitrogen (C% and N%) analysis was done using a Carlo Erba NA 1500 C/N/S analyser, which uses gas chromatographic (GC) separation of the gases produced on total combustion of the sample. The average percentage of N in the as-grown CNTs was 1 % while the *f*N-CNTs contained 3% N. The N % content of the as-grown N-CNTs was low (1%) due to the presence of calcium oxide (CaO) and the catalyst (Fe and Co nanocatalyst) used to synthesise the N-CNTs. However, after acid treatment, the N % (which is in matrix with the carbon) increased. This can be explained by the removal of CaO and amorphous materials in the system. This observation is in agreement with TEM observations, which showed CNTs with bamboo-like compartments (due to the presence of substitutional N).

The N doping level and the types of N-moieties in the N-CNTs were also confirmed by X-ray photoelectron spectroscopy (XPS). Previous work has shown that the N can be incorporated into the CNT lattice in different bonding configurations; namely, (i) pyridine-like N: where the N atom is sp^2 hybridized, bonds to two C atoms, (ii) pyrrole-like N: where the N is sp^3 hybridized in a five-membered ring, (iii) quaternary/graphitic/substitutional N: where a graphitic carbon atom is substituted by a N atom in the graphitic sheet and (iv) pyridinic oxides: which are attributed to oxidized nitrogen on the graphite layers (Fig. 4.5) [3]

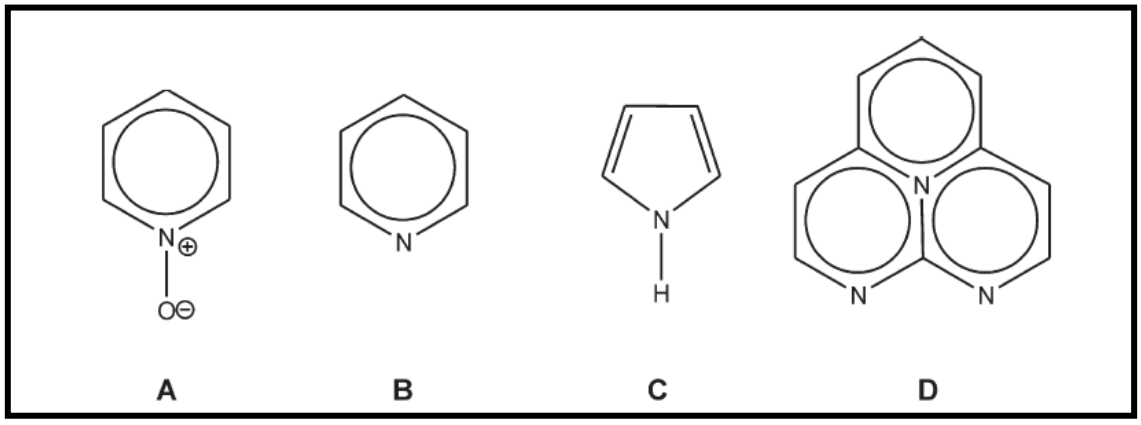

Fig. 4.5. Types of nitrogen moieties that can be incorporated into graphitic carbon: (A) oxidized pyridinic; (B) pyridinic; (C) pyrrolic and (D) quaternary [4].

Figure 4.6a shows a high-resolution N 1s XPS spectrum of the N-CNTs, which shows the presence of nitrogen-based species on the N-CNT structure. The N 1s peak can be deconvoluted into three peaks: pyridinic oxides (NO_x at 405 eV), quaternary nitrogen (N_Q at 401 eV) and pyridinic nitrogen (N_P at 398 eV). The N 1s spectra revealed that N atoms in the outer layer mainly exist as pyridinic oxides while quaternary and pyridinic nitrogen are less abundant. No pyrrolic nitrogen peak was observed on the XPS spectra. However we believe that these N species could be present in the inner walls of the tubes and they could be responsible for the formation of the curvatures (bamboo-like structures) in the inner walls of the N-CNTs (Fig. 4.6b). Indeed, the formation of curvatures e.g. in graphitic carbon spheres occurs as a result of a pentagonal ring in the graphite structure, [5-7] which assumes the same structure observed with pyrrolic nitrogen.

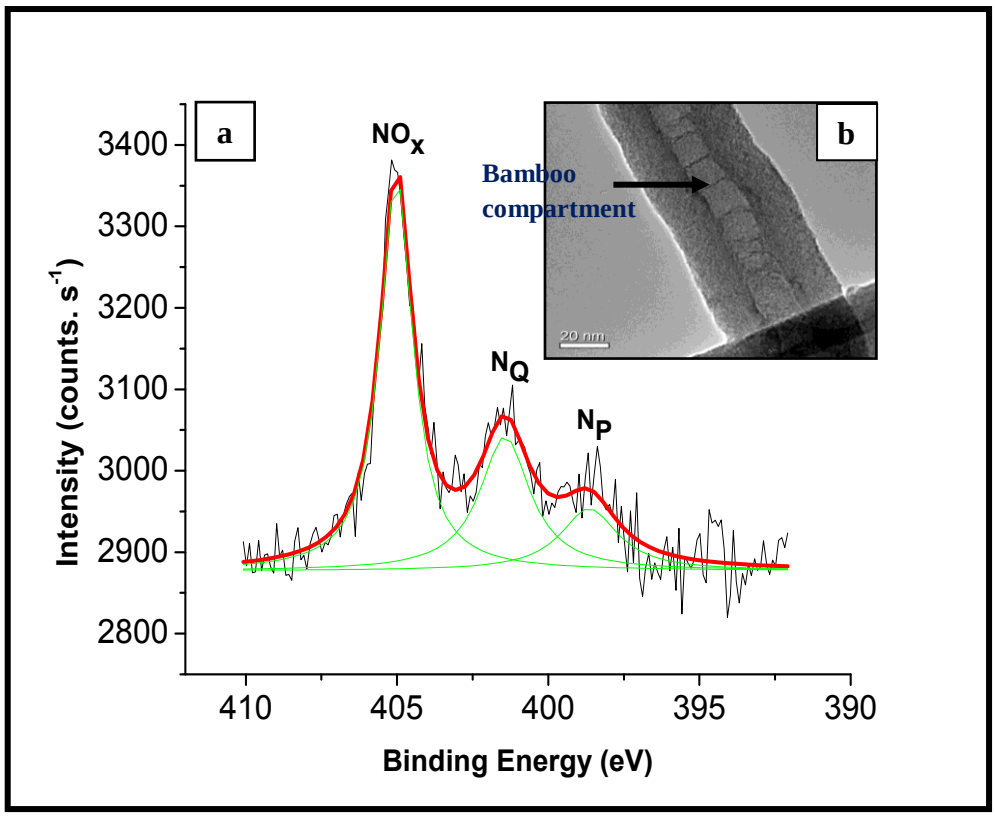

Fig. 4.6. XPS spectrum showing a deconvoluted N 1s spectrum of the functionalized N-CNTs.

4.3.3. TGA and BET surface area analysis

TGA was used to investigate the thermal stability and purity of N-CNTs. Figure 4.7 shows the TGA curves of the as-grown and *f*N-CNTs. The materials were heated in air at 10 °C/min and the profiles show that the materials were stable up to 500 °C. Thereafter a 60 % weight loss was observed when heated to 900 °C. The residual material after the decomposition of the as-grown N-CNTs is due to the Fe-Co/$CaCO_3$ catalyst used during CVD synthesis. The profiles obtained are typical for multi-walled CNTs synthesised using this catalyst [2]. The *f*N-CNTs showed very little residual material (< 3 %). This is because the Fe-Co and CaO present in the as-grown N-CNTs could readily be dissolved in the 35 % HNO_3 solution used to purify and functionalise the N-CNTs.

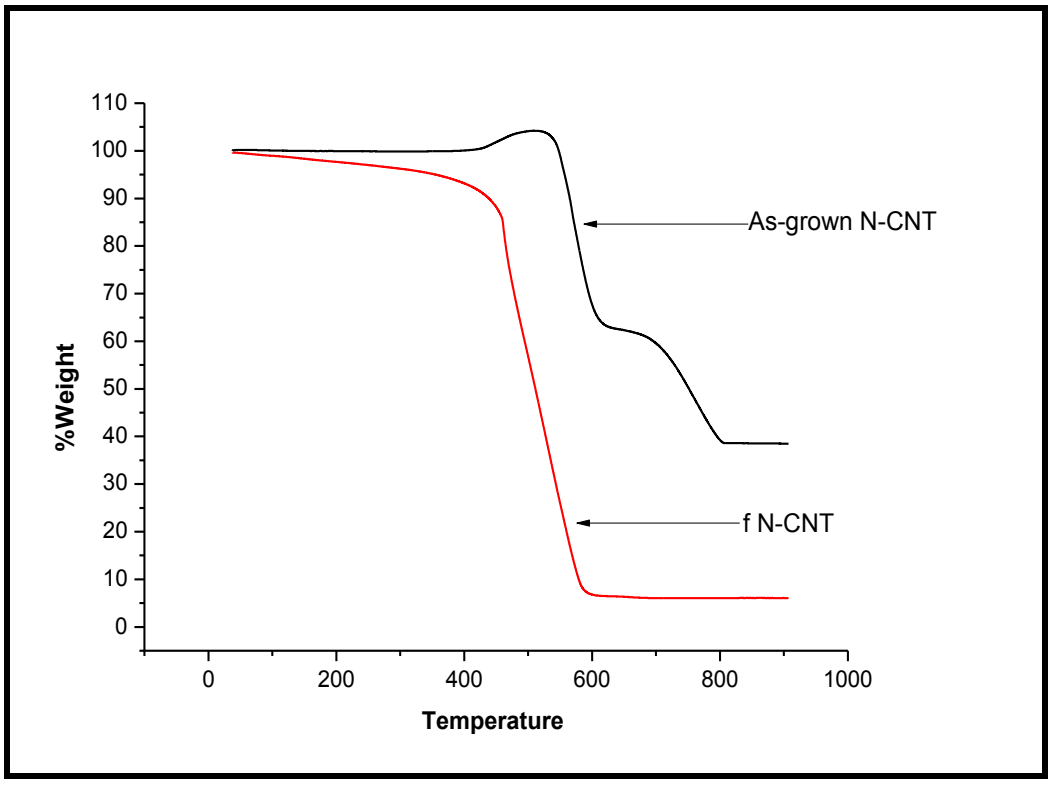

Fig. 4.7: TGA profile of as-grown and *f*N-CNTs.

BET surface areas and pore volumes of the as-grown and *f*N-CNTs are given in Table 4.1. The as-grown N-CNTs have a lower surface area (48.7 m^2/g) and pore volume (0.17 cm^3/g). However, after acid treatment an increase in both surface area (92.2 m^2/g) and pore volume (0.31 cm^3/g) of the as-grown N-CNTs is observed. Again, this is due to the removal of the

low surface area residual Fe-Co/$CaCO_3$ catalyst. A high surface area material is desirable since a small percentage of the *f*N-CNTs is usually added to prepare a nanocomposite matrix. In this case the matrix is the PES membrane matrix.

Table 4.1: BET surface area and pore volume of as-grown and *f*N-CNTs.

Sample	Surface area (m^2/g)	Pore volume (cm^3/g)
As-grown N-CNTs	48.7	0.17
***f* N-CNTs**	92.2	0.31

4.3.4. FTIR spectroscopy and zeta potential measurements

The FTIR spectra for as-grown and *f*N-CNTs are given in Fig. 4.8. The *f*N-CNTs clearly show two peaks of interest corresponding to -CO (1249 cm^{-1}) and $-COO^-$ (1602 cm^{-1}), which are not observed on the spectra of the as-grown N-CNTs. The emergence of these peaks is important because the degree of functionalisation relates to the hydrophilicity of the N-CNTs, which could effectively influence the hydrophilicity and chemical bonding of the membrane composite. Thus, we successfully functionalised the N-CNTs using mild acid treatment by refluxing in 35% HNO_3

To further confirm the presence of the acid groups on the N-CNTs, zeta-potential was measured on samples of well titrated N-CNTs with pHs varying from 2 to 12. These measurements are of interest because they provide information about the hydrophilicity and dispersibilty of carbon nanomaterials in water [2]. Figure 4.9 shows the plots of zeta-potential for the as-grown and *f*N-CNTs with respect to pH. The as-grown N-CNTs have an iso-electric point (point of zero charge) at pH 5. However, after acid treatment, the iso-electric point is not observed. This is due to the introduction of acid/oxygen groups on the surface of the N-CNTs, which causes a shift in the plots to more negative zeta potential values. The results indicate that the point of zero charge is affected by the acid concentration. As such, the higher the concentration of HNO_3, the more surface functional groups, the better the surface (negative) charge and hence the higher the hydrophilicity.

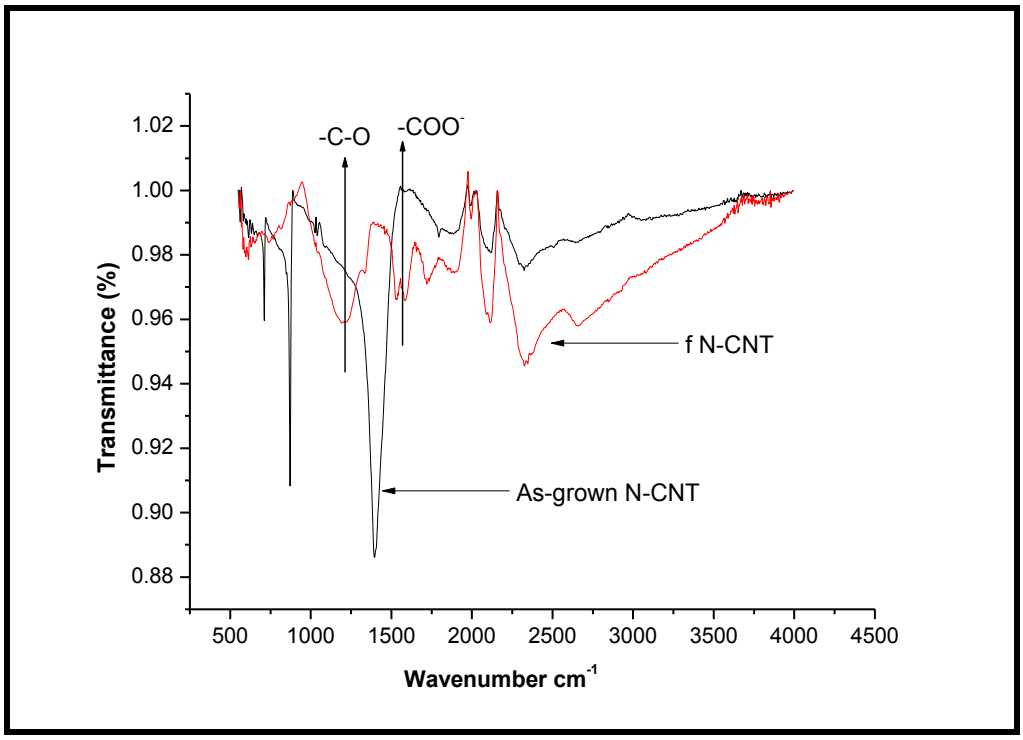

Fig. 4.8: FTIR spectra of as-grown and *f*N-CNTs.

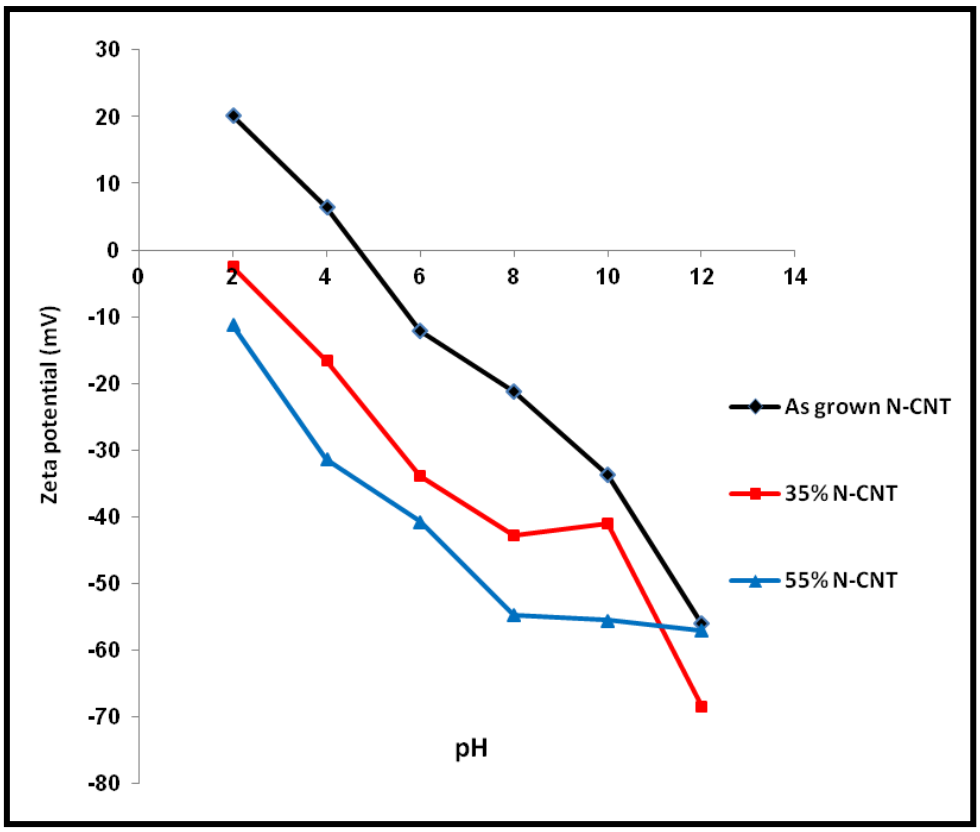

Fig. 4.9: Zeta-potential profile for as-grown and *f*N-CNTs.

4.4 Analysis of N-CNT/PES blend membranes

4.4.1 FTIR spectroscopy analysis

Figure 4.10 shows the FTIR spectra of the pristine PES membrane and the blend membranes with different *f*N-CNT loadings. All spectra show two intense peaks at 1240 cm^{-1} and 1318 cm^{-1} associated with the C-O-C stretch (ether group) and the O=S=O vibrations (sulphonic group), respectively. These are typical peaks of PES [8].

The FTIR bands observed for the *f*N-CNT/PES blend membranes are however slightly different. Three new absorption peaks were identified at 1489 cm^{-1}, 1583 cm^{-1} and 2983 cm^{-1}, representing the skeletal vibrations of the aromatic hydrocarbons, the carboxylate group ($-COO^-$) and the –CH stretch, respectively. This observation confirms the incorporation of *f*N-CNTs in the PES matrix.

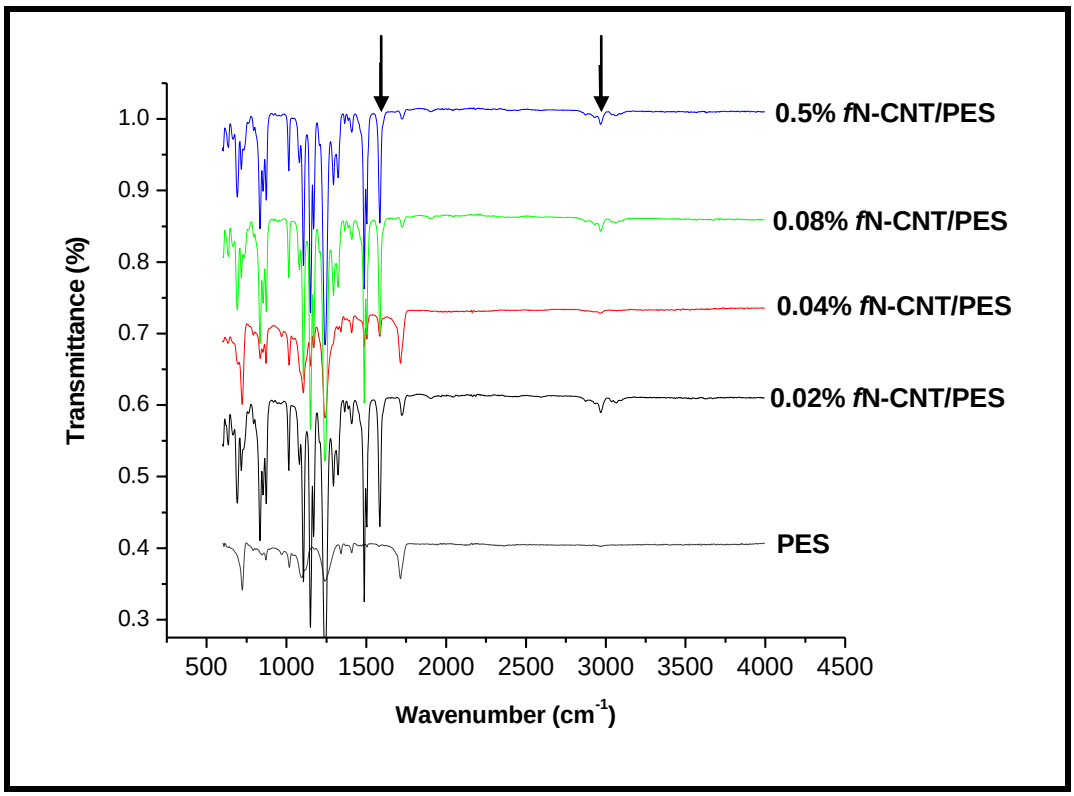

Fig. 4.10: FTIR spectra of the pristine PES and *f*N-CNT blend membranes having different *f*N-CNT loadings.

4.4.2 AFM and SEM analyses

Surface morphology investigations of *f*N-CNTs/PES membrane matrix was carried out using the AFM at a scan-rate of 25 µm. The bright regions represent the highest points on the surface of the membrane, while the darker regions depict the depressions and pores (Fig. 4.11). The surface morphologies of the membranes were influenced by the percentage loading of *f*N-CNTs (Table 4.2). The images show that the surface roughness of the PES membrane is reduced when 0.02, 0.04 and 0.08 wt% *f*N-CNTs was loaded. However, after increasing the *f*N-CNT loading to 0.5 wt%, no further decrease in surface roughness was observed (Table 4.2). Vatanpour *et al* [9] reported that at low CNT loadings, the electrostatic interactions between the CNTs and the membrane matrix is low. Thus, the nanotubes are regularly positioned, giving rise to a smooth surface [9, 10]. However, with high CNT concentrations, agglomeration of the CNTs is observed therefore leading to a slight increase in membrane roughness at 0.5 wt% loadings.

Table 4.2: AFM roughness parameters for different *f*N-CNT loadings in the PES membranes.

Roughness parameter	Pristine PES	0.02% NCNT/PES	0.04% NCNT/PES	0.08% NCNT/PES	0.5% NCNT/PES
$\mathbf{R_q}$	30.13	22.01	20.19	16.00	18.63
$\mathbf{R_a}$	23.85	16.00	15.31	12.69	14.90

R_q: root mean square roughness; R_a: average roughness.

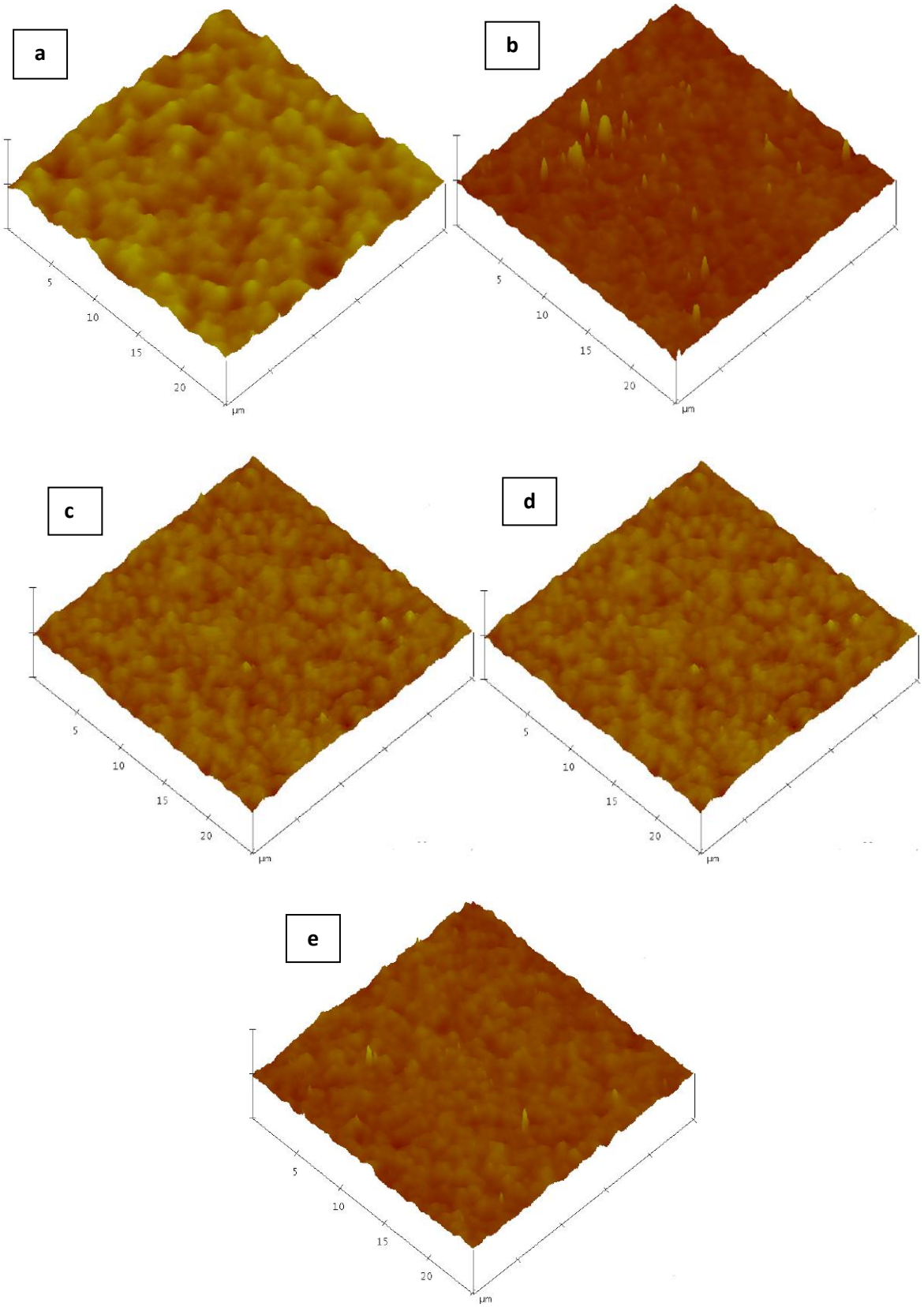

Fig. 4.11: AFM images of (a) pristine PES membrane and blend membranes with different *f*N-CNT loadings: (b) 0.02%, (c) 0.04%, (d) 0.08%, and (e) 0.5%.

The membrane surface morphologies were further studied using SEM at 5 000x magnification. It can be seen that blend membranes have a dense and smooth surface structure (Fig 4.12(a)). This is due to the instantaneous liquid-liquid demixing between the DI water in the coagulation bath and the NMP in the membrane matrix during the phase inversion process.

The cross-section images (Fig 4.12(b)) were also observed using SEM at 5000x magnification. All membranes exhibit the asymmetric structure which is defined by a dense top layer and a highly porous sub-layer. There were no distinct difference observed in the structure between the pristine PES and the N-CNT/PES blend membranes. However, the average widths of pores immediately beneath the surface structure were slightly different.

To quantify the sizes of the pore widths below the membrane surface, the Image J software was used. The widths were found to be 1.95, 1.63, 1.46 and 1.29 μm for PES, 0.02% N-CNT/PES, 0.04% N-CNT/PES and 0.08% N-CNT/PES, respectively. Compared with the pristine PES, the blend membranes had smaller pore widths below the skin layer. This may be attributed to the presence of the N-CNTs in the membrane matrix, mainly occupying the membrane pores. The sizes of the pore widths suggest that they could be used as microfilters.

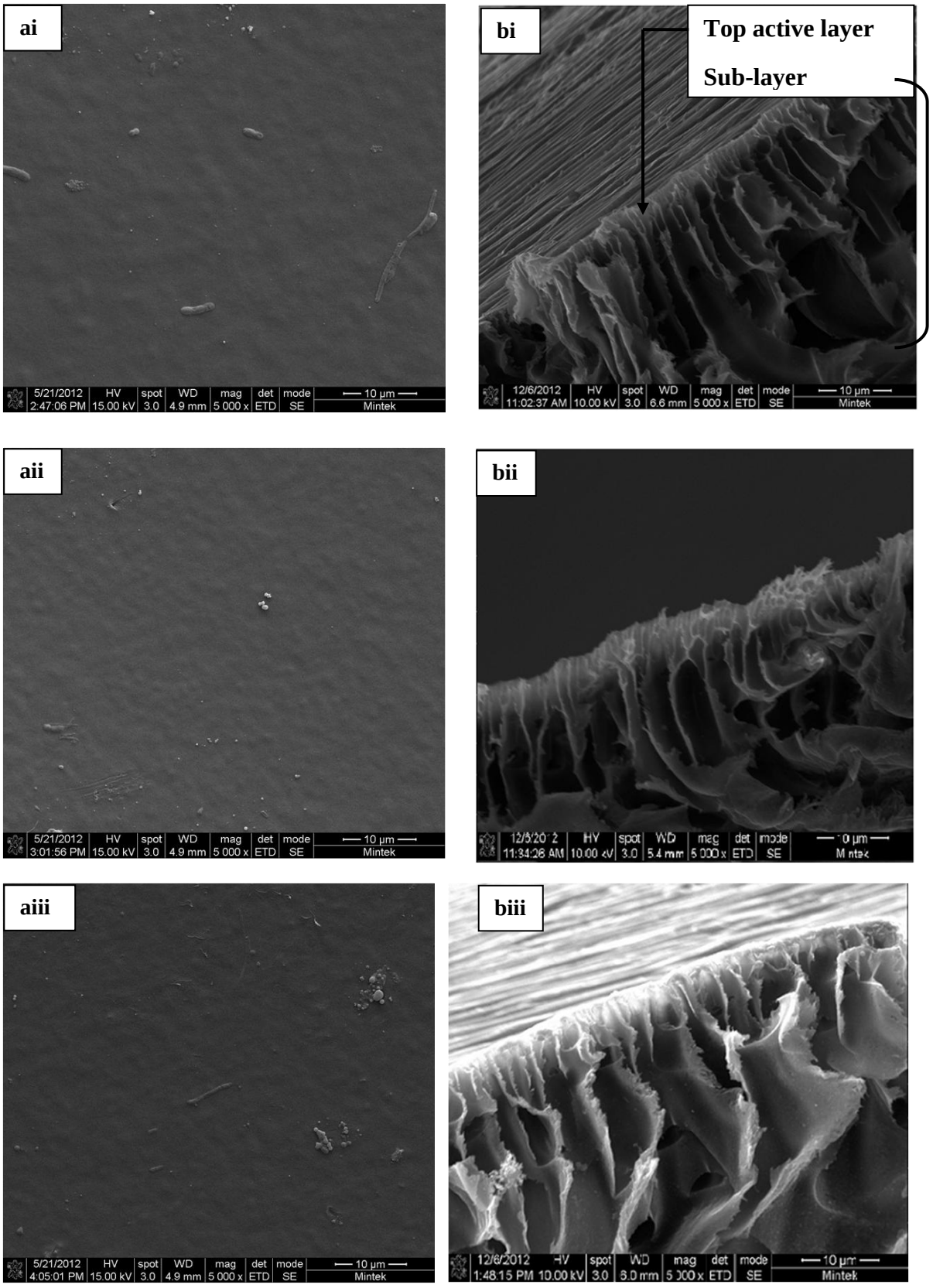

Fig 4.12: SEM images of membrane structure (a) surface structure (b) cross-sectional structure of the pristine PES (ai and bi), 0.04% N-CNT/PES (aii and bii) and 0.5% N-CNT/PES (aiii and biii)

4.4.3 Thermal stability of membranes

Figure 4.13 demonstrates the TGA of pristine PES and N-CNT/PES blend membranes. The membranes generally exhibit a standard decomposition trend which begins above 400 °C. The initial decomposition (400 °C) step can be seen as the loss of the sulphone groups which originates from the PES structure, whereas the second decomposition step (500 °C) may be attributed to the collapse of the polymer chains [11]. The TGA curves of the N-CNT blend membranes also revealed a slight shift from the pristine membrane. This suggests an improved thermal stability. The shift in stability was as a result of the strong hydrogen bond between the functionalised N-CNTs and the PES backbone [12].

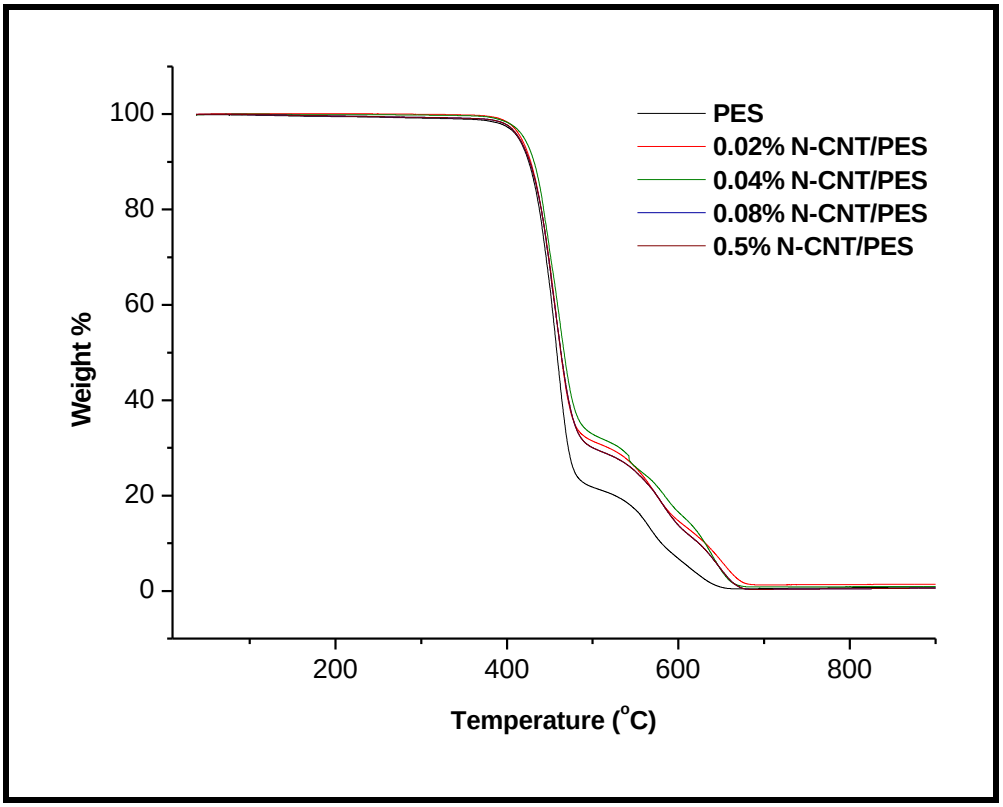

Fig. 4.13: TGA plots for the pristine and N-CNT blend PES membranes.

4.4.4 Mechanical properties of the *f*N-CNT/PES blend membranes

The mean modulus, ultimate tensile strength (UTS), and tensile strain of the blend membranes as a function of N-CNT content are provided in Table 4.3. Increase in modulus and UTS membrane stability was evident at low N-CNT fractions. The increase in N-CNT

loadings from 0 to 0.04 wt% in the PES membrane increased the modulus from 114 to 138 MPa and the UTS from 3.8 to 4.5 MPa. Also, an increase in tensile stress at tensile strength from 3.7 to 4.4 MPa was observed. These improvements are attributed to the strong interaction (hydrogen bonding) between the PES matrix and the N-CNTs at low N-CNT fractions. A decrease in modulus, tensile strength and tensile strain was observed at N-CNT loadings above 0.04 wt%. This is consistent with increase in rigidity of the membrane structure, thus, leading to a decrease in mechanical stability.

Table 4.3: Mechanical properties of *f*N-CNT/PES blend membranes.

Sample Name	Modulus (MPa)	Tensile stress at strength (MPa)	UTS (MPa)	Elongation at break (%)
PES	114	3.7	3.8	22
0.02 N-CNT/PES	138	4.0	4.1	14.5
0.04 N-CNT/PES	135	4.4	4.5	18.2
0.08 N-CNT/PES	100	2.6	2.7	7.8
0.5 N-CNT/PES	123	3.2	3.2	6.6

4.4.5 Membrane performance: flux, contact angle and rejection studies

To investigate the influence of the N-CNTs on the membrane performance, the contact angle and cross-flow system were used. A plot of pure water flux vs. pressure is given in Fig. 4.14. The highest flux was obtained at a N-CNT loading of 0.04 wt% and pressure of 120 psi, beyond which, further loading of N-CNTs led to a decrease in flux. Furthermore, the fluxes for 0.02 and 0.04 wt% N-CNT membranes were higher than that of the pristine PES despite the low loadings.

According to Wu *et al* [13] two factors influence the permeation properties of the CNT blend membranes: (1) hydrophilicity and (2) pore effect. The pure water flux of the pristine PES membrane at 120 psi was 260 L/m^{2}h. The addition of 0.02 and 0.04 wt% N-CNTs to PES enhanced the flux from 260 to 375 and 450 L/m^{2}h, respectively. This enhancement is due to

the hydrophilic N-CNTs at lower loadings (0.02 and 0.04 wt%). Figure 4.14 shows the contact angle of the N-CNT/PES blend membranes. The contact angle of the PES membranes decreased with an addition of 0.02 wt% N-CNT, suggesting that the *f*N-CNTs make the PES membrane surface more hydrophilic and thus has a high water flux. This is typically because the hydrophilicity increases the number of pores on the membrane surface, therefore increasing the flux. It is also important to note, even though 0.02 wt% N-CNT/PES had the highest hydrophilicity than 0.04 wt% N-CNT/PES, the contact angle value of 0.02 wt% N-CNT/PES was not statistically different from that of 0.04 wt% N-CNT/PES membrane. As such, the highest water flux was observed for the PES membrane with 0.04 wt% N-CNT loading. Conversely, when larger amounts of *f*N-CNTs were added to the PES membranes, high contact angles and low water fluxes were observed. This can be explained by the large van der Waals forces experienced between the *f*N-CNTs and the *f*N-CNT-membrane matrix when the density of the *f*N-CNTs is high in the membrane structure. The high density causes an increase in viscosity of the casting solution [12, 14],

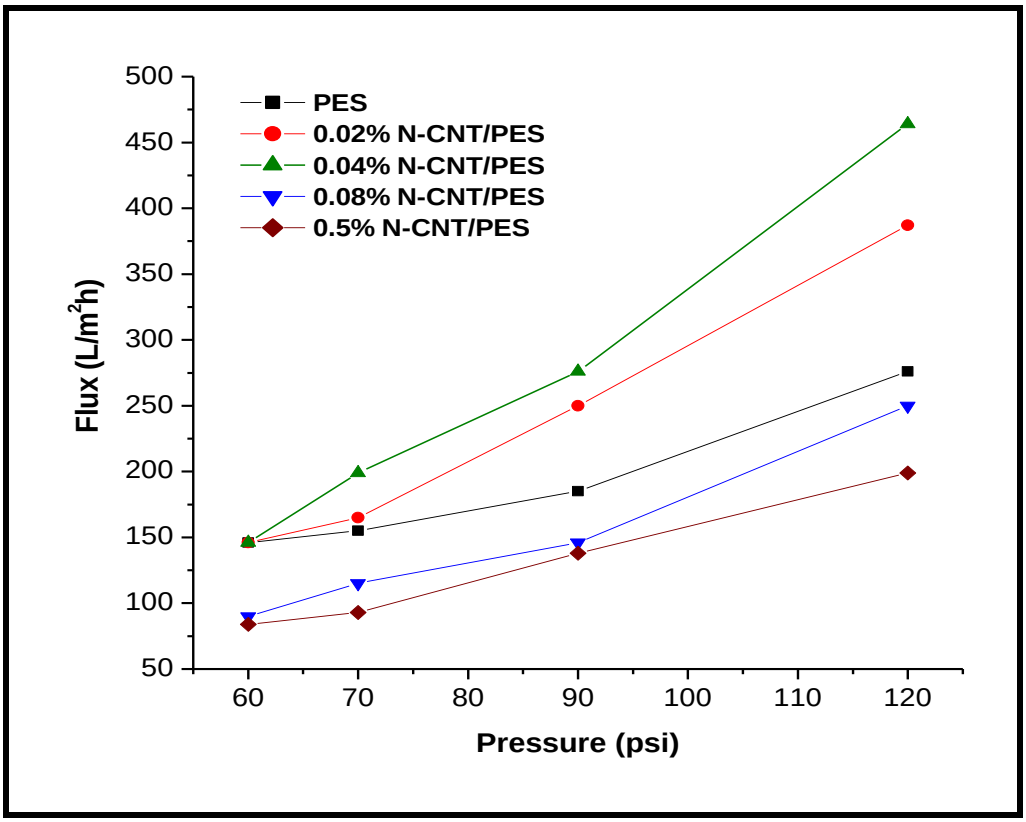

Fig. 4.14: Pure water flux as a function of pressure for the *f*N-CNT/PES membranes and the pristine membrane.

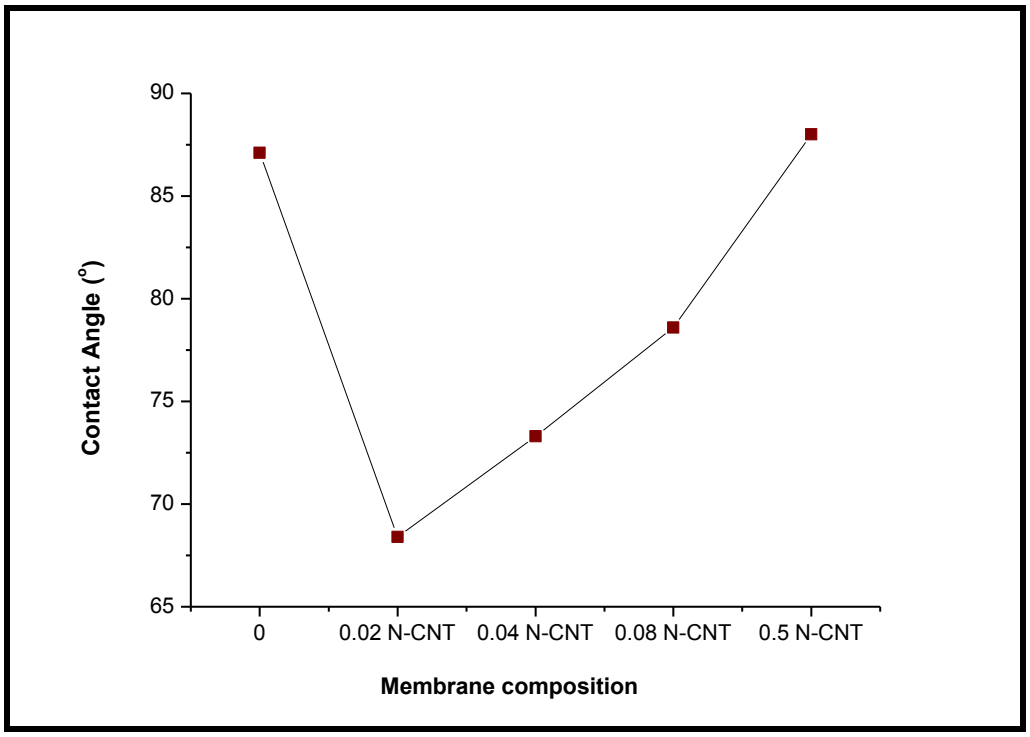

Fig. 4.15: Surface contact angle for the *f*N-CNT/PES blend membranes.

which subsequently slows down the rate of liquid-liquid exchange (water and NMP) in the coagulation bath during the phase inversion process. Thus, more hydrophobic and less porous membranes are formed. These results are expressed in Figures 4.12 and 4.15, which showed a reduction in pore sizes and high contact angle values with higher N-CNT loadings respectively. As such, we also observe low flux values for blend membranes with high *f*N-CNT loadings.

Based on the SEM cross-section images, the pore sizes of the PES membranes were in a range of 1 – 2 µm. Thus suggesting microfiltration PES membranes. According to literature, such a membrane is selective towards high molecular weight pollutants e.g. proteins, bacteria, viruses etc. As such, polyethyleneglycol (PEG) of molecular weight 10 000 was used as a model pollutant for the rejection study.

The rejection properties of the N-CNT/PES blend membranes were observed using 500 ppm aqueous solution of PEG (10.000 M_w) as the feed. Figure 4.16 shows the rejections relative to the membranes under study. The order of rejections was as follows: 0.04 < 0.08 < 0.02 < PES < 0.5. This trend is inverse to what was obtained with water flux studies, with the exception

of the membrane with 0.08 wt% N-CNTs. The membrane with the highest flux (0.04 wt% N-CNT/PES) showed the lowest rejection, whereas the membrane with the lowest flux showed the highest rejections. Previous studies have reported this observation [12, 14]. The behaviour can be explained by the presence of pore structures on the membranes, when various amounts of *f*N-CNTs are incorporated into the membrane matrix As mentioned above, the increase in flux for 0.04 wt% N-CNT/PES (and 0.02 wt% *f*N-CNT/PES) is mainly because of the increase in hydrophilicity and porosity. As a consequence, lower rejections are observed for 0.04 wt% *f*N-CNT/PES. On the contrary, when higher amounts of *f*N-CNTs are added to the PES membranes, more structurally compact membrane composites are formed as a result of the agglomeration of the *f*N-CNTs. This forms a complex network within the membrane structure, which decreases the pore sizes. Hence lower fluxes and higher rejections are observed for PES membranes with large fractions of *f*N-CNTs.

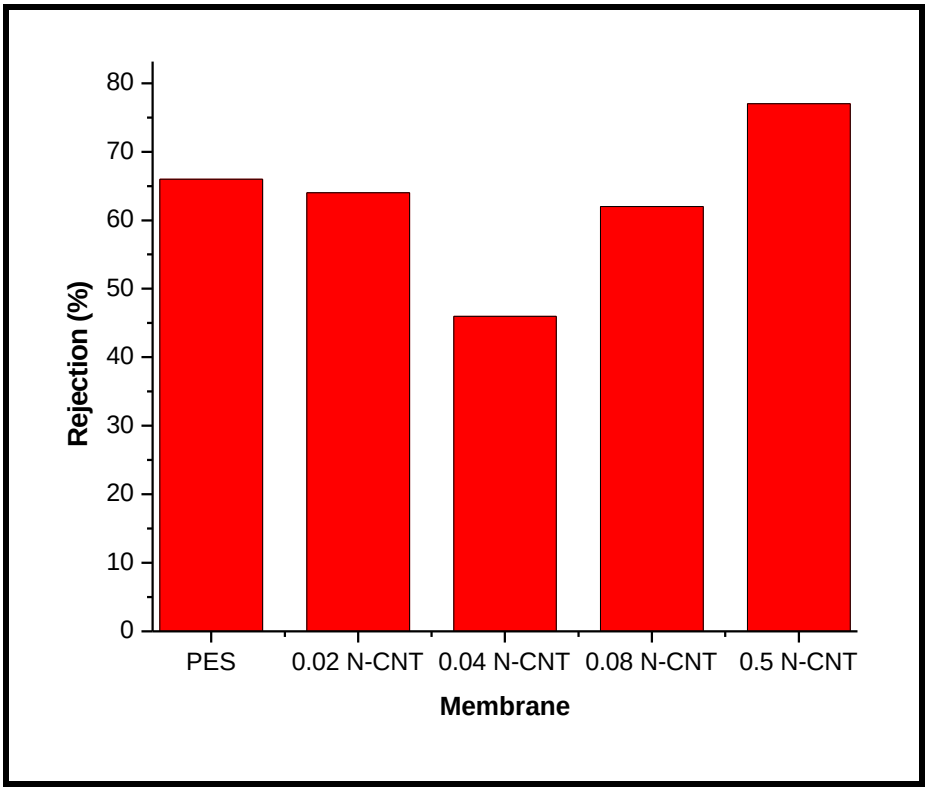

Fig. 4.16: Rejection of a 500 ppm PEG in aqueous solution using the *f*N-CNT/PES blend membranes.

4.5 Fouling studies of N-CNT/PES membranes

The flux performances for PES and N-CNT/PES blend membranes using humic acid spiked deionised water as feed at room temperature and at a pressure of 100 psi are shown in Fig. 4.17. The plots show the permeate flux over time during fouling of the blend membranes with humic acid. Although membrane fouling was not observed in the absence of humic acid, fouling was quite prominent for solution containing 20 mg/L humic acid. The greatest fraction of flux decline was observed after the first few minutes of introducing the feed solution. This initial decline can be attributed to the adsorption of the humic acid on the surface of the membrane upon initial introduction of the solution. According to Wang *et al* [15] membrane fouling can be observed by the reduction in permeate flux with time. This can be explained by four mechanisms [15, 16]:

(i) Complete blockage of membrane pore: which prevents flow of any liquid medium or solutes.
(ii) Partial blockage of membrane pore: which prevents flow of certain foulants but allows movement of the solvent.
(iii) Cake layer formation: which is due to the aggregation or adsorption of foulants on the membrane surface.
(iv) Constriction of membrane pores: due to adherence of small foulants on the walls of the pores.

Based on the mechanisms provided above, we can assume that the initial flux decline was due to the formation of the cake layer on the surface structure. Conversely, after the rapid fouling, a steady decrease in flux decline was observed. According to Nghiem *et al* [17] this is attributed to the compaction and thickening of the cake layer. It must be noted that when water was used no decline in flux was observed suggesting that the decrease was indeed caused by the humic acid, which acted as foulants.

It is also important to note that within a given set of prepared materials there are variations in the membrane properties. For this reason, different flux values were observed for 0.08% N-CNT/PES blend membrane in Fig. 4.14 and for the fouling study (Fig 4.17). The flux values varied by ± 30% for the same operating conditions (temp: 25 °C, pressure: 100 psi). This is a statistically significant value, however, this never altered a trend that was envisaged.

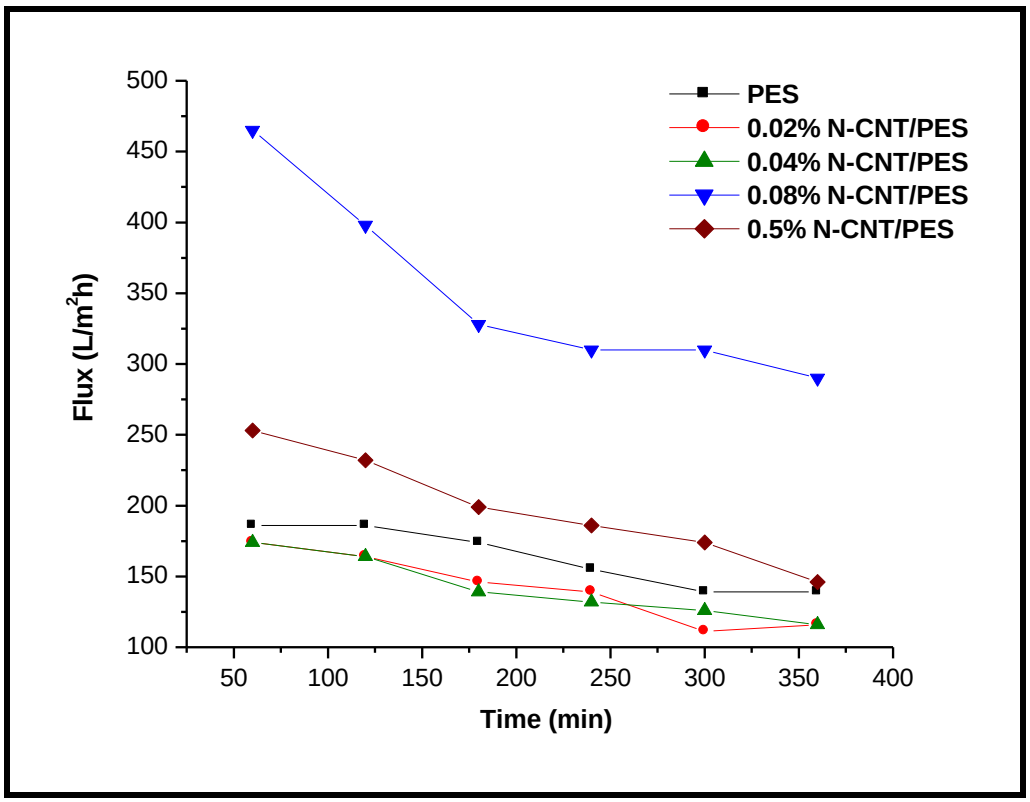

Fig. 4.17: Flux decline behaviour of membranes during fouling studies with humic acid.

Figure 4.18 shows the normalised flux for the filtration/backwashing experiments. In which case the blend membranes were first fouled with the humic acid feed for a few hours (as was done above), then washed with DI water to try and recover the initial flux. Comparing the flux in the three cycles, one can observe that the flux is not fully recovered. In actual fact a flux decline is observed for all membranes over the three cycles. This trend suggests an irreversible type of fouling even after rinsing the membranes with DI water. These results are consistent with those of several other authors [17-19].

Humic acid fouling had a major impact on the surface properties of the membranes. AFM analysis of fouled membranes revealed a change in the surface properties of the membranes (Fig. 4.19). The surface structures showed an increase in the average surface roughness (Fig. 4.20). Furthermore, an increase in membrane hydrophobicity was also observed. This confirms the idea of the cake layer on the surface of the membranes after fouling.

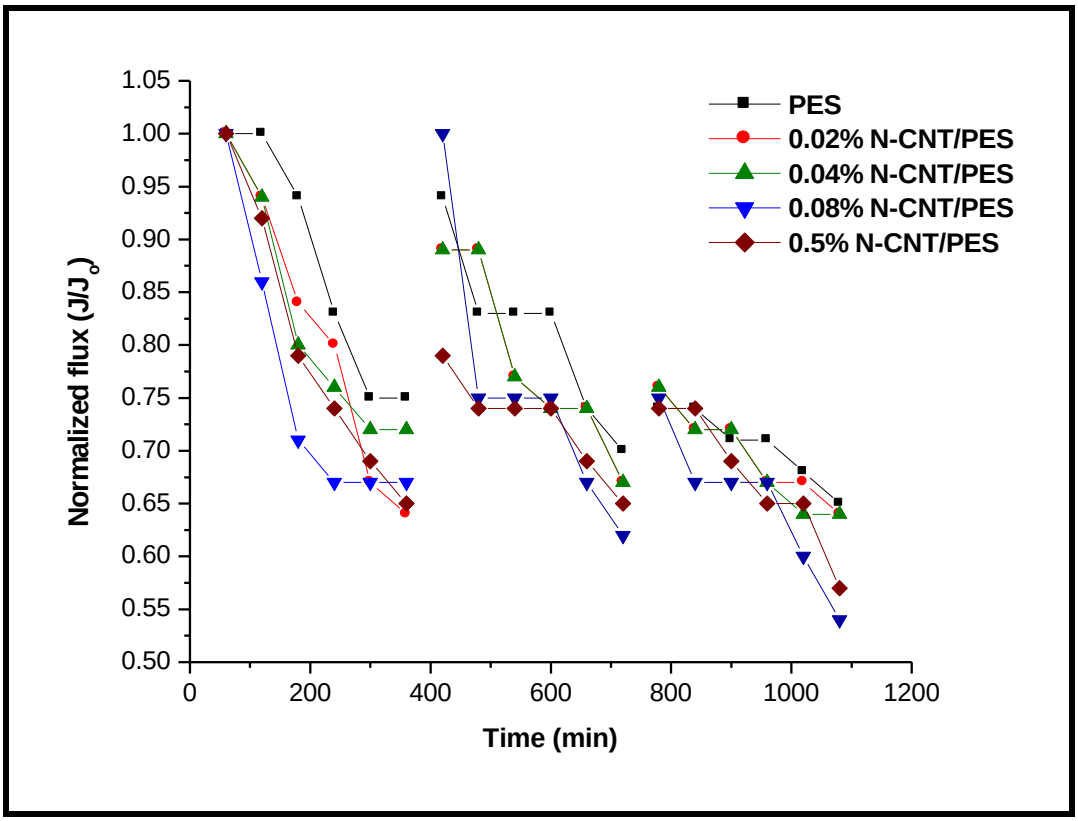

Fig. 4.18: Normalised flux for the filtration/backwashing experiments using humic acid as the foulant.

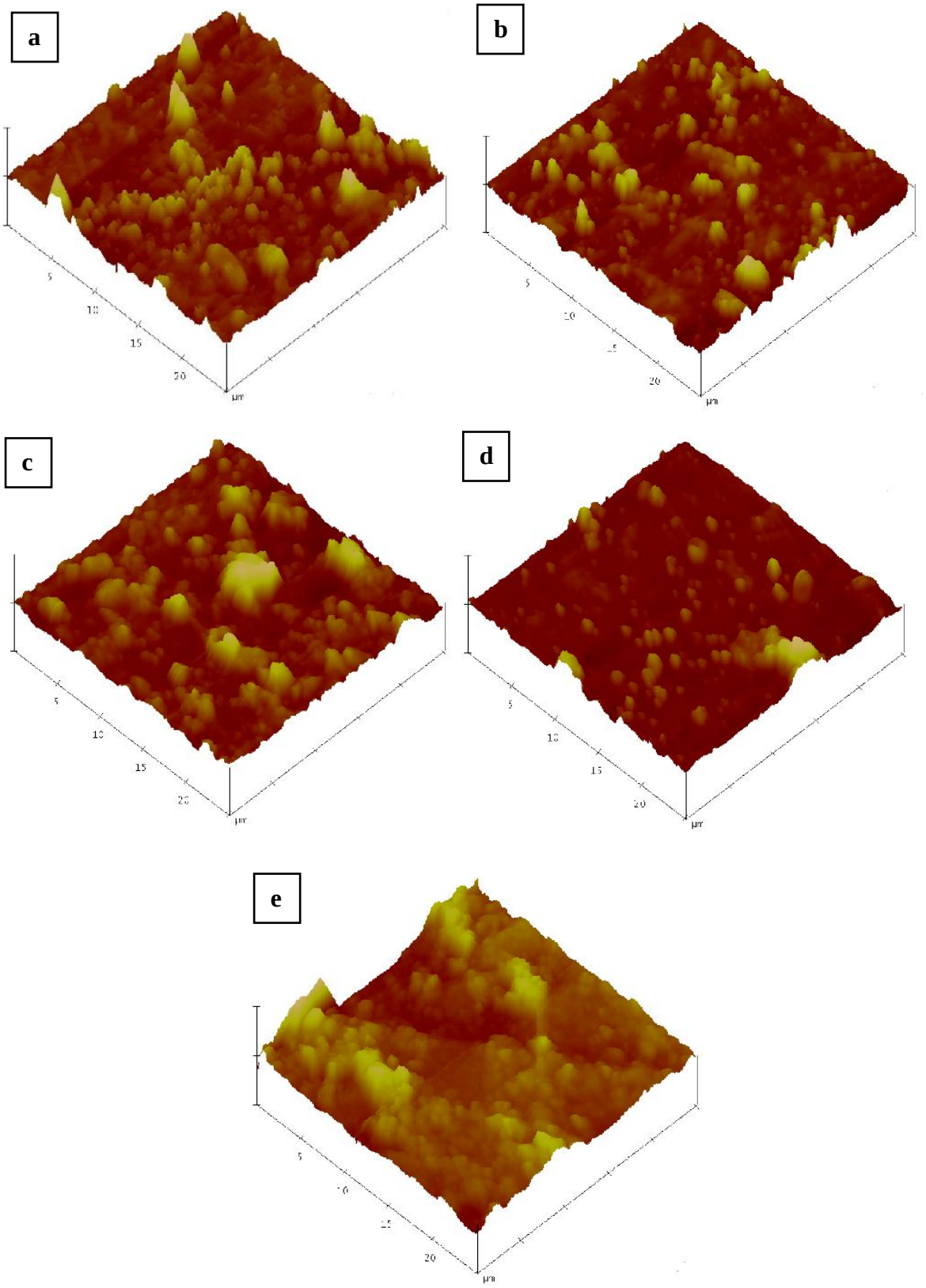

Fig. 4.19: AFM images of humic acid fouled membranes (a) Pristine PES (b) 0.02% N-CNT/PES (c) 0.04% N-CNT/PES (d) 0.08% N-CNT/PES (e) 0.5% N-CNT/PES.

Having considered the impact of humic acid fouling on the PES and the N-CNT/PES membranes, it is however important to note that even with the negative impact of the fouling on the membranes, the N-CNT/PES blend membranes still maintained a higher flux output. It is thus reasonable to suggest the difference in flux is due to the difference in initial surface roughness. In comparison, less rough membrane surfaces (e.g. 0.08% N-CNT/PES) tend to foul less due to little or no valleys (pore like structures) available for clogging or accumulation of pollutants as compared to highly rough surfaces (pristine PES) (Fig. 4.20).

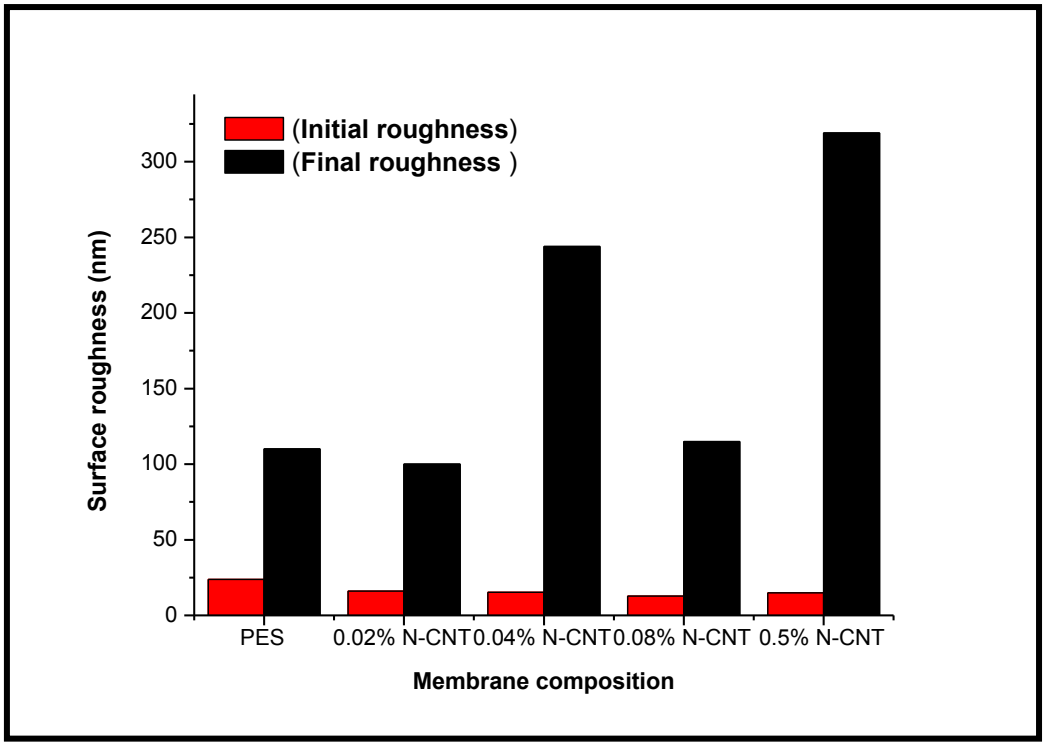

Fig. 4.20: Surface roughness before and after fouling

4.6 Synthesis of Ag/N-CNTs composites

N-CNTs are more chemically active than pristine CNTs. Moreover, the presence of acid functional groups (e.g. –COOH, COO- etc) further enhances their surface properties by increasing the number of active sites for interaction with other materials (e.g. anchoring sites for metal nanoparticles) [20]. The structural morphology and size distribution of AgNPs loaded onto N-CNTs prepared in this study were analysed using the TEM. Figure 4.21(a) shows a TEM image of AgNPs impregnated on the surface the N-CNTs.

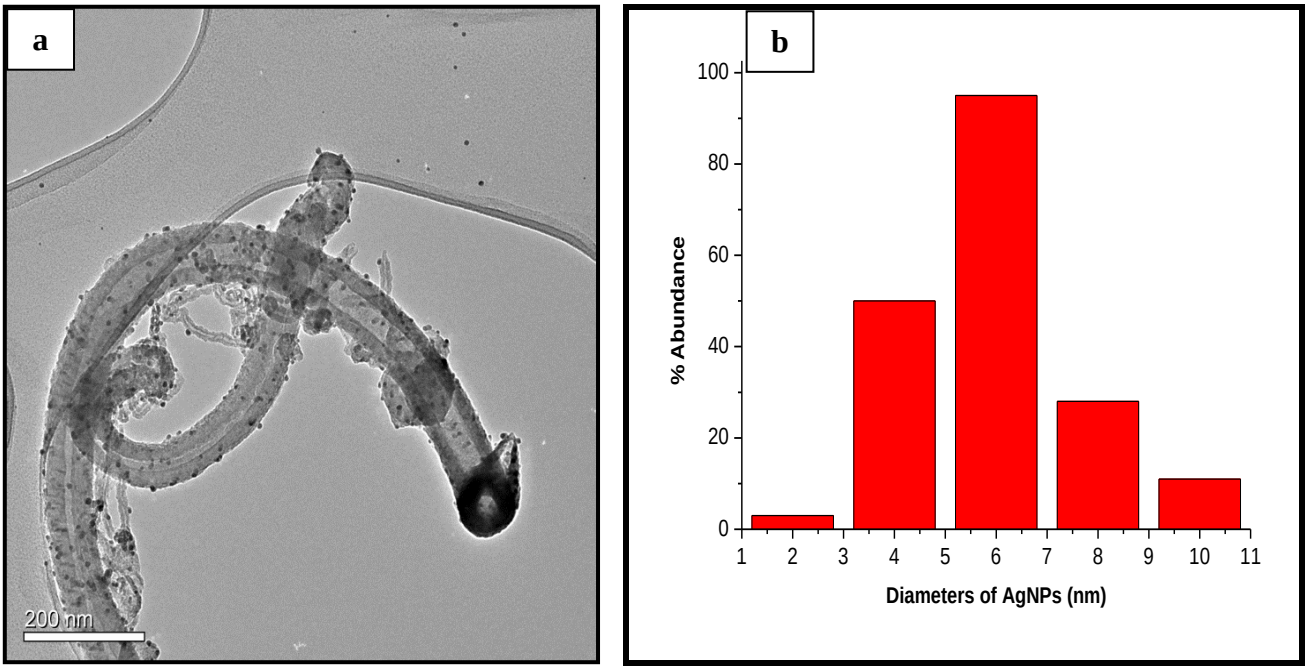

Fig. 4.21: (a) TEM image Ag/N-CNTs (AgNPs can be seen as dark spots on surface of N-CNTs); (b) Diameter size distribution of AgNPs.

The AgNPs can be identified as tiny circular spots on the outer walls of the N-CNTs. The AgNPs were uniformly dispersed on the N-CNTs, exhibiting diameters ranging from 2 – 10 nm. The mean size of the AgNPs was 6.4 nm (see Fig. 4.21b). Previous work on the antimicrobial properties of AgNPs suggests their activity is size dependent. Thus the smaller the particles, the greater the contact surface area with the bacteria and the better their antibacterial activity [21].

The Ag/N-CNTs were also characterised using EDS and scanning electron microscopy (SEM) (Fig. 4.22). The EDS spectra confirmed the elemental content of AgNPs by the presence of four Ag peaks between 2 and 4 keV. The spectra also showed the presence of a major carbon peak, which is due to the carbon composition of N-CNTs. To further confirm the Ag loading on the N-CNTs XRD analysis was performed. Figure 4.23 shows the XRD patterns of functionalised N-CNTs and Ag/N-CNTs with 5% loading of Ag on the N-CNTs. The patterns differed with respect to Ag bound peaks. Three diffraction peaks for Ag positioned between 40–90° were observed for Ag/N-CNTs, these peaks were absent for functionalised N-CNTs.

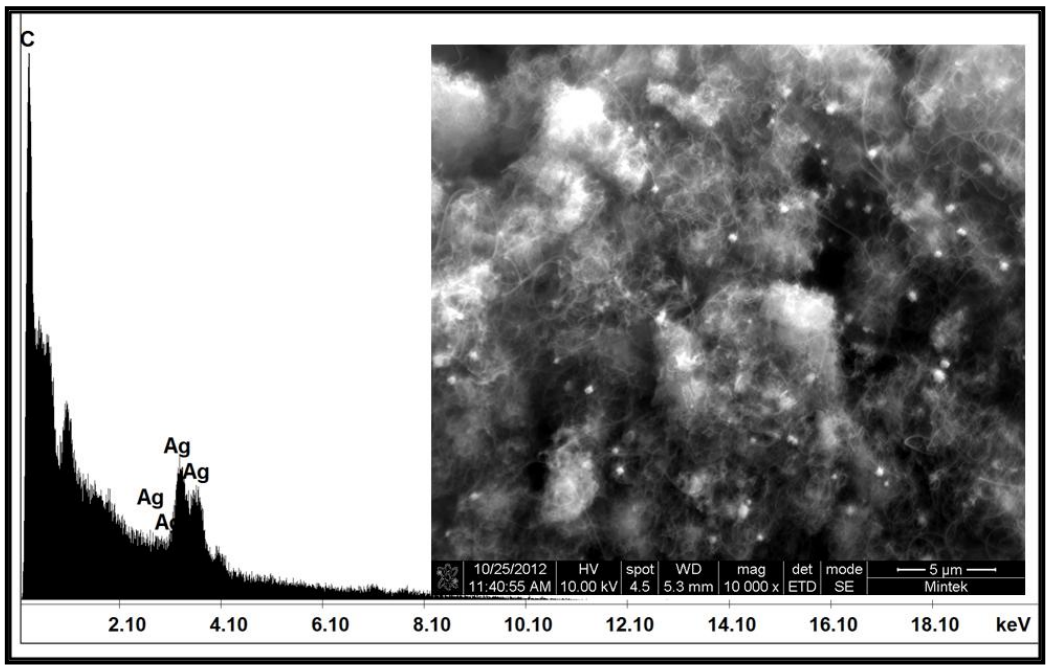

Fig. 4.22: An EDS spectrum and SEM image of 5% Ag/N-CNTs

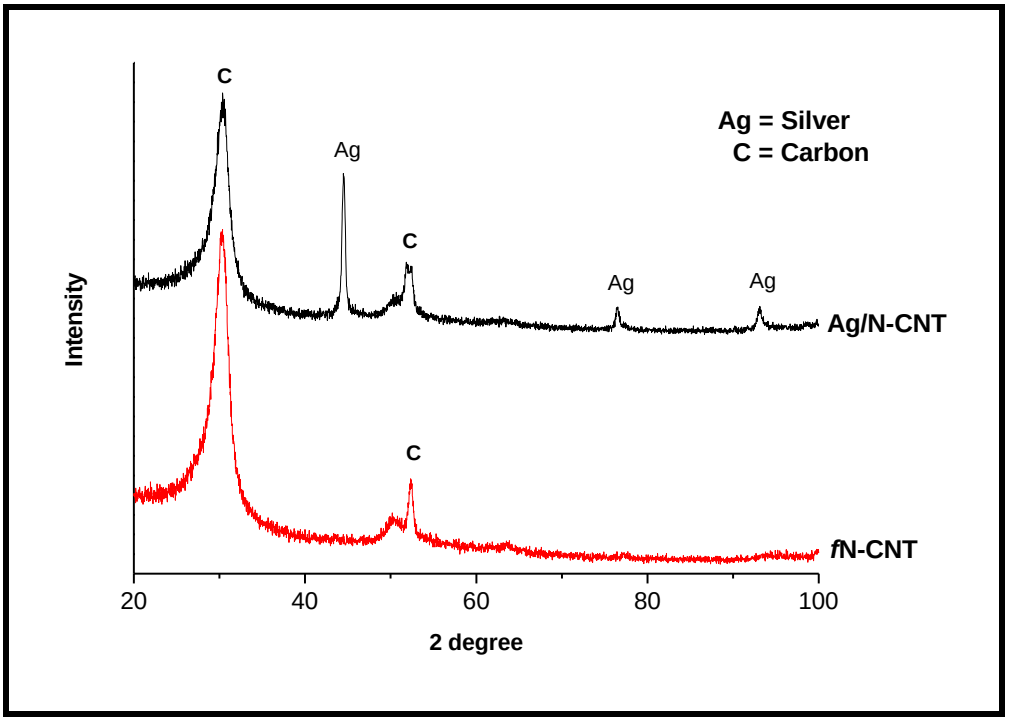

Fig 4.23: XRD patterns of the pristine N-CNTs and the 5% Ag/N-CNTs.

4.6.1 Leaching studies for Ag/N-CNTs

To measure the level of leaching of Ag from the N-CNTs, the 5%, 10% and 20% Ag/N-CNTs samples were sonicated in DI water for 12 h in a beaker. Small portions of the water were sampled at 1 h intervals and analysed using ultra-violet (UV) spectroscopy. AgNPs are generally identified by absorption peaks at ± 400 nm. Figure 4.24 shows the UV spectra of the sonicated samples. The spectra were found to contain one absorption peak at 260 nm, which is associated with MWCNTs. At a wavelength of 400 nm no absorption peak was observed, thus suggestion little or no leaching occurred. TEM revealed that the AgNPs were still bound to the surface of the N-CNTs even after sonication (Fig. 4.25).

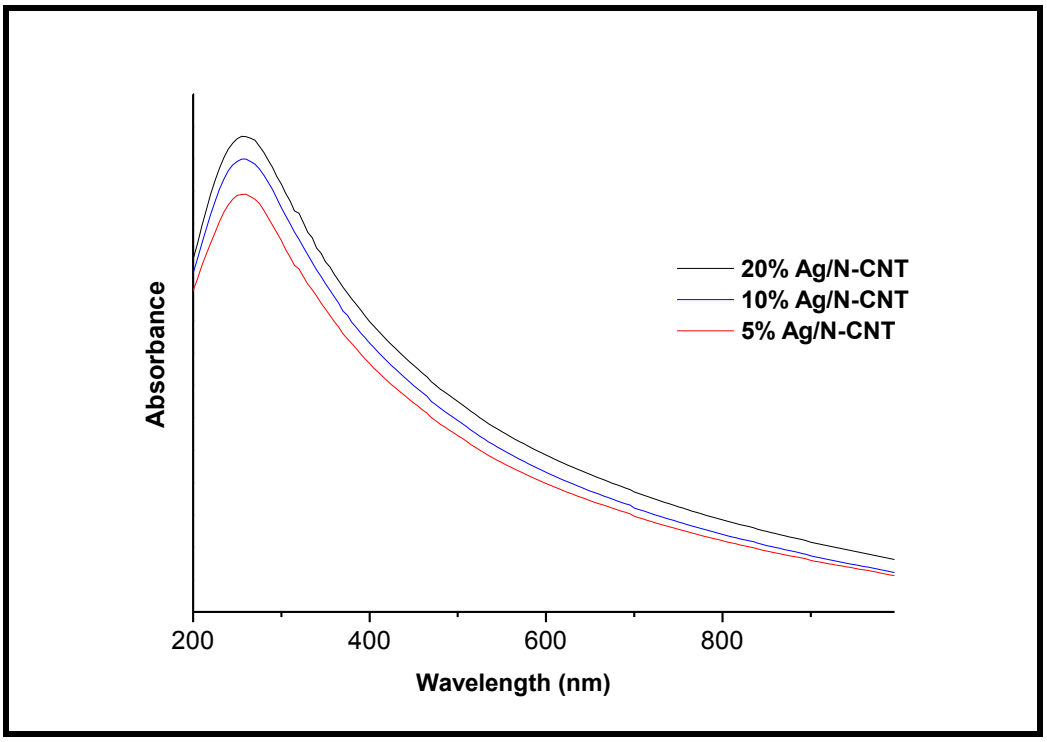

Fig 4.24: UV-vis spectra of DI water samples extracted from the sonicated samples containing Ag/N-CNTs.

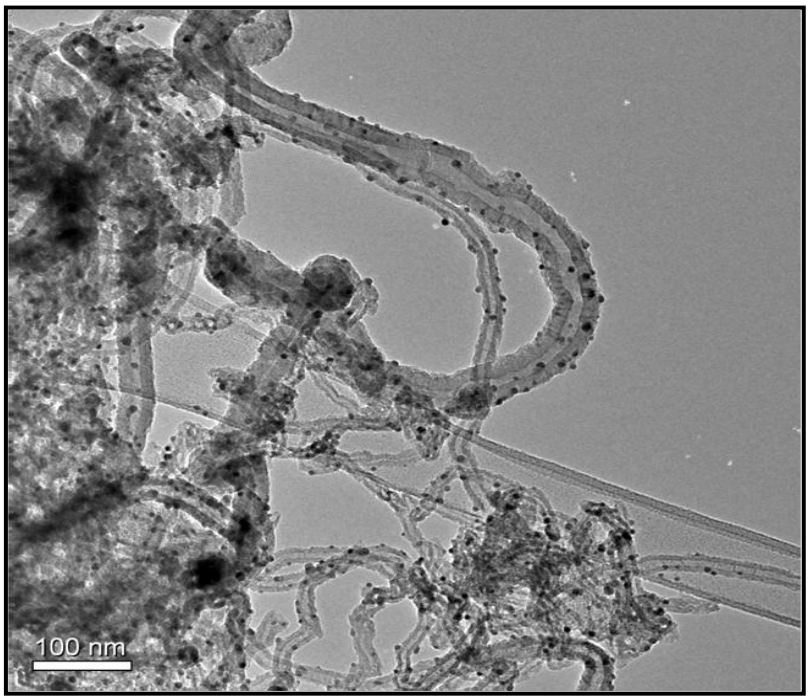

Fig 4.25: TEM image for Ag/N-CNTs after sonication

4.6.2 Anti-microbial study of Ag/N-CNTs

Before assessing the membranes modified with Ag/N-CNTs, the influence of Ag/N-CNTs alone on the *Enterohaemorrhagic E. coli* (EHEC) was studied. Antibacterial tests were performed for pristine N-CNTs and Ag/N-CNTs as shown in Fig. 4.26. In the case of pristine N-CNTs no antibacterial activity was observed. On the other hand, Ag/N-CNTs showed a positive growth inhibition wherein colonies of EHEC were not detected on regions surrounding the Ag/N-CNTs. Moreover, the higher the concentration of AgNPs on the N-CNTs, the better the antibacterial activity. Figure 4.26(d) shows a larger zone of inhibition for N-CNTs with 20% loading than Fig. 4.26(b) and (c) which contained 5 and 10% Ag loading respectively. These results suggest that Ag/N-CNTs are effective in destroying/inhibiting the growth of bacteria due to the presence of AgNPs (Table 4.4). These results correlate well with literature [22-24] despite the fact that the AgNPs were dispersed for the first time on N-CNTs.

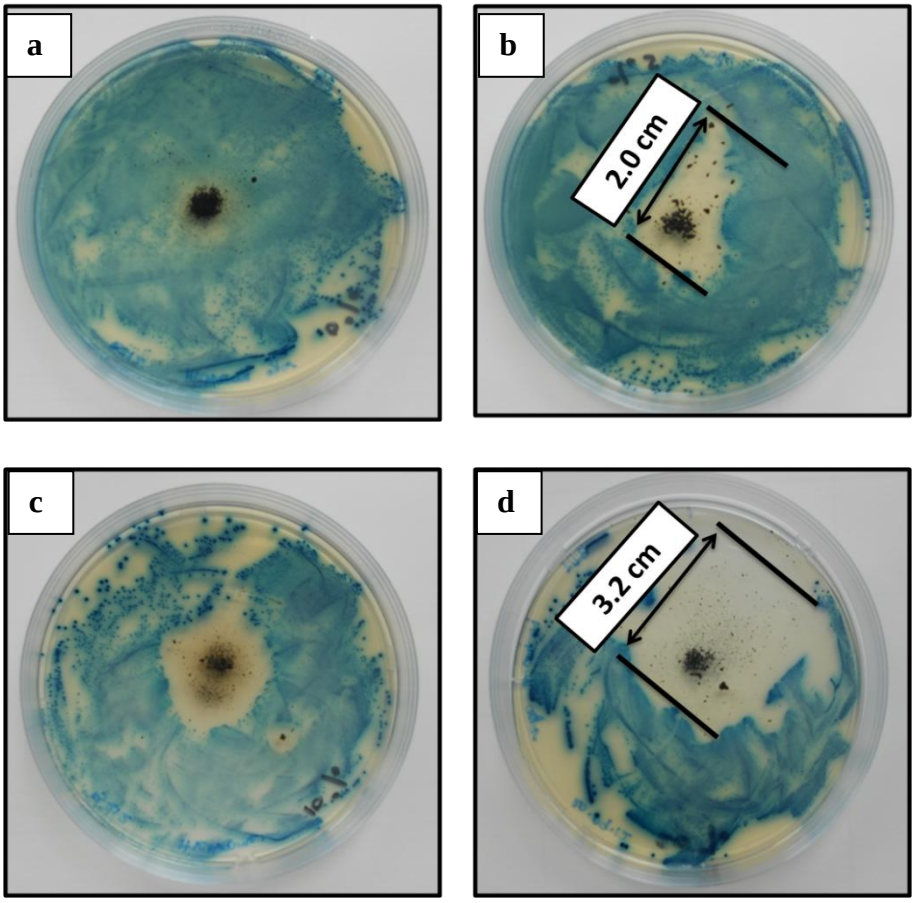

Fig. 4.26: Antibacterial activity of Ag/N-CNTs (a) N-CNTs (b) 5% Ag/N-CNT (c) 10% Ag/N-CNT (d) 20% Ag/N-CNT.

Table 4.4: Zones of inhibition for Ag/N-CNTs.

Ag loadings on N-CNTs (%)	Diameter of zone of inhibition (cm)
20	3.2
10	2.4
5	2.0
0	0.0

Furthermore when the same samples were suspended in a solution containing EHEC cells of concentration 3 x 10^5, a increase in cell concentration was observed for N-CNTs with 0, 5 and 10% Ag as opposed to 20% Ag/N-CNTs which showed a decrease in cell concentration (Fig. 4.27) (see Table 4.5). The results expressed here suggest that at lower Ag loadings the Ag/N-CNTs in suspension are unable to kill nor prevent the growth of the bacteria. As such, a 3 fold concentration increase is observed for N-CNTs with 0, 5 and 10% Ag loadings.

Table 4.5: Cell concentrations of suspensions with Ag/N-CNTs. Initial concentration: $3x10^5$

Ag loadings on N-CNTs (%)	Cells/ml after 24 hrs
20	4.7×10^3
10	4×10^8
5	1.9×10^8
0	4.5×10^8

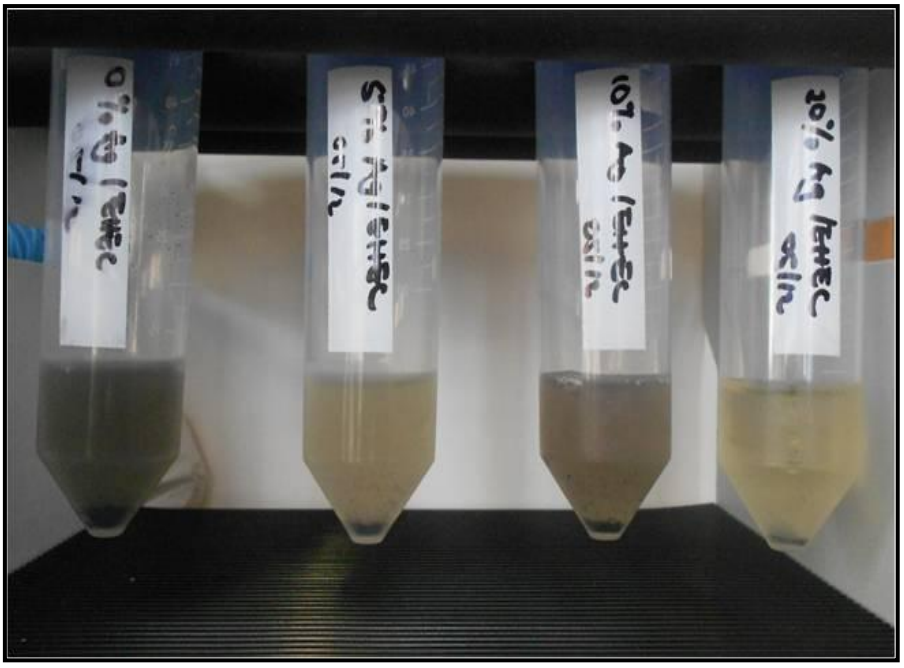

Fig. 4.27: Bacterial suspension incorporated with Ag/N-CNTs for antibacterial activity. From left to right is 0% Ag/N-CNT, 5% Ag/N-CNT, 10% Ag/N-CNT and 20% Ag/N-CNT.

4.7 Synthesis of Ag/N-CNTs/PES membranes

Based on the results obtained in section 4.4.5 about the performance and properties of N-CNT/PES blend membranes, we chose the 0.02% N-CNT/PES as our best membrane. Evidently, this membrane showed a limited trade–off between the flux performance and rejection measurements. Moreover, it was observed that the membrane had improved structural properties (with reference to the mechanical strength, thermal stability and the surface roughness). As such, we decided to load the same fraction of Ag/N-CNTs (different Ag concentrations) to the PES membranes.

4.7.1 AFM and SEM analysis

Figure 4.28 shows the AFM surface morphology and SEM cross-section images of Ag/N-CNT blend membranes prepared via the phase inversion method. The AFM topography images reveal homogenous, defect free structures with evenly distributed valleys and peaks on the membrane surfaces. Comparing the roughness parameters between the 0.02% N-

CNT/PES and the 0.02% Ag/N-CNT/PES membranes obtained from the AFM images confirmed that the surface roughness of the membranes was not affected by the addition of AgNPs (Table 4.6). The roughness values are in close correlation with each other and the slight changes can be ignored. To further evaluate membrane structural changes, the SEM was used. The cross-section images revealed the typical asymmetrical structure as a result of the phase inversion procedure. The addition of Ag/N-CNT did not show any distinct physical changes to the membrane structure [25]. Compared with the 0.02% N-CNT/PES membrane, the 0.02% Ag/N-CNT/PES membranes had an average pore width of 0.8 μm, which is only a slight decrease from the 1 μm of the 0.02% N-CNT/PES membrane.

Table 4.6: Surface roughness before and after Ag incorporation.

Sample	**0.02% N-CNT/PES**	**5% Ag/N-CNT/PES**	**10% Ag/N-CNT/PES**	**20% Ag/N-CNT/PES**
Surface roughness (nm)	16.00	16.6	17.4	19.1

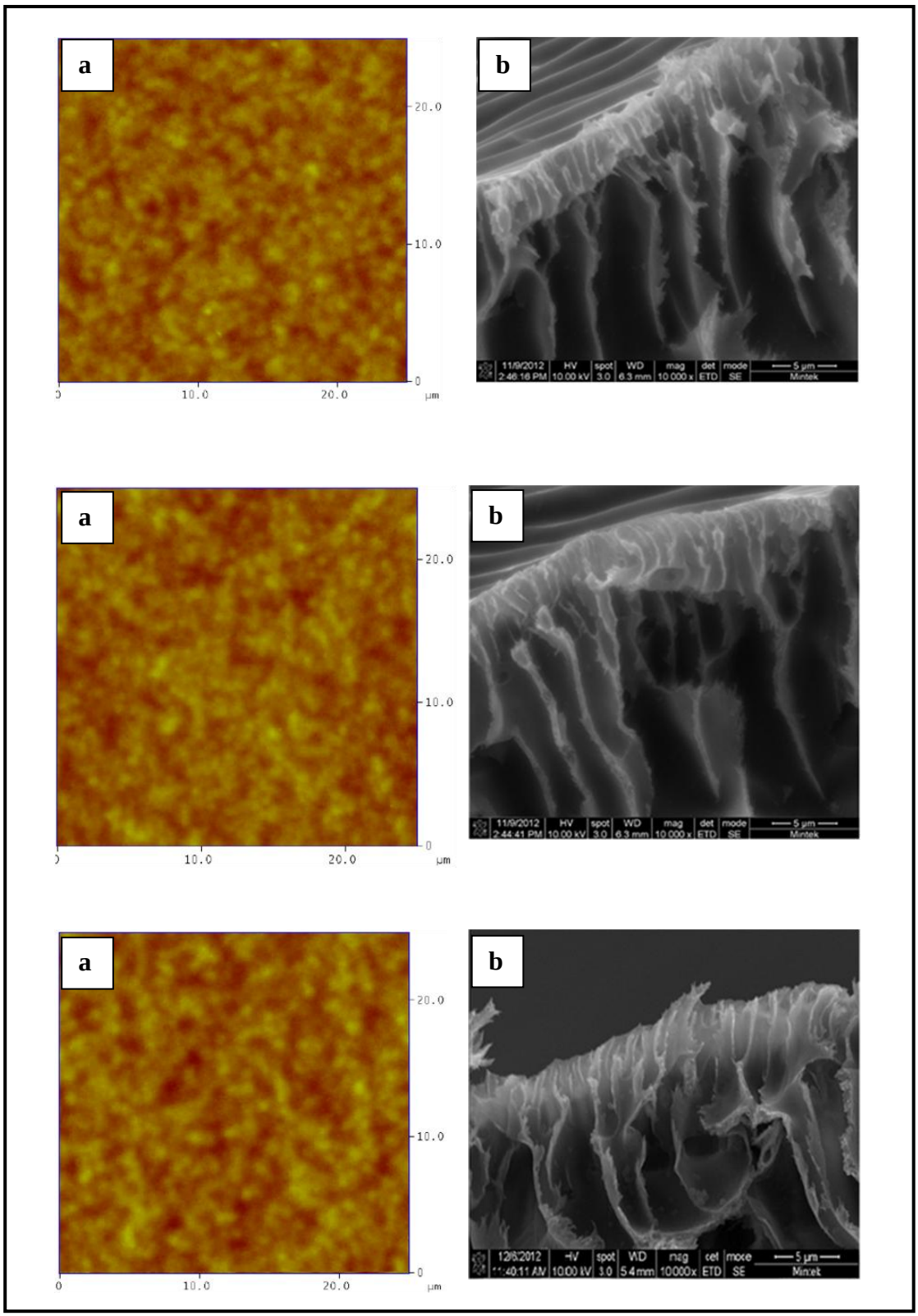

Fig 4.28: (a) AFM surface morphology and (b) SEM cross section images of Ag/N-CNT/PES membranes.

4.7.2 Anti-microbial study Ag/N-CNT/PES

The antibacterial activity of the Ag/N-CNT/PES and the pristine N-CNT/PES membranes was studied using the inhibition zone method. It was observed that the membranes showed no antibacterial activity against the EHEC even with varying the mass ratio of Ag and N-CNTs incorporated in the PES membranes (e.g. 0:1, 5:1, 10:1 and 20:1 respectively) (Fig. 4.29).

According to Huang *et al* [26] Ag poses an antibacterial effect by either coming in contact with the bacteria or leaching out Ag^{+} ions into the solution containing the microorganisms. In the former case it is predicted that the AgNPs attach to the cell membrane (of bacteria) and disrupts metabolic processes (e.g. respiration). Similarly, it is expected that the Ag^{+} ions (travelling through media) can hamper metabolic functioning by denaturing of proteins [27].

However, since no antibacterial activity was observed for the membranes despite the incorporation of Ag/N-CNTs. It is believed that the AgNPs were unavailable for interaction with the bacteria as a result of their low concentration in the skin layer of the membrane. Moreover, due to their altered bioavailability as a consequence of polymer wrapping of the N-CNTs incorporated with Ag (Ag/N-CNTs being trapped in the membrane matrix) [28, 29].

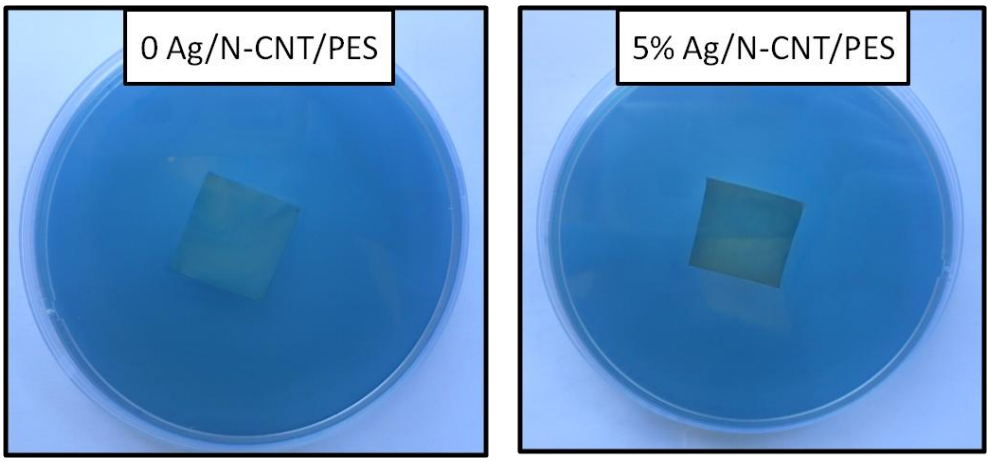

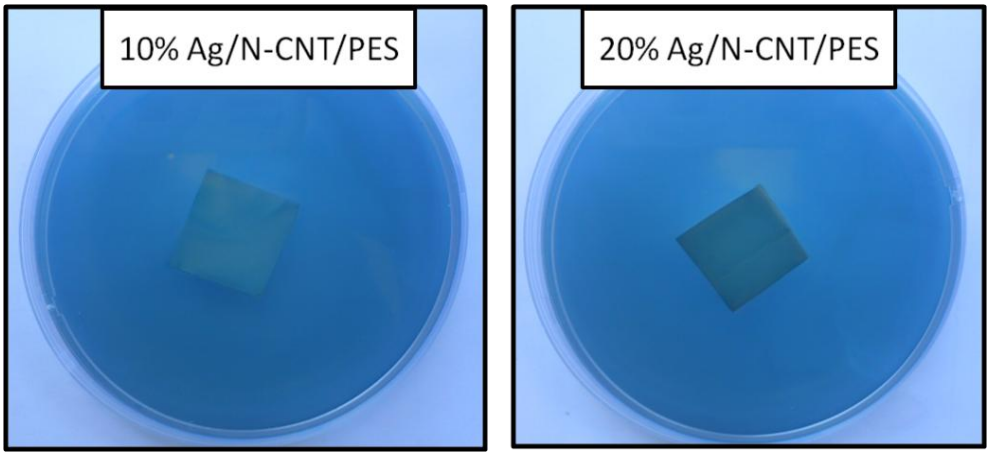

Fig. 4.29: Zone inhibition study of PES membrane with different concentration Ag incorporated onto N-CNTs.

To further establish the antibacterial capabilities or lack thereof for the Ag/N-CNT/PES membranes, a second test was conducted. In this test filtration experiments were performed on EHEC suspension of concentration 1.76 x 10^7 colony forming units (cfus)/ml. The EHEC samples were filtered through membrane coupons using a vacuum filtration system. The filtrate was then assessed to quantify the antibacterial activity of the membranes. The concentration of the suspension after filtration was found to be 1.75 x 10^7, which is not any different from the initial concentration. This result corroborates the lack of antibacterial activity in the zone inhibition study, as explained above.

In summary, these results suggest that the Ag/N-CNTs/PES membranes synthesised in this study were not effective in inhibiting or destroying EHEC as envisaged. The increase in Ag loading on the N-CNTs did not enhance the antibacterial properties of the membranes. However, this does not confirm that the materials are inactive because the Ag/N-CNTs alone were found to inhibit any form of growth. This suggests more extensive modifications and tests of these materials may be necessary. However due to limited time allocated to the study, these have been left out for future studies.

4.8 References

1. Mhlanga, S.D., Nxumalo, E.N., Coville, N.J., and Srinivasu, V.V. 2011. Nitrogen doping of CVD multiwalled carbon nanotubes: Observation of a large g-factor shift. Materials Chemistry and Physics, 130, 1182-1186.
2. Motchelaho, M.A.M., Xiong, H., Moyo, M., Jewell, L.L., and Coville, N.J. 2011. Effect of acid treatment on the surface of multiwalled carbon nanotubes prepared from Fe–Co supported on $CaCO_3$: Correlation with fischer–tropsch catalyst activity. Journal of Molecular Catalysis A: Chemical, 335, 189-198.
3. Biddinger, E.J., Deak, D.V., and Ozkan, U.S. 2009. Nitrogen-containing carbon nanostructures as oxygen-reduction catalysts. Topics in Catalysis, 52, 1566-1574.
4. van Dommele, S., Romero-Izquirdo, A., Brydson, R., de Jong, K.P., and Bitter, J.H. 2008. Tuning nitrogen functionalities in catalytically grown nitrogen-containing carbon nanotubes. Carbon, 46, 138-148.
5. Li, Q., Yan, H., Zhang, J., and Liu, Z. 2004. Effect of hydrocarbons precursors on the formation of carbon nanotubes in chemical vapor deposition. Carbon, 42, 829-835.
6. Kang, Z.C. and Wang, Z.L. 1996. On accretion of nanosize carbon spheres. The Journal of Physical Chemistry, 100, 5163-5165.
7. Wang, Z.L. and Kang, Z.C. 1996. Pairing of pentagonal and heptagonal carbon rings in the growth of nanosize carbon spheres synthesized by a mixed-valent oxide-catalytic carbonization process. The Journal of Physical Chemistry, 100, 17725-17731.
8. Drioli, E. and Giorno, L. 2010. Comprehensive membrane science and engineering, Kidlington, OX: Elsevier.
9. Vatanpour, V., Madaeni, S.S., Moradian, R., Zinadini, S., and Astinchap, B. 2011. Fabrication and characterization of novel antifouling nanofiltration membrane prepared from oxidized multiwalled carbon nanotube/polyethersulfone nanocomposite. Journal of Membrane Science, 375, 284-294.
10. Qiu, S., Wu, L., Pan, X., Zhang, L., Chen, H., and Gao, C. 2009. Preparation and properties of functionalized carbon nanotube/psf blend ultrafiltration membranes. Journal of Membrane Science, 342, 165-172.
11. Lawrence Arockiasamy, D., Alam, J., and Alhoshan, M. 2012. Carbon nanotubes-blended poly(phenylene sulfone) membranes for ultrafiltration applications. Applied Water Science, 1-11.

12. Celik, E., Park, H., Choi, H., and Choi, H. 2011. Carbon nanotube blended polyethersulfone membranes for fouling control in water treatment. Water Research, 45, 274-282.
13. Wu, H., Tang, B., and Wu, P. 2010. Novel ultrafiltration membranes prepared from a multi-walled carbon nanotubes/polymer composite. Journal of Membrane Science, 362, 374-383.
14. Choi, J.-H., Jegal, J., Kim, W.-N., and Choi, H.-S. 2009. Incorporation of multiwalled carbon nanotubes into poly(vinyl alcohol) membranes for use in the pervaporation of water/ethanol mixtures. Journal of Applied Polymer Science, 111, 2186-2193.
15. Wang, C., Zhao, S., and Wei, Y. 2012 Hydrophilic modification of microporous polysulfone membrane via surface-initiated atom transfer radical polymerization and hydrolysis of poly(glycidylmethacrylate). Chinese Journal of Chemistry, 2473-2482.
16. Wang, S., Liu, C., and Li, Q. 2011. Fouling of microfiltration membranes by organic polymer coagulants and flocculants: Controlling factors and mechanisms. Water Research, 45, 357-365.
17. Nghiem, L.D., Vogel, D., and Khan, S. 2008. Characterising humic acid fouling of nanofiltration membranes using bisphenol a as a molecular indicator. Water Research, 42, 4049-4058.
18. Goosen, M.F.A., Sablani, S.S., Al-Hinai, S., Al-Obeidani, S., Al-Belushi, R., and Jackson, D. 2004. Fouling of reverse osmosis and ultrafiltration membranes: A critical review. Separation Science and Technology, 39, 2261-2298.
19. Katsoufidou, K., Yiantsios, S.G., and Karabelas, A.J. 2008. An experimental study of uf membrane fouling by humic acid and sodium alginate solutions: The effect of backwashing on flux recovery. Desalination, 220, 214-227.
20. Castle, A.B., Gracia-Espino, E., Nieto-Delgado, C., Terrones, H., Terrones, M., and Hussain, S. 2011. Hydroxyl functionalized and n-doped multiwalled carbon nanotubes decorated with silver nanoparticles preserve cellular function. ACS Nano, 5, 2458-2466.
21. Mauter, M.S., Wang, Y., Okemgbo, K.C., Osuji, C.O., Giannelis, E.P., and Elimelech, M. 2011. Antifouling ultrafiltration membranes via post-fabrication grafting of biocidal nanomaterials. ACS Applied Materials & Interfaces, 3, 2861-2868.

22. Li, Z., Fan, L., Zhang, T., and Li, K. 2011. Facile synthesis of Ag nanoparticles supported on mwcnts with favorable stability and their bactericidal properties. Journal of Hazardous Materials, 187, 1-3.
23. Wang, J., Dong, Z., Huang, J., Li, J., Liu, K., Jin, J., and Ma, J. 2013. Synthesis of Ag nanoparticles decorated multiwalled carbon nanotubes using dialdehyde starch as complexant and reductant for antibacterial purposes. RSC Advances, 3, 918-922.
24. Mohan, R., Shanmugharaj, A.M., and Sung Hun, R. 2011. An efficient growth of silver and copper nanoparticles on multiwalled carbon nanotube with enhanced antimicrobial activity. Journal of Biomedical Materials Research Part B: Applied Biomaterials, 96B, 119-126.
25. Hilal, N., Khayet, M., and Wright, C.J. 2012. Membrane modification: Technology and applications. Boca Raton: Taylor & Francis.
26. Huang, J., Arthanareeswaran, G., and Zhang, K. 2012. Effect of silver loaded sodium zirconium phosphate (nanoagz) nanoparticles incorporation on pes membrane performance. Desalination, 285, 100-107.
27. Rai, M., Yadav, A., and Gade, A. 2009. Silver nanoparticles as a new generation of antimicrobials. Biotechnology Advances, 27, 76-83.
28. Ismail, A.F., Goh, P.S., Sanip, S.M., and Aziz, M. 2009. Transport and separation properties of carbon nanotube-mixed matrix membrane. Separation and Purification Technology, 70, 12-26.
29. Brunet, L., Lyon, D.Y., Zodrow, K., Rouch, J.C., Caussat, B., Serp, P., Remigy, J.C., Wiesner, M.R., and Alvarez, P.J.J. 2008. Properties of membranes containing semi-dispersed carbon nanotubes. Environmental Engineering Science, 25, 565-576.

CHAPTER 5

CONCLUSIONS AND RECOMMENDATIONS

5.1 Conclusions

The main aim of this study was to synthesise and functionalize a membrane filtration system incorporating nitrogen doped CNT supported Ag nanoparticles (NPs) and to characterise the system using TEM, SEM, FTIR, TGA, contact angle and the cross-flow filtration system, and finally test this system for its potential use in water treatment by removing model pollutants such as PEG and humic acids. This study was successfully done and the following conclusions are drawn

- N-CNTs with bamboo compartments were synthesised using the chemical vapour deposition (CVD) method. In this research, a Fe-Co/$CaCO_3$ catalyst was used as a template for growth of the N-CNTs. Acetylene was used as a carbon source, nitrogen gas as a carrier and acetonitrile as the nitrogen source. This catalyst system was used in our group.

- The N-CNTs were readily purified and functionalised by acid treatment in order to remove any excess residues from the catalyst and to also introduce acid functional groups (e.g. carboxyl groups) onto the surface of the N-CNTs. The purity was > 97%. Success of functionalisation was confirmed by FTIR, and the degree of functionalisation was ascertained by zeta potential measurement. A decrease in the iso-electric point of the N-CNT surface was observed with an increase in acid treatment. As the degree of functionalisation increased the iso-electric point values decreased correspondingly. From the measurements, we could ascertain the saturation of the surface of the N-CNTs with acid functional groups.

- Composite membranes containing PES and N-CNTs were successfully prepared by the phase inversion method. This involved dispersing the N-CNTs in N-methylpyrrolidone (NMP) followed by adding the PES polymer to the solution and blending the components together to give a homogeneous mixture. The mixture was cast on a glass plate and submerged in DI water to give a thin film (membrane).

- Characterisation of the membranes by FTIR confirmed successful incorporation of N-CNTs. Furthermore, the reduced surface roughness showed by AFM analysis indicated the uniform distribution of the carbon materials in the membrane matrix.

- Characterisation of the membrane surfaces using SEM revealed a dense and smooth structure. However the cross section images showed highly porous sub-layers with pore widths ranging between 1 and 2 μm, suggesting a microfiltration type of membrane.

- Mechanical and thermal analysis demonstrated that the incorporation of N-CNTs even at low wt% to the pristine PES membrane could increase both the mechanical and thermal stability of the blend membranes.

- The N-CNT blend PES membranes were also tested for any improvements in water flux and PEG rejections. Generally, improved performances were observed for membranes with low fraction of N-CNT. A 46% increase in water flux was observed with only 0.04 wt% of N-CNTs to PES membrane. A 13% increase in PEG rejection was also observed with addition of 0.5 wt% of N-CNT in PES membranes. Moreover a 58% improvement in fouling performance was also observed with only 0.08 wt% of N-CNTs to PES membrane.

- To further establish an advanced membrane filtration system. The functionalised N-CNTs were modified with AgNPs (due to their antibacterial properties) using $AgNO_3$ as the Ag source and ethylene glycol as a reducing agent. The Ag embedded N-CNTs

were then characterised with XRD, TEM and EDX to confirm the Ag loading. In each case the AgNPs were observed, which served as confirmation for the Ag loading.

- The Ag/N-CNTs were tested for their antibacterial activity before they could be incorporated in the PES membrane. Indeed the Ag/N-CNTs showed antibacterial activity towards a pathogenic strain of *E-coli.* The zone inhibition method was used. The more the AgNPs loaded onto the N-CNTs, the better the performance observed.

- The Ag/N-CNT/PES membranes were found not to have any antibacterial activity even with high concentrations of Ag. This was attributed to the entrapment of the Ag/N-CNT in the membrane matrix as well as their low concentration at the membrane surface, thus preventing their interaction with the bacterial cell wall.

  It can be concluded from these results that apart from the poor antibacterial properties of the Ag/N-CNT/PES membranes, improvement in blend membranes was observed as compared to the pristine membrane.

5.2 Recommendations for future work.

- It has been demonstrated that the incorporation of N-CNTs into PES membrane using the simple solution blending can improve the properties of the membranes. However, if the N-CNTs could be tactically placed (e.g. aligning) within the membrane matrix this could potentially elevate the membrane properties even further.

- Preliminary studies of Ag/N-CNT/PES membranes in our laboratories suggested poor antibacterial activity towards *E-coli*. It will be necessary to apply different strategies towards incorporation of Ag/N-CNT into PES membranes such that the AgNPs are readily available to interact with bacteria. For example, post modification of the pristine PES membrane with the Ag/N-CNTs rather than solution blending.

- The membranes presented here have micropores. It would be worthwhile to synthesise membranes with even smaller pores (e.g. nanopores) for better separation of pollutants. This would require control of the synthesis conditions.

- All experiments were conducted using model pollutants. It would be beneficial to investigate the performance of the membranes using real water samples.